

# American Journal of Science

SEPTEMBER 2022

## DETERMINATION OF AN INTRACONTINENTAL TRANSFORM SYSTEM ALONG THE SOUTHERN CENTRAL ASIAN OROGENIC BELT IN THE LATEST PALEOZOIC

JIN ZHANG<sup>\*,†</sup>, JUNFENG QU<sup>\*</sup>, BEIHANG ZHANG<sup>\*</sup>, HENG ZHAO<sup>\*</sup>,  
RONGGOU ZHENG<sup>\*</sup>, JIANFENG LIU<sup>\*</sup>, JIE HUI<sup>\*\*</sup>, PENGFEI NIU<sup>\*</sup>,  
LONG YUN<sup>\*\*\*</sup>, SHUO ZHAO<sup>\*</sup>, and YIPING ZHANG<sup>§</sup>

**ABSTRACT.** Intracontinental transform structures are important forms of continental deformation, such as the Altyn Tagh fault on Tibetan Plateau. Although many intracontinental transform structures have developed throughout geological history, their identification is relatively difficult due to later deformation and sedimentary covering. Strike-slip faults played an important role in the formation and subsequent transformation of the Central Asian orogenic belt (CAOB). In this study, a group of nearly EW-trending dextral shear zones along the southern CAOB in the Beishan, Alxa, northern margin of the North China Craton and the Great Xing'an Mountains to the east, is reported. Regional strike-slip duplex systems were developed and strongly superimposed on the CAOB in the Beishan and Alxa regions. Meanwhile, to the west of the Beishan, coeval ductile shear zones with the same kinematics also developed along the CAOB. The ages of the shear zones range from 280 Ma to 230 Ma and become younger to the east. This megashear system may also connect with the shortening in the Ural Orogenic belt to the west and the convergence along the eastern margin of the Eurasian continent, which is approximately more than 9000 km long in the Asian continent and consists of an intracontinental transform structure in the central Pangea continent. Further west, the dextral shear system may also connect with the coeval shear zones with the same kinematics along the southern Variscan orogenic belt in Europe and even the South Appalachian Orogenic Belt in the southeastern North America, which we call the Intra-Pangean Megashear (IPM) after Irving (2004). The rotation and approach of the Baltic Craton and Siberian Craton and the northern Pangean lithosphere heated by mantle plumes and its lateral (eastward) spreading may have caused the development of the IPM and intracontinental deformation from Pangea B to Pangea A.

Key words: Central Asian Orogenic Belt (CAOB), dextral shearing, latest Paleozoic, Pangea, intracontinental transform system, Intra-Pangean Megashear

### INTRODUCTION

Transform faults are one of the most important boundaries in plate tectonics (Wilson, 1965). They are mainly distributed in the ocean regime. Intracontinentally, there are large fault systems or continental transform faults such as the San Andreas system in California, the Altyn Tagh fault and Red River-Ailaoshan fault in China, the North Anatolian fault in Turkey, and the Alpine fault in New Zealand (Şengör and

\* Key Laboratory of Deep-Earth Dynamics of Ministry of Natural Resources, Institute of Geology, Chinese Academy of Geological Sciences, Beijing, 100037, China

\*\* University of Chinese Academy of Sciences, Beijing, 100049, China

\*\*\* Beijing Research Institute of Uranium Geology, Beijing, 100029, China

§ Chinese Academy of Geological Sciences, Beijing, 100037, China

† Corresponding author: zhangjinem@sina.com

others, 2019a). However, the identification of similar transform structures developed during geological history is relatively few and difficult, and the most important reason for this is the strong superimposition or cover in later periods (Şengör and others, 2019a). Previous studies have shown that the role of strike-slip shearing is of great significance in the evolution of the Central Asian Orogenic Belt (CAOB), however, the role played by strike-slip shearing is in enthusiastic discussions (Şengör and Natal'in, 1996; Windley and others, 2007; Xiao and others, 2015, 2018), and later intracontinental strike-slip shearing may also cut and duplicate various units, including ophiolites, which often causes difficulties in interpreting of the original structures of the CAOB and its evolution (Şengör and others, 2019a).

At present, various studies have different understandings of the age, role and nature of these strike-slip shear zones in CAOB. Strike slipping has not only caused the stacking of primitive magmatic arcs in the CAOB (Şengör and others, 1993; Şengör and Natal'in, 1996) but has also affected the large-scale rotation and translation between different cratons (plates) (Şengör and others, 1993; Allen and others, 1995; Şengör and Natal'in, 1996; Buslov and others, 2004a, 2004b; Yakubchuk, 2004; Natal'in and Şengör, 2005; Wang and others, 2007, 2010; Buslov, 2011). However, there are still many different interpretations of regional-scale strike-slip faults in the CAOB, such as kinematics, ages and tectonic settings (Buslov, 2011; Şengör and others, 2019a).

A series of late Paleozoic shear zones have been identified in the Tianshan Mountains in the western part of the southern CAOB, which have the same kinematics and ages (Shu and others, 1999; Laurent-Charvet and others, 2002, 2003; Wang and others, 2007, 2010; Charvet and others, 2011; Cai and others, 2012; He and others, 2021). Similar structures are also recognized on the southern margin of the "Silk Road arc" farther west (Natal'in and Şengör, 2005). However, there have been few related reports of coeval ductile shear zones in the Beishan and Alxa areas in the central CAOB. Although shear zones with similar kinematics occur along the northern margin of the North China Craton (NCC) (Wang and Wan, 2014; Zhao and others, 2015), the age is relatively young (Late Triassic) (Ma, 2009; Wang and Li, 2020). Do these shear zones along the southern CAOB belong to a large-scale transform system? How are they connected, what are their ages, and what tectonic setting do they represent? In addition, the Beishan-Alxa region are also the key region connecting the Tianshan to the west and the Xing'an-Mongolian orogenic belt to the east: however, there are few structural and geochronological data of ductile deformation from this region.

In addition, in the reconstruction of Pangea, Pangea A1 (Bullard and others, 1965), A2 (Van der Voo and French, 1974), Pangea B (Irving, 1977, 2004; Muttoni and others, 2003, 2009) and Pangea C (Smith and others, 1981) have been proposed according to paleomagnetic data. Pangea A1 is the typical Pangea reconstruction of Wegener, and Northwest Africa is connected to the eastern edge of North America, but there is basically no overlap between North and South America. Pangea A2 is similar to the classic Wegener Pangea reconstruction; northwestern Africa is connected with the eastern edge of North America, but North and South America overlap widely and occupy the position of the whole Gulf of Mexico. In Pangea B, the northwestern edge of South America is connected with the eastern edge of North America, while Northwest Africa is directly connected with southern Europe. Pangea C is similar to Pangea B, but the northwestern edge of South America is directly connected with southern Europe. There is no further work because the restoration of Pangea C is quite different from the geological evidence. At present, there are different views on whether Pangea B existed in the reconstruction process of the Pangea Supercontinent. The transition from Pangea B to A requires a nearly EW-trending dextral twist on the southern margin of the present Variscan orogenic belt (central Pangea Supercontinent), which is named the Intra-Pangean Megashear (Irving, 2004). However, some studies argued that the relatively

dextral movement was caused by oblique subduction of the ocean between Gondwana and Laurasia (Torsvik and others, 2012; Wu and others, 2021).

Since most of the above reconstruction studies were from the perspective of paleomagnetism, whether there was such a giant shear zone has always been in doubt, which is also the main basis for some scholars to oppose the existence of the Pangea B model (Domeier and others, 2012). However, an increasing number of studies have found a large amount of dextral transpression deformation at the end of the Paleozoic orogeny in the Variscan orogenic belt and confirmed the existence of a *ca.* 2500 to 3000 km dextral strike-slip along the shear zone constrained by displaced tectonic units such as the Galician-Castillian zone, the axial zone of the Variscan belt, or displaced granitic plutons (Arthaud and Matte, 1977; Gates and others, 1986; Shelley and Bossière, 2000; Matte, 2001; Franke and Żelaźniewicz, 2002; Natal'in and Şengör, 2005; Martínez Catalán, 2011; Şengör, 2013). These studies have mainly focused on the European part of the Pangea Supercontinent. In the eastern part of the supercontinent, the scissor-like closure of the Paleo-Asian Ocean from west to east occurred in the Tianshan region during 340–310 Ma (Han and others, 2016; Jourdon and others, 2017), the Beishan-Alxa region during 280–260 Ma (Mao and others, 2012; Liu and others, 2019; Zheng and others, 2020), and farther east in the Solonker Suture during 280–225 Ma (Eizenhöfer and others, 2014; Xiao and others, 2015; Liu and others, 2017), and then the convergence of the NCC and Siberian Craton, as well as the Mongolian terranes between them, was completed. It is not clear whether the dextral displacement of nearly 3000 km between the Gondwana continent in the south and Laurasia continent in the north affected the CAOB in the east, how the deformation behaved in this period, and how it transformed eastward into other structures. Moreover, the dextral shearing in the eastern CAOB may be key evidence for the existence of Pangea B and the Intra-Pangean Megashear, but its distribution, age, and displacement are unknown.

In this study, structural data of ductile dextral shearing in the central and eastern-most CAOB are reported, their ages and displacements are also constrained, and the tectonic setting in which dextral shearing occurred is discussed. Combined with data from the western CAOB and Variscan Orogenic Belt, an intracontinental transform system which cut through the Kazakhstan oroclinal-bending structure to the west and may continue to extend westward along the southern Variscan orogenic belt in Europe even to the South Appalachian orogenic belt in North America, forming a mega-shear system in the core of the Pangea Supercontinent, is proposed.

#### GEOLOGICAL SETTING

The CAOB, mainly located between the Baltic, Siberia, Tarim and North China cratons, is one of the world's largest Phanerozoic accretionary orogens (Şengör and others, 1993; Windley and others, 2007; Xiao and others, 2015). Scholars have various understandings of the "Central Asian orogenic belt" and have proposed different names. The most influential ones are the "Central Asian fold belt" (Khain and others, 2002), "Altaids" (Şengör and Natal'in, 1996; Şengör and others, 2018) and "Central Asian Orogenic Belt" (CAOB) (Jahn and others, 2000). Among them, CAOB is widely accepted by the majority of scholars, and the abbreviation CAOB is also adopted in this paper. The orogenic belt has undergone a long-lasting evolution from the Neoproterozoic (~1020 Ma) to the early Mesozoic (Windley and others, 2007). It is the product of long-term subduction of the Paleo-Asian Ocean and is composed of a large number of accretionary complexes, arcs, arc-related basins, ophiolites, seamounts and continental fragments (Windley and others, 2007). Large-scale ductile shear zones, thrust structures, block rotation, oroclinal bending, and later intracontinental superimposition are important features of the CAOB (Şengör and Natal'in, 1996; Zhang and Cunningham, 2012; Li and others, 2015, 2021; Xiao and others, 2015, 2018; Şengör and others, 2018; Jiang and others, 2019; Zhang and others,

2021f). The ophiolites in the CAOBS are generally younger from north to south, indicating that the orogenic belt grew gradually from north to south (Xiao and others, 2003). Most ophiolites in the western CAOBS formed from the Ordovician to Devonian and are preserved in a vast area to the north of the Tarim Craton. The ophiolites in the eastern orogenic belt were mainly formed in the Carboniferous-Permian/Triassic. The western CAOBS in China is called Tianshan, which is divided into North Tianshan, Central Tianshan and South Tianshan and connected with the Beishan orogenic belt eastward; the eastern part of the orogenic belt is traditionally called the Xing'an-Mongolian orogenic belt (Liu and others, 2017), and the Xing'an-Mongolian orogenic belt is connected with Beishan through the northern margin of the Alxa Block.

The Beishan is located between the East Tianshan and Alxa Block (fig. 1). Previous studies suggested that it was the convergence position between the Tarim Craton and the Kazakhstan Plate (Zuo and He, 1990; Zuo and others, 1990). Several ophiolitic mélanges developed in this orogenic belt, but the formation time and mechanisms of these mélanges are in dispute (Zuo and He, 1990; Zuo and others, 1990; Xiao and others, 2010; Mao and others, 2012; Yu and others, 2016; Xin and others, 2020; Gao and others, 2022). For example, Mao and others (2012) argued that the late Paleozoic Liuyuan complex is an SSZ-type ophiolite formed in a forearc environment. However, other authors have suggested that it was the product of a "Red Sea-type" rift zone (Gao and others, 2022). Similarly, Xiao and others (2010) suggested that the Yueyashan-Xichangjing ophiolitic mélange was formed in a back-arc basin, which, however, Yu and others (2016) argued formed in a middle ocean ridge.

To the east of the Beishan is the Alxa Block (fig. 1). It is traditionally considered to be a Precambrian block and is assigned to a part of the NCC (Huang, 1945; Zhao and others, 2005); however, some studies have argued that it may have been an independent block in the early Paleozoic (Zhang and others, 2015a, 2016). The Alxa Block ranges from the Engeer Us ophiolite belt in the north to the northern edge of the Hexi Corridor in the south (Huang, 1945). Precambrian rocks in the Alxa Block are mainly exposed in the area of Longshoushan-Beidashan-Bayanwulashan-Langshan along the southern and eastern margins, while the early-middle Permian granitic rocks are exposed in the northern Alxa Block, most of which are distributed in a nearly EW direction. Recent studies have indicated that the northern boundary of the Alxa Block is the Chaganchulu ophiolite belt (Zhang and others, 2015b; Zheng and others, 2018) instead of the Engeer Us ophiolite belt (Zheng and others, 2014). Previous studies have shown that in the Early Permian, the northern margin of Alxa was an active continental margin upon which voluminous plutons and volcanic rocks occurred in a post collisional environment (Zhang and others, 2015b; Ye and others, 2016). Recent studies have also shown that the Alxa Block is not an intact block but is divided by multiple ophiolite belts or ductile shear zones (Zhang and others, 2013, 2014, 2021a, 2021b; Zheng and others, 2014, 2018; Zhao and others, 2022). During the closing of the Paleo-Asian Ocean and subsequent intracontinental evolution, a large number of Mesozoic basins developed in the orogenic belt (Graham and others, 2001). At the same time, multiple stages of compression and extension activities and intracontinental ductile strike-slip shear zones/faults developed in the Alxa Block, forming many Mesozoic basins, such as the Chaoshui, Yingen-Ejina, and Yabulai basins (Heumann and others, 2014; Zhang and others, 2021f).

#### METHODS

In this contribution, previous data of various shear zones in different segments of the CAOBS were collected, in which the structural and geochronological data are the focus (figs. 1, 2; table 1). In addition, because the structural studies are not equal along the whole CAOBS, especially its eastern part, we also performed structural mapping,



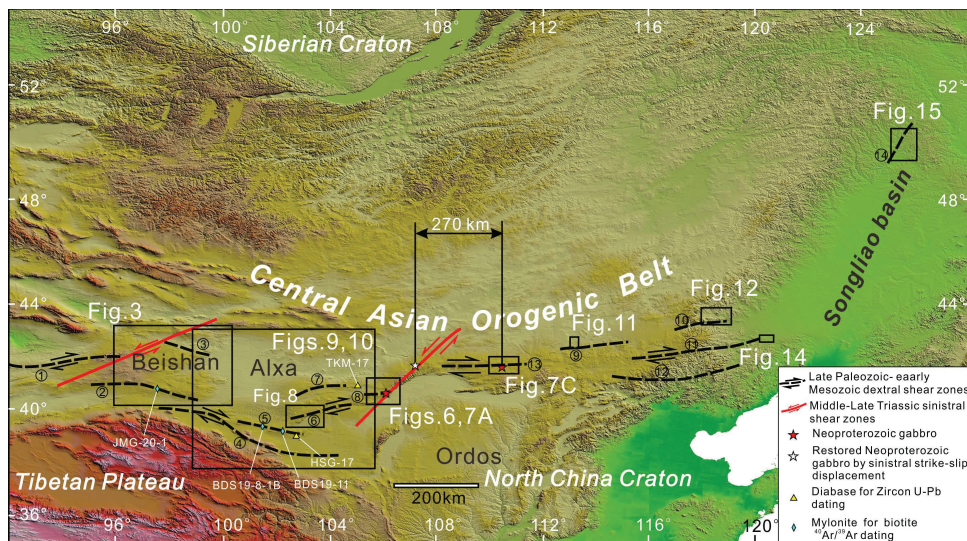


Fig. 2. Shear zones in eastern CAOB, their index numbers used in table 1, and sample locations dated in this study.

analysis, and age dating on some shear zones in the eastern CAOB to constrain the ages of the abovementioned ductile deformations. We tested a total of five samples including  $^{40}\text{Ar}/^{39}\text{Ar}$  dating on three samples from the Beidashan shear zone in the Alxa Block and the Jinmiaogou shear zone in the Beishan, and zircon U–Pb dating on two samples and dikes (Tukemu diorite dike in the northeast and Hongshagang diabase in the southwest) intruding the Paleozoic granites in the Alxa Block (fig. 2). Detailed information about the sample locations, geological mapping, dating methods and results are described in detail in the Supplementary Data, and the interpretation of field data and its potential problems are also included in it.

#### DISTRIBUTION OF SHEAR ZONES

The distribution of the late Paleozoic ductile shear zones in the southern CAOB can be traced from the Tianshan in the west to the Greater Xing'anling in the east (figs. 1, 2; table 1). Our main work is concentrated to the east of the Beishan (fig. 2; table 1). The shear zones are introduced from west to east. As many studies have reported many datasets on the distributions, ages, orientations, kinematics and displacements of shear zones in the Tianshan in the west (Shu and others, 1999; Laurent-Charvet and others, 2002, 2003; Chen and others, 2005; Wang and others, 2010; Cai and others, 2012; Liu and others, 2022), this study will not introduce them in detail.

#### Central CAOB

*Beishan.*—Eight late Paleozoic ductile dextral shear zones with unknown displacements have been reported in the Beishan and Dunhuang Blocks to the south (fig. 3; Zuo and Zheng, 1991; Zhang and Cunningham, 2012; Gao and others, 2016; Feng and others, 2020). Among them, there are three large-scale shear zones in southern, central, and northern Beishan. The southern zone is the Baidunzi-Xiaoxigong ductile shear zone (Chen and others, 2007), the Gongpoquan shear zone developed in the central zone and the Sangejing-Gonglujing shear zones are in the northern zone (Gao and

TABLE 1  
Main features of shear zones in the eastern CAOB

Shear zone name	Location	Latitude (N)	Longitude (E)	Length (km)	Width (km)	Strike	Displacement (km)	Shear sense indicators	Age (Ma)	Methods	Source	Index in fig. 2
North Tianshan shear zone	Tianshan Orogen	43.0°-46.06°	80.83°-87.6°	-600	No data	WNW-ESE	No data	Macroscopic scale: Microscopic scale: S-C fabrics, quartz c-fabrics; asymmetrical porphyroclasts	285-255	<sup>40</sup> Ar/ <sup>39</sup> Ar of Whole rocks, Mus. And Bt.; Zircon U-Pb	de Jong and others, 2009; Shu and others, 1999;	
Main Tianshan shear zone	Tianshan Orogen	41.51°-42.8°	87.63°-95.25°	-650 -700	25-75	EW	125-375*	Macroscopic scale: asymmetrical synkinematic plutons. Microscopic scale: S-C fabrics, quartz c-fabrics; asymmetrical porphyroclasts	~280-250	<sup>40</sup> Ar/ <sup>39</sup> Ar of Whole rocks, Hbl, Mus. And Bt.; Zircon U-Pb	Shu and others, 1999; Laurent-Charvet and others, 2003; Chen and others, 2005 Cai and others, 2012; Wang and others, 2008, 2014; Hu and others, 2021; Li and others, 2020, 2021	1
Baidunzi-Xiaoxigou shear zone	Beishan Orogen	40.32°-41.07°	94.52°-98.60°	-350	8-15	WNW-ESE	40-75*	Macroscopic scale: asymmetrical synkinematic plutons and folds. Microscopic scale: S-C fabrics, asymmetrical porphyroclasts	~250	<sup>40</sup> Ar/ <sup>39</sup> Ar of Hbl. Mus.; Zircon U-Pb	Ding and others, 2019	2
Sangcijing-Gonglujin shear zone	Beishan Orogen	41.8°-42.71°	95.61°-99.6°	-300 -350	2-8	WNW-ESE	10-40*	Macroscopic scale: asymmetrical folds and lens; NW-SE trending dyke swarms. Microscopic scale: S-C fabrics, mica fish, asymmetrical porphyroclasts	300-230	Zircon U-Pb	Gao and others, 2016	3
Southern Alxa shear zone	southern Alxa	38.39°-40.14°	97.33°-102.7°	-500	1.5-2	NW-S E	40-50	Macroscopic scale: sheath folds asymmetrical folds and displaced granites. Microscopic scale: S-C fabrics, mica fish, asymmetrical porphyroclasts	269-240	<sup>40</sup> Ar/ <sup>39</sup> Ar of Mus. Bt; Zircon U-Pb	Zhang and others, 2021	4
Beidashan shear zone	central Alxa	39.13°-39.57°	101.05°-102.63°	-120 -145	0.5-1	ENE-WSW	2.5-5*	Macroscopic scale: asymmetric folds. Microscopic scale: S-C fabrics, mica fish, asymmetrical porphyroclasts	274-264	<sup>40</sup> Ar/ <sup>39</sup> Ar of Bt.	This study	5
Yabrai shear zone	central Alxa	39.67°-40.22°	102.8°-104.8°	-150 -180	2-3	ENE-WSW	21-30	Macroscopic scale: sheared pluton. Microscopic scale: S-C fabrics, quartz c-fabrics; asymmetrical porphyroclasts	270-250	<sup>40</sup> Ar/ <sup>39</sup> Ar of Mus.; Zircon U-Pb	Zhao and others, 2022	6

In this study, most shear zones reported to the east of Beishan have gradual boundaries, only several of them were cut by later faults, however, the faults are mainly developed in the interior of the shear zones. The width we employed is a lower limit if discrete faults or later faults occurred along the shear zones, because these later faults are mainly thrust faults.

\* calculated by shear strain of 5 as a lower limit (Ramsay and Graham, 1970; Simpson, 1983; Fossen and Cavalcante, 2017).

TABLE 1  
(continued)

Shear zone name	Location	Latitude (N)	Longitude (E)	Length (km)	Width (km)	Strike	Displacement (km)	Shear sense indicators	Age (Ma)	Methods	Source	Index in fig. 2
Aergashun shear zone	central Alxa	40.61°-40.87°	103.04°-104.9°	~160-180	0.15-2	ENE-W SW	0.75-1.0*	Macroscopic scale: regional asymmetrical folds. Microscopic scale: S-C fabrics and asymmetrical porphyroclasts	264-257	Zircon U-Pb	Guan, ms, 2010	7
Langshan shear zone	eastern Alxa	40.5°-40.7°	105.4°-106.35°	>80-90	0.3-2	EW	45-82	Macroscopic scale: sheared pluton, asymmetrical folds. Microscopic scale: S-C fabrics and $\delta$ -type feldspar porphyroclasts	274-249	Zircon U-Pb	Zhang and others, 2022; Tian and others, 2020	8
Ondor Sum shear zone	eastern CAOB	42.23°-42.46°	112.47°-114.20°	>140	18-22	EW	~102-104	Macroscopic scale: regional asymmetrical folds. Microscopic scale: S-C fabrics	241±19	<sup>40</sup> Ar/ <sup>39</sup> Ar of Mus.	Zhang and others, 2018	9
Xar Moon shear zone	eastern CAOB	42.9°-43.3°	117.2°-118.5°	>120	3-10	EW	15-50*	Macroscopic scale: regional asymmetrical folds. Microscopic scale: S-C fabrics; asymmetric $\sigma$ -type feldspar	227-209	<sup>40</sup> Ar/ <sup>39</sup> Ar of Mus.	Zhao and others, 2015	10
Chifeng shear zone	northern NCC	41.81°-42.66°	114.18°-119.37°	~400-440	8-20	ENE-W SW	40-100*	Macroscopic scale: synkinematic granitic dikes. Microscopic scale: S-C fabrics; asymmetric porphyroclasts; bookshelf, mica fish	227-219	Ar/Ar of Mus. Zircon U-Pb	Wang and Li, 2020	11
Fengning-Longhua shear zone	northern NCC	41.03°-41.53°	114.85°-118.08°	~280-300	0.5-3	ENE-W SW	2.5-15*	Macroscopic scale: shear folds. Microscopic scale: imbrication, mica fish, S-C fabric, and pressure shadows.	255-234	<sup>40</sup> Ar/ <sup>39</sup> Ar of Mus.	Wang and others, 2013; Wan and Wang, 2014	12
Guyang-Wuchuan shear zone	northern NCC	40.89°-41.25°	109.32°-111.28°	>170	~5-30	EW	~270	Macroscopic scale: dextral duplex, imbrication of lens. Microscopic scale: S-C fabric, and mica fish.	253-247	K/Ar of Sericite	Zhang and others, 1999	13
Keluo shear zone	Great Xing'an Mountain	49.26°-50.25°	125.53°-126.58°	>100-130	10-20	NNE-S SW	50-100*	Macroscopic scale: shear folds. Microscopic scale: mica fish, S-C fabric, and asymmetric porphyroclasts	~216±3M <sub>a</sub>	Zircon U-Pb	Miao and others, 2003; Zhao and others, 2017	14

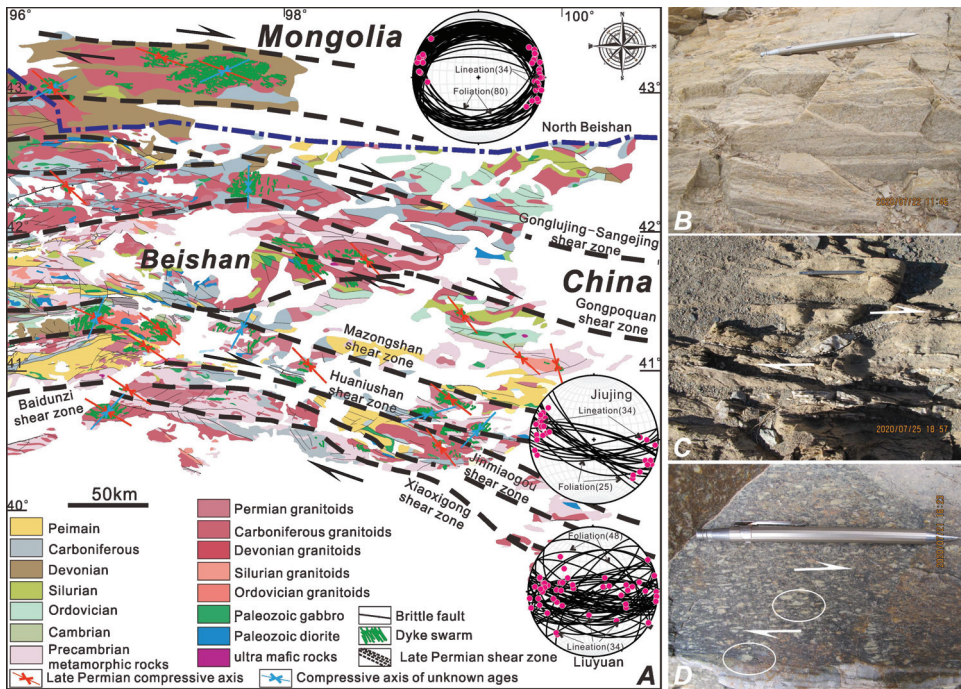


Fig. 3. Distribution of the late Paleozoic shear zones in Beishan region. A. Geological map and stereographic projection of foliations and lineation of main shear zones. B. Felsic mylonite and quartz stretching lineation in the Xiaoxigong shear zone. C. Mylonite and asymmetrical structures of felsic veins in the Baidunzi shear zone, indicating dextral shearing. D. Granitic mylonite and  $\sigma$ -type quartz porphyroblasts in the Jinmiaogou shear zone, indicating dextral shear.

others, 2016). These shear zones are connected westward with the Gubaoquan-Hongliuyuan and southern and northern marginal shear zones of central Tianshan, respectively (Cai and others, 2012). Due to the coverage by Quaternary deserts, the extension of these shear zones to the east is unknown, and there has been no specific study either. However, aeromagnetic data show that the Sangejing-Gonglujing shear zones extend eastward to the Yagan area to the north of the Alxa Block (Zhao and others, 2022), where the latest mapping found a late Paleozoic shear zone in this area (Cui and others, 2019). The Gongpoquan-Hongliuyuan shear zone in the central zone may extend to the north of Zongnaishan in the Alxa Block, but there have been no further studies on the shear zone. The Baidunzi-Xiaoxigong ductile shear zone in the southern zone may be connected with the Alxa shear system, as indicated by aeromagnetic data (Xiong, 2019).

The Baidunzi-Xiaoxigong shear zone is located in the southernmost Beishan (fig. 3), close to the northern margin of the Dunhuang Block. The rocks involved include Precambrian medium- to high-grade metamorphic rocks, lower Paleozoic medium- to low-grade metamorphic rocks and late Paleozoic granites. The shear zone is very obvious in satellite images featuring well-developed S-C fabrics at the map scale, with an outcrop length of 160 km and a width of 5–8 km. The shear zone is composed of wavy bands of light-colored ductile-sheared clastic rocks “interbedded” with black bands of basalts. The foliations are distributed around circular or oval granites and often merge at diagonal corners of granite bodies in map view, showing characteristics similar to the asymmetrically rotated porphyroblast systems under the microscope. Generally, the shear zone is nearly EW-trending, but the western segment (Baidunzi-Panjiaying section) is NE-

trending, and the eastern segment (Xijianquan-Xiaoxigong section) is NW-trending (fig. 3). In the shear zone, felsic mylonite, coarse mylonite, mylonite and ultramylonite are developed. The foliations and lineations in the shear zone are well developed. The mylonite foliation is nearly EW-trending with steep dip angles ( $60^{\circ}$ – $85^{\circ}$ ) (fig. 3). Since the strike of the shear zone is not consistent, the rake is relatively large in the western shear zone and nearly horizontal in the near east–west-trending part. A previous study (Chen and others, 2007) and our field observations found a large number of shear indicators (fig. 3C, D), which indicate dextral shearing of this shear zone.

At present, there are few age constraints for the shear zone, and most previous studies have indicated that the shear zone developed in the late early Paleozoic to Permian (Zuo and Zheng, 1991; Chen and others, 2007). The sericite  $^{40}\text{Ar}/^{39}\text{Ar}$  dating of the shear zone was also performed, whose plateau age is *ca.* 250 Ma (Ding, 2021).

The Sangejing-Gonglujing ductile shear zone is located between the Mingshui Block and the Paleozoic Gongpoquan island arc (fig. 3). It is generally nearly EW-trending, with a width of 1.5–8 km and a regional extension of more than 300 km (Gao and others, 2016). The rocks involved in the shear zone include early Silurian quartz diorite and metamorphic rocks of the Beishan Group (Proterozoic). It is mainly composed of granitic mylonite and mylonitized quartzite. The mylonitic foliation is nearly EW-trending, which is consistent with the overall extension direction of the ductile shear zone in the Beishan area, with a dip angle of  $30^{\circ}$  to  $50^{\circ}$ . The trend of lineation is generally close to east–west (fig. 3A). S-C fabric/asymmetric small folds all indicate dextral shearing, and the age is constrained between 300 Ma and 230 Ma (Gao and others, 2016).

There are abundant Paleozoic acid, medium, and basic dike swarms in the Beishan. The development of dike swarms was related to many environments, such as mantle plumes, regional extension, and regional strike slipping (Dewey, 2002). Dike swarms are often used for reconstruction of paleocontinent and regional tectonic environments and inversion of regional tectonic stress fields (Dewey, 2002; Şengör, 2013). The dike swarms in the Beishan are generally distributed in nearly NW-SE and NE-SW directions (figs. 4, 5). The occurrence of most dikes is nearly vertical. The exposed widths of single dikes range from 10 cm to several meters, and lengths range from several meters to tens of kilometers. In the Beishan, the strike of basic dikes is mainly nearly north–south or northwest, while that of intermediate acidic dikes is mainly northwest or nearly east–west. Generally, the dike swarms mainly intruded into Paleozoic granodiorite, quartz diorite and Permian strata. Many geochronological and geochemical studies have been carried out in the Beishan; diabase dikes were formed in the Late Carboniferous-Early Permian, while quartz diorite dikes were generally formed in the Mid-Late Permian (Zhang and others, 2015c, 2017; Zheng and others, 2020). We chose the area north of the Yingao valley in the central Beishan for mapping (fig. 4A). Previous work in this area constrained the ages of dikes and surrounding rocks (fig. 4, Zheng and others, 2020). Two types of dikes occur in the Yingao valley granite ( $\sim$ 280 Ma, Zheng and others, 2020): Group I dikes (267 Ma) are calc-alkaline gabbros trending NW (fig. 4A); and Group II dikes are high-Mg diorites trending NE-SW (fig. 4A). Both mapping and field observations show that Group II was cut by Group I (fig. 4A).

The NW-SE-trending dikes in the Beishan area are the youngest dikes found at present, while the former intermediate dikes (doleritic dikes) were mostly formed in a subduction environment (Zhang and others, 2017; Zheng and others, 2020) or in a slab break-off scenario (Zhang and others, 2015c). However, many basic dikes are considered to have formed in an intraplate extensional environment (Peng and others, 2020). The NW-SE-trending dikes in figure 4A were likely derived from an E-MORB-like source mainly metasomatized by subduction-related fluids. NE-SW-trending dikes were likely derived from interactions between melts of subducted sediments and overlying mantle peridotites (Zheng and others, 2020).

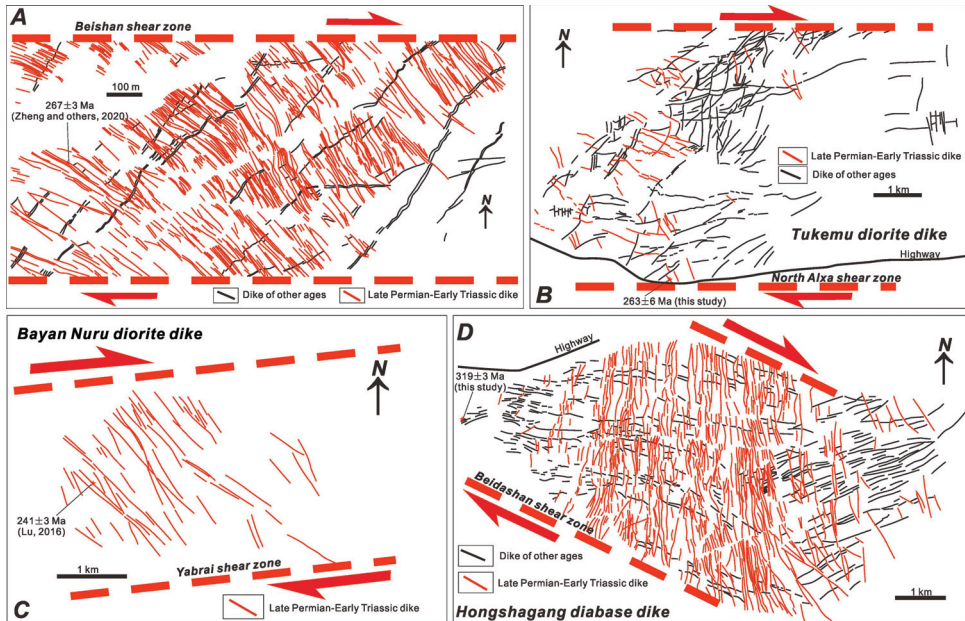


Fig. 4. Dike swarms in the Beishan-Alxa region. A. Northern Yingao Valley in the Beishan. B. Tukemu in the northeastern Alxa. C. Bayan Nuru in the central Alxa. D. Hongshagang in the southern Alxa. See figs. 2 and 5 for locations of dikes.

There are Jinmiaogou and Mazongshan dextral shear zones in the northern and southern parts of the mapping area (fig. 3). These two shear zones are thought to have developed in the late Paleozoic (Zuo and Zheng, 1991), and  $^{40}\text{Ar}/^{39}\text{Ar}$  dating of the Jinmiaogou ductile shear zone in the Jiujing area shows that the shear zone is *ca.* 258 Ma (table S1; fig. S1, see Supplementary Data for details). The ages of the shear zones

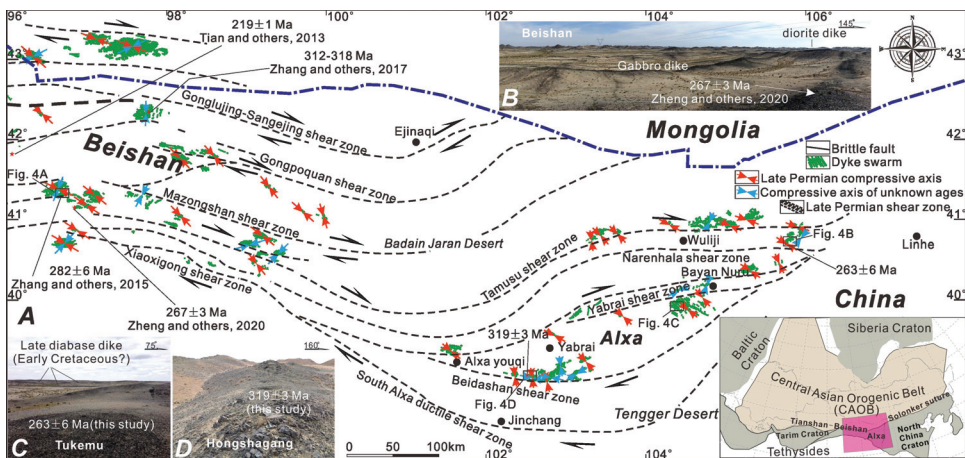


Fig. 5. Dike swarms, ductile shear zones in Beishan-Alxa region with local stress field directions causing the development of dike swarms (locations of shear zones are based on fig. 3 and later discussion). A. Two sets of dikes to the north of Yinao Valley in the Beishan. B. Northwest-trending diorite dikes in Tukemu region. C. Nearly east-west-trending dikes of intermediate-acid rocks in Hongshagang region in the southern Alxa.

in the mapping area are later than the emplacement age of the NW-trending dike swarms. Considering the different isotopic closure temperatures, the formation ages of the shear zones and the NW-trending dike swarms are consistent. Because the shear zones on the northern and southern sides are both dextral strike slip, the NW-trending dike swarms in the mapping area are only in the direction of the extensional structures in the shear zone. In the Beishan, there are many NW-trending dike swarms, which are distributed between the dextral shear zones without exception (fig. 5). Recently, the ages of dike swarms in the central Beishan were reported, and the latest NW-trending acidic dike swarms were emplaced at approximately 260 Ma (Qi and others, 2016). Combined with regional data, Qi and others (2016) also argued that the Beishan underwent regional extension during 260–255 Ma, which was probably the induced “T-type” extension caused by the dextral shearing of east west-trending shear zones across the entire Beishan region reported by Zuo and Zheng (1991) (fig. 5).

*Langshan.*—The NE-SW-trending Langshan is located in the northeastern Alxa Block, which is mainly composed of the Meso-Neoproterozoic Langshan Group, Paleoproterozoic metamorphic basement rocks and late Paleozoic intrusive rocks (fig. 6). The shear zone is dextral and separates the late Paleozoic granite to the south and the Langshan Group to the north (fig. 6; Zhang and others, 2021a, 2022). Our previous work determined that the age of the shear zone is between 270 and 250 Ma (Tian and others, 2020). Quartz in granitic mylonite shows strongly undulated extinction and dynamic recrystallization, and quartz-stretching lineation is developed. S-C fabric and  $\sigma$ -type K-feldspar porphyroblasts indicate dextral shearing. The thickness of the shear zone changes from tens of meters to 300 meters along the strike, and the steeply well-developed mylonitic foliations strike east-west. The zircon U-Pb ages of coarse-grained biotite granites in this area are approximately 270–260 Ma.

To the west, a series of small Permian granite bodies are exposed along the shear zone (fig. 7; Hui and others, 2021; Zhang and others, 2021a, 2022). They were sheared by the shear zone. These rocks are connected with the same Permian granite batholith to the southwest. The displacement of the shear zone can be calculated by using the western intrusive boundaries between Permian granites and the Neoproterozoic Langshan Group on two sides of the shear zone as markers (fig. 7). General calculations show that the dextral displacement was 45 to 82 km (fig. 7).

Similar to the Beishan, a series of intermediate-acidic dike swarms are also distributed in the Yingen and Tukemu areas to the west of Langshan (figs. 4B, 5). The dikes in the Yingen area mainly strike northwest-southeast, and dikes in the Tukemu area to the east of the Yingen area have both NW-SE and NE-SW strikes, and some dikes are even folded (fig. 4B). Among them, the NW-SE-trending diorite dikes cut the NE-SW- or nearly EW-trending granite porphyry dikes (figs. 4B, 5B). The NW-trending diorite dikes, with widths of 10–15 m and lengths of several meters to several hundred meters, are straight along the strike, and these dikes intruded into the late Paleozoic granite ( $294 \pm 2$  Ma, Zhang, ms, 2013). Zircon U-Pb dating of these NW-SE-trending diorite dikes indicates  $263 \pm 6$  Ma (table S2; fig. S2). This age is consistent with the activity time of the nearly EW-trending dextral ductile shear zone in the Langshan area, 270–250 Ma (Tian and others, 2020). Moreover, the development of NW-SE dikes is consistent with the distribution of extensional structures caused by E-W ductile shear. The late Paleozoic NW-SE-trending dikes in the Yingen and Tukemu areas may be derived structures caused by the EW ductile shears in northern Alxa (fig. 5).

*Yabrai region.*—The Yabrai Mountains are located in the middle of the Alxa Block. The mountains are divided into the South Yabrai and North Yabrai mountains, which are separated by the nearly east-west-trending Yabrai dextral shear zone (fig. 8). The lithology of the Yabrai Mountains is mainly Permian granite (286–272 Ma), monzogranite, syenogranite, gabbro, *etc.* (fig. 8; Ye and others, 2016). Mid-Late Jurassic-Early

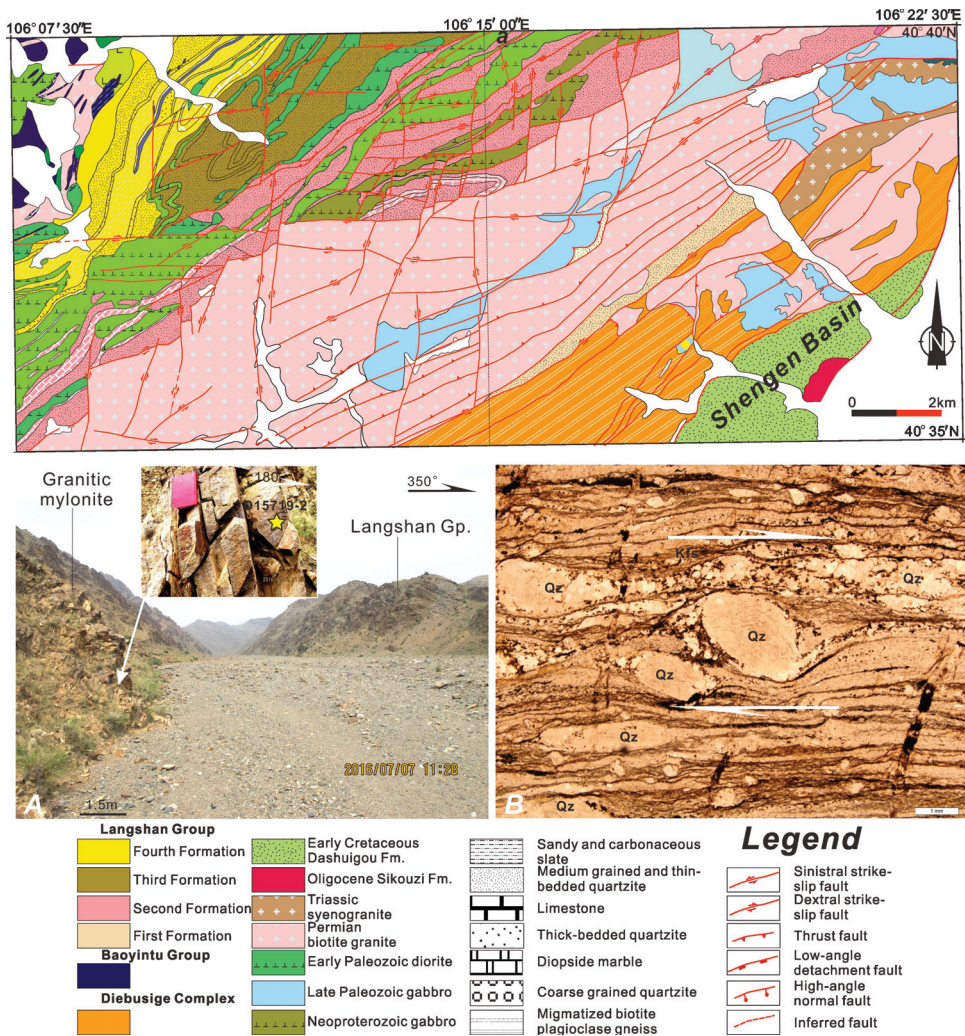


Fig. 6. Geological Map of the Langshan region. A. Geological map. B. Boundary between nearly east-west trending granitic mylonite and Meso-Neoproterozoic Langshan Group. C. Granitic mylonite and quartz stretching lineations. D.  $\delta$ -type feldspar porphyroclast in the XZ plane, indicating dextral shearing. Pl-Plagioclase, Qz-Quartz, Ms-Muscovite, Kfs-K-feldspar (same below).

Cretaceous continental sediments are exposed in the southwest and cover the Permian granite with a nonconformity (fig. 8). The mountain range and the Early-Middle Permian granites in the Bayan Nuru area in the east form a nearly EW-trending continental margin arc (Zhang and others, 2015b).

The NEE-trending Yabrai shear zone is exposed along the eastern edge of Badain Jaran Desert, and extends for more than 60 km in a direction of 75° (fig. 8). The width of the shear zone is approximately 200–1000 m. The foliation is nearly vertical with quartz-stretching lineation. In some parts, a dark stretching enclave lineation is developed, and the rotation plunges to WSW, with a pitch angle less than 10° (fig. 8B). The  $\sigma$ -type rotational porphyroblasts, S-C fabric, bookshelf of K-feldspar and mica fish indicate nearly horizontal dextral shearing (fig. 8). Far from the main shear zone, diffused NNE-trending weakly foliated granitic gneiss is developed in the North

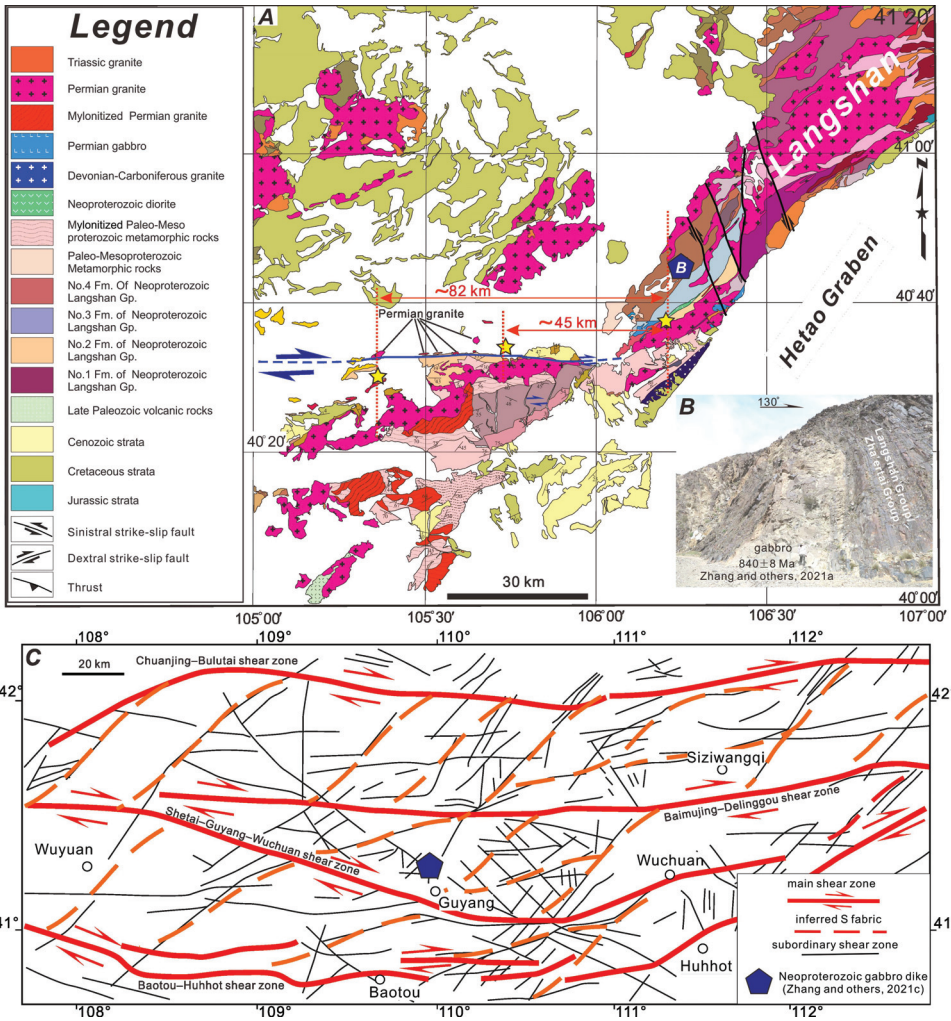


Fig. 7. Dextral shear zones in the northeastern Alxa and northern North China Craton (NCC). A. Displacement of EW-trending shear zone in Langshan. B. Neoproterozoic gabbro dike parallel to the bedding of the Langshan Group/Zha'ertai Group in Langshan. C. EW-trending shear zones in the northern NCC and location of Neoproterozoic gabbro dike parallel to the bedding of the Langshan Group/Zha'ertai Group in Guyang (modified from Zhang and others, 1999; See fig. 2 for location of C).

Yabrai Mountains. These foliations extend southward and were cut by the ENE-trending main shear zone. The NNE-trending foliations may be magmatic fabrics formed during the syn-tectonic emplacement of plutons (Zhao and others, 2022). There are no foliations to the south of the main shear zone.

Since the Yabrai shear zone cuts the Permian granite (272 Ma), the shear zone was formed after 272 Ma. Zhao and others (2022) performed  $^{40}\text{Ar}/^{39}\text{Ar}$  dating of the shear zone, in which the muscovite plateau age is 254–251 Ma, and argued that the age of the Yabrai shear zone is approximately 250 Ma. The age of the Yabrai shear zone is therefore consistent with that of the Langshan shear zone (that is, 270–250 Ma, Tian and others, 2020).

A set of NW-SE-trending diorite porphyrite dikes and gabbro dikes were developed in the early Permian biotite monzogranite (Lu, ms, 2016,  $277 \pm 1$  Ma) approximately 60

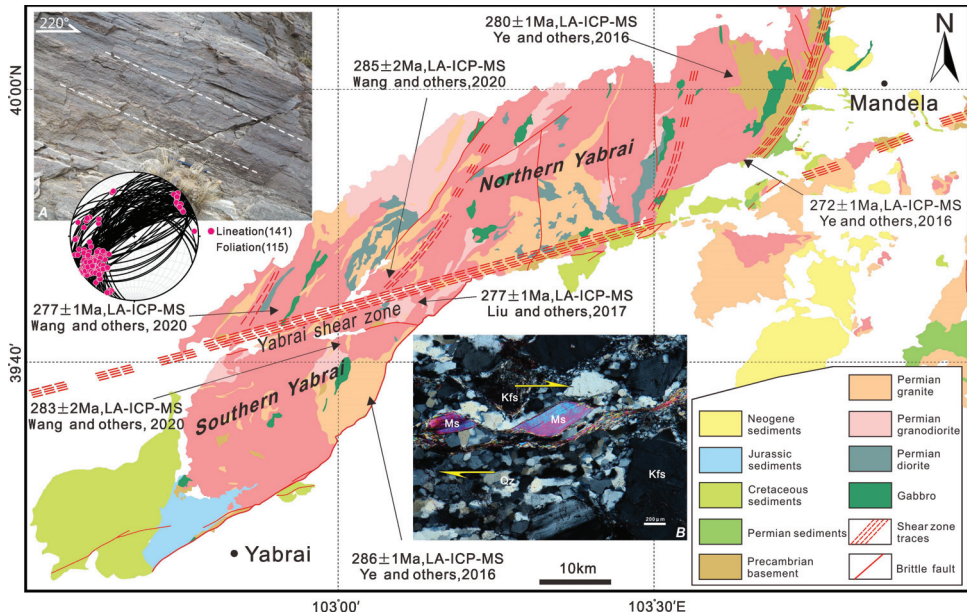


Fig. 8. Geological map of Yabrai region. A. Geological map. B. Granitic mylonite, quartz stretching lineation and their stereographic projection. C. Mica fish indicating dextral shearing.

km south of the Yabrai shear zone (figs. 3C, 4). The dikes extend far and vary in length. The visible length ranges from 200 m to 1000 m, and the width ranges from 0.4 m to 6 m. The dikes are nearly vertical. A previous study showed that these dikes were formed in an intraplate environment with an age of  $241 \pm 3$  Ma (Lu, ms, 2016). The age of these dikes is almost the same as that of the Yabrai shear zone in the north, and the strike of the dikes intersects the shear zone at a large angle ( $40\text{--}45^\circ$ ) (figs. 4C, 5), they are likely extensional structures derived from dextral shearing. The sheared late Paleozoic Mandela pluton indicates that the dextral displacement was 21 to 30 km (Zhao and others, 2022; fig. 9G).

*Beidashan and Longshoushan.*—The late Paleozoic Beidashan dextral shear zone with unknown displacement is mainly distributed along the northern and southern margins of the Beidashan in the central Alxa Block (fig. 9). Some scholars discovered a new Tebai ophiolite (mélange) associated with the subduction of the Paleo-Asian Ocean on the northern side of the Beidashan and suggested that it can be connected with the Chaganchulu ophiolite (mélange) on the northern margin of the Alxa Block on the northeastern side, representing the final subduction and extinction of the Paleo-Asian Ocean (Zheng and others, 2018).

Our field investigation shows that the northern Beidashan shear zone trends nearly NW-SE, with a width of 0.5–1 km and an exposed length of more than 10 km. In the shear zone, felsic mylonite is developed, and the protoliths include Precambrian mica quartz schist and late Paleozoic granite ( $327\text{--}324$  Ma, Gong and others, 2018). Asymmetric folds and S-C fabric all indicate dextral shearing. Biotite from two mylonite samples yielded two plateau ages of  $264.7 \pm 2$  Ma (BDS19-11) and  $274.7 \pm 2$  Ma (BDS19-8-1b) (table S1; fig. S1). Microscopically, quartz shows undulate extinction and bulging (BLG), indicating that the deformation temperature was  $300\text{--}400^\circ\text{C}$  (Passchier and Trouw, 2005), while the closure temperature of biotite was  $300 \pm 50^\circ\text{C}$  (McDougall and Harrison, 1999). Therefore, the age of the Beidashan shear zone is between 274 and 264 Ma.

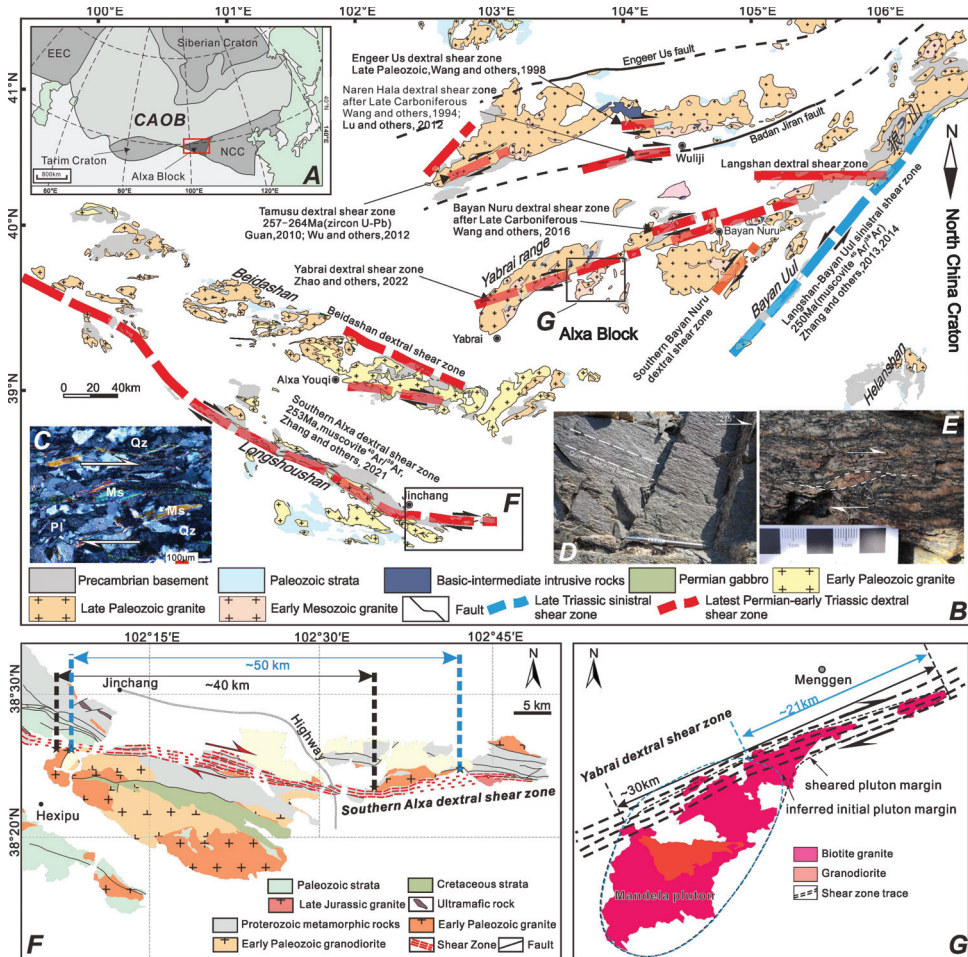


Fig. 9. Distribution of shear zones in Alxa region. A. Tectonic location of Alxa region in the CAOB. B. Locations of shear zones of different ages in Alxa. C. Mica fish indicating dextral shearing (Southern Alxa dextral shear zone). D. Quartz stretching lineation (Southern Alxa dextral shear zone). E. “σ” type porphyroclast of K-feldspar indicating dextral shearing. F. Measurement of dextral displacement of Southern Alxa dextral shear zone. G. Measurement of dextral displacement of Yabrai dextral shear zone (sheared Mandela pluton).

There are two sets of dike swarms in the Hongshagang area on the southern side of the Beidashan shear zone (figs. 4D, 5). Among them, the most developed dikes belong to the diabase dike set, which trends nearly north–south. A single dike is 0.5–3 m in width, 30 m in maximum width, more than 100 m to several km in length, and the longest is more than 10 km. The second set is composed of granite porphyry dikes (fig. 5C), whose main strike is nearly east–west. A single dike is 0.2–3 m in width, more than 10 m in maximum width, and 100 m in length, and several kilometers in some cases. The zircon U–Pb dating on these north–south dikes in this study showed wide concordant  $^{206}\text{Pb}/^{238}\text{U}$  ages ranging from  $2456 \pm 26$  Ma to  $231 \pm 3$  Ma, six of which are concentrated with a weighted mean age of  $318.9 \pm 3.5$  Ma ( $2\sigma$ ) (MSWD = 1.2) (table S2; fig. S2, see Supplementary Data for details).

Both sets of dikes intruded into early Paleozoic gneissic granite (408 Ma, Zhou and others, 2016) and late Paleozoic granite. The north–south-trending diabase dikes

cut the nearly east–west-trending granite porphyry dikes (fig. 4D). The zircon U–Pb dating of these east–west dikes in this study showed that the zircon composition of the dike is complex, and there are many captured zircons from the country rocks (Hoskin and Schaltegger, 2003; table S2; fig. S2, see Supplementary Data for details). The weighted average age of the youngest zircon is  $318.9 \pm 3.5$  Ma, which may represent the emplacement age of the nearly EW-trending dikes. The age of the NS-trending diabase dikes cutting the EW-trending dikes should be younger. Although there is no further test on the age of the NS-trending dikes, considering that the intersection angle between the NS-trending dikes and the Beidashan shear zone is approximately  $40\text{--}60^\circ$  (fig. 4D), they may be derived structures of the Beidashan ductile shear zone, and their formation was at the end of the late Paleozoic (274–264 Ma).

On the southern side of the Beidashan shear zone, we recently discovered a late Paleozoic dextral ductile shear zone, the southern Alxa ductile shear zone (SADSZ) (fig. 9; Zhang and others, 2021b). The SADSZ is NW–SE-trending and basically parallel to the Beidashan shear zone. It is located along the Longshoushan in southern Alxa (fig. 9), starting from Kuantanshan close to the Altyn Tagh fault in the west (Zhang and others, 2020, 2021c), turning nearly EW in the east and covered by the Tengri Desert (fig. 9). The overall exposed length of this shear zone is approximately 500 km, and its width ranges from 0.15 to 2.5 km. Various kinematic indicators indicate dextral shear. The sheared early Paleozoic granite on two sides of the SADSZ indicates that the dextral displacement was between 40 km and 50 km (Zhang and others, 2021b). The zircon U–Pb ages of the granite sheared by the SADSZ and the  $^{40}\text{Ar}/^{39}\text{Ar}$  ages of the muscovite from mylonites formed within the SADSZ indicate that the SADSZ formed *ca.* 269–240 Ma (Zhang and others, 2021b).

There are several shear zones along the boundaries of the Alxa Block (fig. 9), including the Late Triassic NE-trending Langshan-Bayanwula sinistral ductile shear zone (*ca.* 210 Ma, Zhang and others, 2013), the late Paleozoic–early Mesozoic dextral WNW-trending ductile shear zone on the southern margin of the Alxa Block (*ca.* 269–240 Ma, Zhang and others, 2021b) and the dextral EW-trending shear zone of unknown age in the Eengeer Us belt along the northern margin of the Alxa Block (Wang and others, 1998). In addition, there are also shear zones within the block, including the dextral NE-trending shear zone in Tamusu (Guan, *ms.*, 2010; Wu and others, 2012), the near EW-trending dextral shear zone in Bayan Nuru (Zhao and others, 2022) and the dextral ductile shear zone in Beidashan (fig. 9). The activities of these shear zones were concentrated in the late Paleozoic to early Mesozoic (Zhang and others, 2013, 2021a, 2021b, 2022; Zhao and others, 2022).

The relationship of these shear zones in and around the Alxa Block is not clear because of poor outcrops. We plotted all the known shear zones on the aeromagnetic anomaly map of the Alxa Block and show that the distributions of these shear zones are consistent with the aeromagnetic anomaly belts (fig. 10). The arcuate array of the aeromagnetic anomaly belts shows that the dominant structural trend in the Alxa Block transforms from NW–SE to EW (fig. 10). Because most of these shear zones in the Alxa Block formed in the Late Permian and with the same kinematics, these shear zones may be connected to form a large shear system, with a giant S–C-style geometry in map view, indicating dextral shearing (fig. 10; Zhang and others, 2021b; Zhao and others, 2022). A similar large ductile strike-slip duplex was also reported from NE Brazil, that is, the Borborema shear zone system in the Pan-African Orogenic Belt (Corsini and others, 1996; Neves and others, 2021).

#### *Eastern CAO (Xing'an-Mongolian Orogenic Belt)*

The eastern CAO is the segment to the east of the Langshan-Bayanwula ductile sinistral shear zone (Zhang and others, 2013, 2014). Because many dextral shear

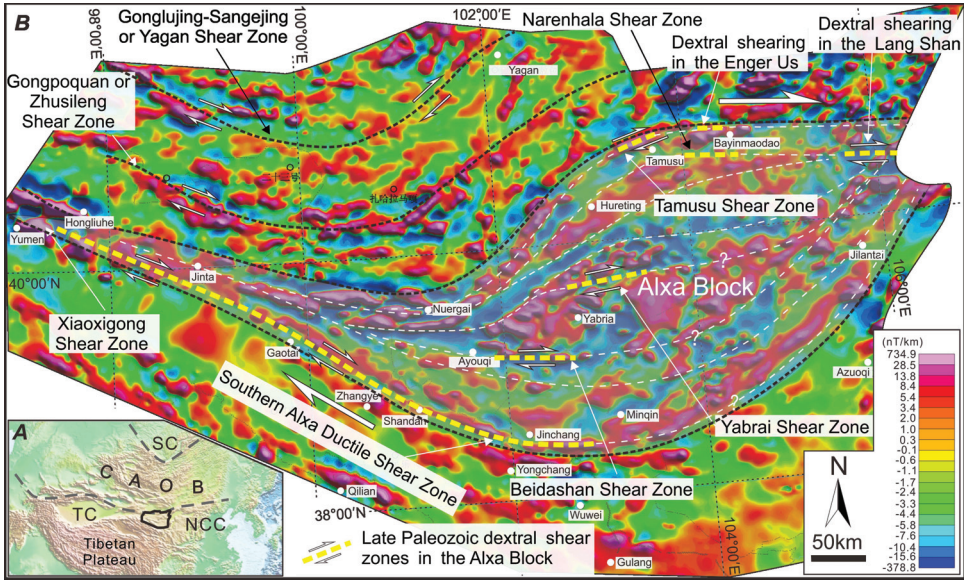


Fig. 10. A. Physiographic map of the eastern Eurasia showing the region of the aeromagnetic pattern (irregular polygon). B. A dextral ductile strike-slip duplex shown by the aeromagnetic pattern in the Alxa Block, central part of the southern CAO B (aeromagnetic data from Xiong, 2019).

zones in the latest Permian–Early Triassic have been reported in the northern North China Craton (NCC), we also include the northern NCC in this section. The regional tectonic line gradually changes from nearly EW to NNE in the east (figs. 1, 2, 7C).

*Northern NCC region.*—Previous studies have identified at least four EW-trending major ductile dextral shear zones that consist of a major shear zone (that is, the Guyang–Wuchuan Shear Zone; Sun and others, 1990; Zhang and others, 1999; table 1, fig. 7C). These shear zones are several hundreds of meters to 10 km wide and more than 280–300 km long (fig. 7C). These shear zones formed mainly along the ancient cratonic margin of the NCC, cutting through the Archaean Wulashan Complex, Paleoproterozoic Seertengshan Complex, Neoproterozoic Zha’ertai Group and Paleozoic granite related to the CAO B. K–Ar dating of sericite from the shear zones yielded ages of 253–247 Ma (Zhang and others, 1999).

The Wulashan Complex in the study region is composed of high-grade metamorphic rocks such as gneiss and migmatite. The Seertengshan Complex is mainly composed of schist and marble. The Zha’ertai Group, however, is similar to the Langshan Group in the Langshan region (fig. 7A) and is mainly composed of low-grade metamorphic rocks such as sandstone, limestone and slate. In the Zha’ertai Group, several bedding-parallel gabbro dikes were reported in the region to the north of Guyang (Zhang and others, 2021d; figs. 2, 7C), which are similar to the gabbro dikes in the coeval Langshan Group in northeastern Alxa (fig. 7B; Zhang and others, 2021a). Because no Neoproterozoic (900–800 Ma) mafic dikes have been found along the northern boundary of the NCC except in the Guyang and Langshan regions (Zhang and others, 2021a, 2021d) and the characteristics of gabbros in these two regions and their wallrocks are the same, the Zha’ertai Group in the northern NCC and Langshan Group in northeastern Alxa all experienced strong dextral shearing (fig. 7), and we infer that the gabbro in the Guyang in the northern NCC was dextrally sheared from the Langshan region. If this correlation is correct, then the dextral displacement

between northeastern Alxa and Guyang in the northern NCC was approximately 270 km after restoring the Triassic sinistral strike-slip distance along the northeast south-west-trending Langshan-Bayanwula Shear Zone (fig. 2).

*Ondor Sum region.*—The ophiolitic mélangé in the Ondor Sum region represents the early Paleozoic southward subduction zone along the northern NCC (Xiao and others, 2003), and the basin was closed at the end of the Ordovician (de Jong and others, 2006). Field mapping reveals nearly EW-trending dextral ductile shear zones in the interior and northern and southern margins of the Paleozoic ophiolitic mélangé (fig. 11). The shear zone along the southern margin of the ophiolitic mélangé zone is the largest, with an outcropping length of more than 140 km. The involved Ondor Sum mélangé developed mylonite foliations (fig. 11C), which are nearly EW-trending and steep. Felsic mylonite containing muscovite is developed, and its protolith is quartzite, with nearly horizontal quartz-stretching lineation (fig. 11B). The early Paleozoic granite to the south of the shear zone was also involved in deformation, and a quartz-stretching lineation was developed (fig. 11E).

Mapping in the Ondor Sum region shows that there were mainly two stages of folding in the area. The first stage of deformation produced nearly east–west tight folds. The folds in this stage are generally recumbent and verge to the north. They are mainly developed in the chlorite sericite quartz schist in the northern mélangé (fig. 11). On the outcrop scale, the folds in this direction are characterized by axial cleavage, crenulation lineation and kinking. The early nearly EW-trending tight fold hinge was superimposed by nearly NS-trending folds. The formation of early nearly EW-trending folds is generally believed to be related to the deformation of the accretionary wedge caused by the southward subduction of the Paleo-Asian Ocean (Xiao and others, 2003; Shi and others, 2013). However, the formation of the later nearly NS-trending folds has not been determined. Nearly EW-trending ductile shear zones were found to the north and south of the mélangé, and the nearly NS/NNE-trending folds show asymmetric Z-shapes in cross-sections at different scales, which shows that their formation was controlled by later dextral shearing, resulting in the folding of early nearly EW-trending folds and foliations. If the early fold hinge is regarded as a passive marker, it would be rotated and deformed continuously during dextral shearing and would then form a Z-shaped fold. At present, the width of the shear zone is approximately 18–22 km. Taking the EW-trending fold hinge as a marker, the shear strain angle is approximately 80°, and the dextral displacement is 102–124 km (fig. 11F).

The  $^{40}\text{Ar}/^{39}\text{Ar}$  ages of the amphibole schists in the Ondor Sum region obtained by scholars are not consistent. de Jong and others (2006) obtained  $^{40}\text{Ar}/^{39}\text{Ar}$  plateau ages of phengites from quartz mylonites (that is,  $453 \pm 2$  Ma and  $449 \pm 2$  Ma), which are considered the formation ages of accretionary complexes. Similarly, Tang and Yan (1993) and Tang (1990) also reported a  $^{40}\text{Ar}/^{39}\text{Ar}$  age of  $426 \pm 15$  Ma for sodic amphibole in the accretionary complex, representing the metamorphic age of blueschist. However, Zhang and others (2018) obtained an actinolite  $^{40}\text{Ar}/^{39}\text{Ar}$  apparent age of  $241 \pm 19$  Ma, which is considered to represent the metamorphic age. Since our mapping shows that the accretionary complex suffered strong ductile deformation in the later stage, the age obtained by Zhang and others (2018) likely represents the age of later shearing related metamorphism.

*Linxi region.*—There are a series of nearly EW-trending, Triassic dextral ductile shear zones with unknown displacements on both sides of the Xar Moron River in the southern Greater Xing'anling, Inner Mongolia (that is, the Xar Moon Shear Zone; fig. 12). The width of a single shear zone can exceed 2–3 km. The shear zones not only cut the early “Shuangjing schist” and the late Permian-early Triassic thick conglomerate (Kedehe conglomerates) but also control/cut the early-middle Triassic Shuangjingzi pluton (Zhao and others, 2015; Zhang and others, 2021e).

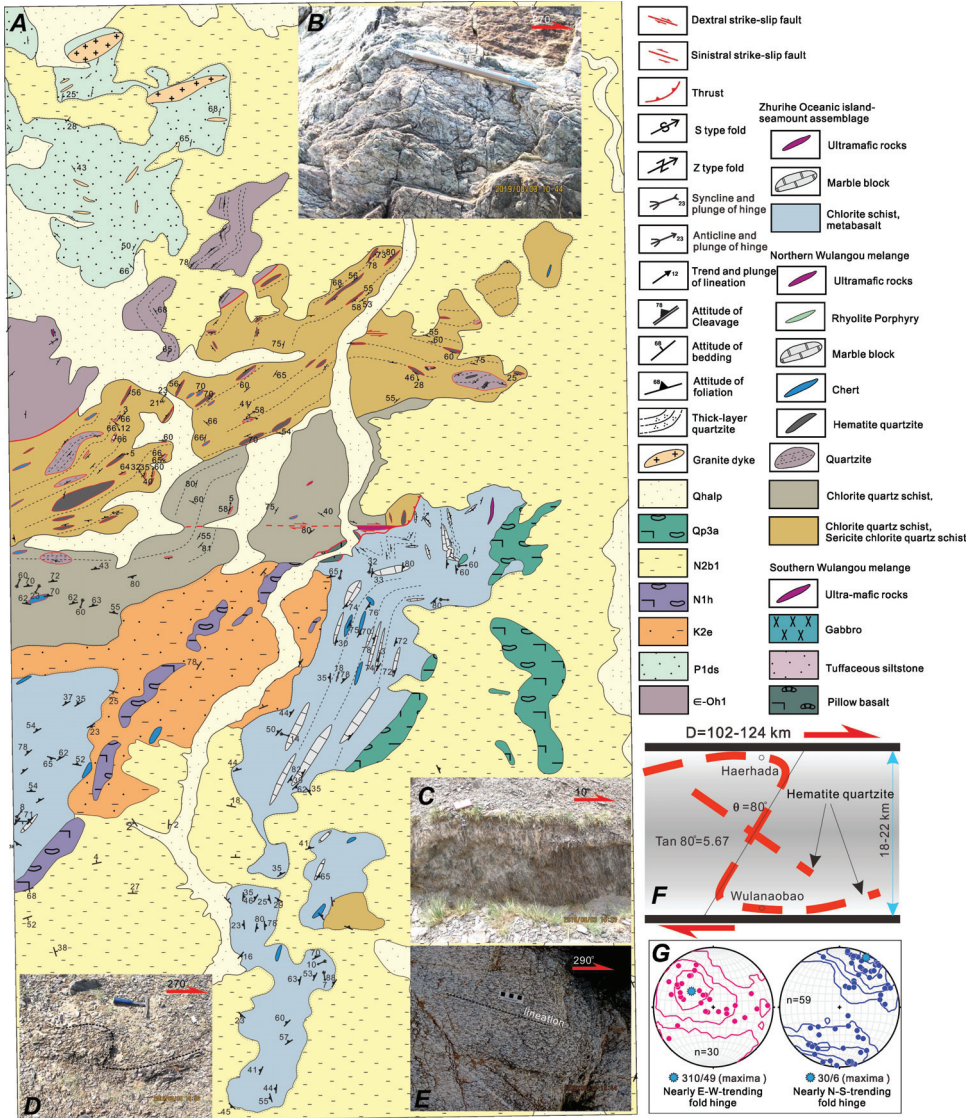


Fig.11. Geological map of Ondor Sum. A. Geological map. B. Felsic mylonite of the Ondor Sum Group in Wulanaobao and quartz stretching lineation. C. Felsic mylonite of the Ondor Sum Group in Wulanaobao. D. Asymmetrical folds in felsic mylonite of the Ondor Sum Group in Wulanaobao, indicating dextral shearing. E. Mylonitic Ordovician granite to the south of Ondor Sum Group in Wulanaobao. F. Distribution of hematite quartzite and shear strain. G. Stereographic projection of fold hinges in the Ondor Sum Group.

The Shuangjing schist exposed on both sides of the Xar Moron River is composed of metamorphic supracrustal rocks and plutonic rocks. Its age was assigned as the early Precambrian by early geological survey (BGM RIMAR, 1991), but recent high-precision dating shows that it is very young, and the metamorphic plutonic rocks are mainly late Paleozoic in age (283 Ma, Li and others, 2007). Ductile deformation is well developed in the Shuangjing schist. Mylonitic foliations are developed in plutonic rocks and schists. The foliations are steep, trending nearly east-west. The quartz-stretching lineation is

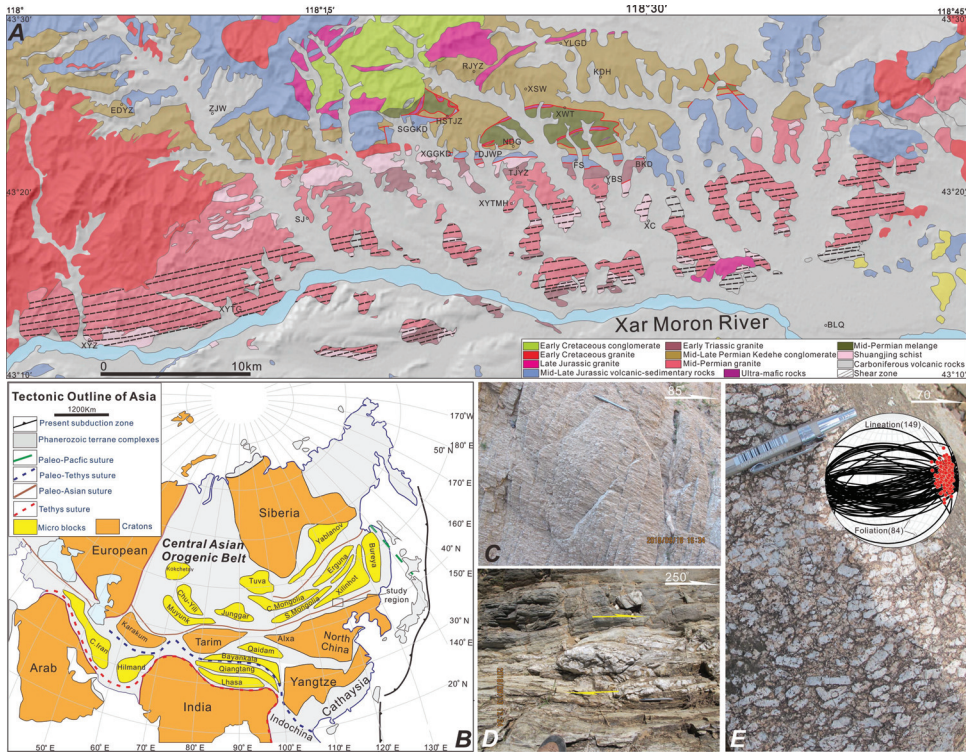


Fig.12. Geological map of Shuangjing region. A. Geological map. B. Felsic mylonite and quartz stretching lineation. C. Shear sense indicator of quartz vein (dextral). D. Mica-fish (dextral). E. Oriented K-feldspar phenocrysts in Triassic granite. BKD: Beikundui, BLQ: Balinqiao, DJWP: Daijiawopu, EDYZ: Erdaoyingzi, FS: Fangshen, KDH: Kedeche, NDG: Nadaga, RJYZ: Renjiayingzi, SGGKD: Shangganggangkundui, SJ: Shuangjing, TJYZ: Tongjiayingzi, XC: Xiachang, XGGKD: Xiaganggangkundui, XSW: Xingshuwa, XYTMH: Xiayingtaomohe, XYZ: Xiayingzi, XYTG: Xiyingtaogou, XWT: Xiaoweitang, YBS: Yuanbaoshan, YLGD: Yeligendai, ZJW: Zhaojiawan.

well developed (fig. 12C) and gently plunges to the east or west (fig. 12E). A series of asymmetric structures, such as quartz vein lenses (fig. 12D), small folds and mica fish indicate dextral shearing.

The Shuangjingzi granite, which is a Triassic granite, is adjacent to the Shuangjingzi schist. Because of the ductile shear deformation, NE-trending foliation developed with ENE-trending quartz-stretching lineation. Meantime, K-feldspar phenocrysts were developed, and the long axis of phenocrysts is nearly EW (fig. 12E), which is consistent with the quartz-stretching lineation in the Shuangjing schist in the nearby region. The oriented K-feldspar phenocrysts suggest that the Shuangjingzi pluton may be a syntectonic pluton, and a previous study reached a similar conclusion (Zhao and others, 2015). If this conclusion is correct, the emplacement age of Shuangjingzi was the age of ductile shear (that is, 229–237 Ma, Li and others, 2007). Zhang and others (2018) also obtained a muscovite  $^{40}\text{Ar}/^{39}\text{Ar}$  age of Shuangjing schist at  $240 \pm 2$  Ma, which is considered to represent the metamorphic age.

In Shuangjing schist in the study area (north of Nadaga), syntectonic intrusive rock is also found (fig. 13). There are a series of dioritic enclaves distributed in the granitic rock body (fig. 13). The long axis of these enclaves is parallel to the quartz-stretching lineation in the Shuangjing schist (fig. 13). Moreover, the development of mylonite foliation becomes strong outward in the granitic rock body, the enclaves are

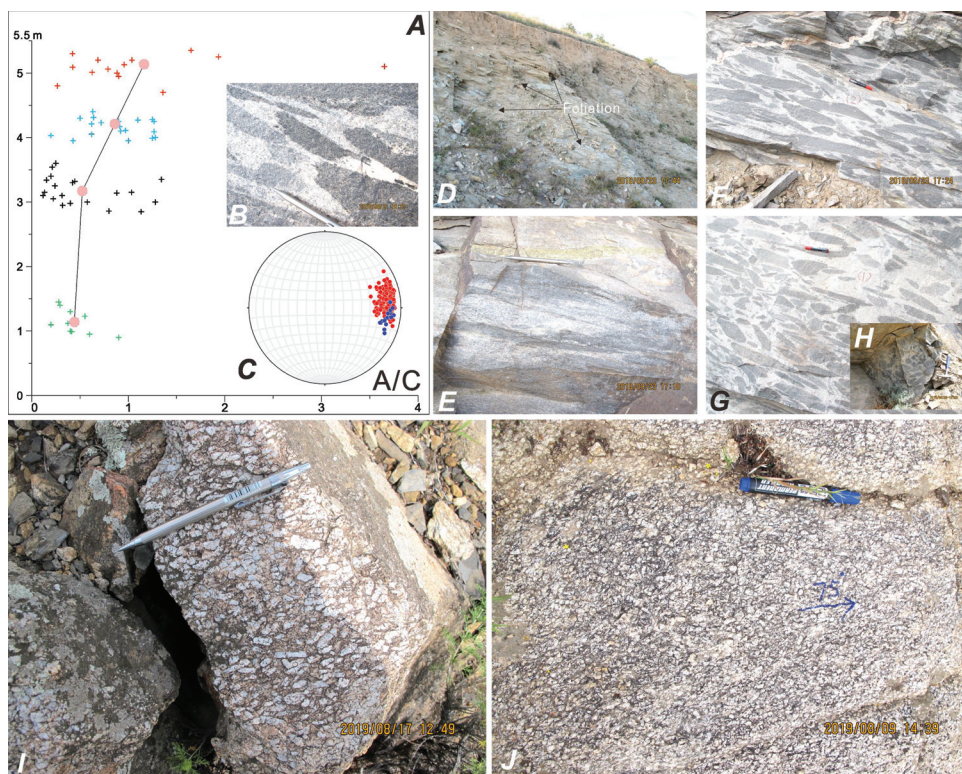


Fig. 13. Syntectonic granite and oriented dioritic enclaves in the Shuangjing schist. A. Relationship between the axial ratio of dioritic enclaves and their locations above the ground, A/C represents the ratios of long and short axes of elliptic enclaves, which were measured in XZ plane. B. Torn dioritic enclaves. C. Relationship between quartz stretching lineation (red) of mylonite in Shuangjing schist and long axis of dioritic enclaves (blue). D. Strongly developed mylonitic foliations outwards. E. Intensely sheared dioritic enclaves without obvious boundaries. F. Dioritic enclaves approximately 4 m above the ground. G. Dioritic enclaves approximately 1 m above the ground. H. Crossing section of dioritic enclaves approximately 1 m above the ground. I and J. Oriented K-feldspar phenocrysts in the Shuangjing granite.

also strongly sheared, and their outlines are totally indistinguishable (fig. 13). The age of the enclave is 260–250 Ma, and the metamorphic age of the granite in the wall rock is also approximately 250 Ma (Li and others, 2014). Under the microscope, the ductile deformation of minerals in granite and diorite enclaves is not obvious, but the minerals were oriented to a certain extent (fig. 13I and J), which indicates that the deformation temperature was higher and may have been in a plastic state. Therefore, we suggest that the ductile dextral shearing in the Shuangjing schist occurred at the end of the Permian. There are at least two more shear zones of the same scale formed to the north of Linxi region, which are parallel to the Xar Moon Shear Zone; however, few studies have been performed, and we do not have any detailed information about these shear zones except their dextral kinematics.

*Chifeng region.*—To the east of the Linxi region, the Jiefangyingzi area of Chifeng on the northern margin of the NCC also experienced strong dextral shearing (fig. 14), and the Silurian Badangshan Formation and early Paleozoic intrusions were all involved in ductile deformation. The ductile deformation was approximately 10 km wide; however, the displacement is not constrained. In the zone, nearly horizontal ENE–WSW-trending quartz-stretching lineations were strongly developed (fig. 14). The Late Triassic granodiorite (229 Ma, Liu and others, 2012) in the study area is

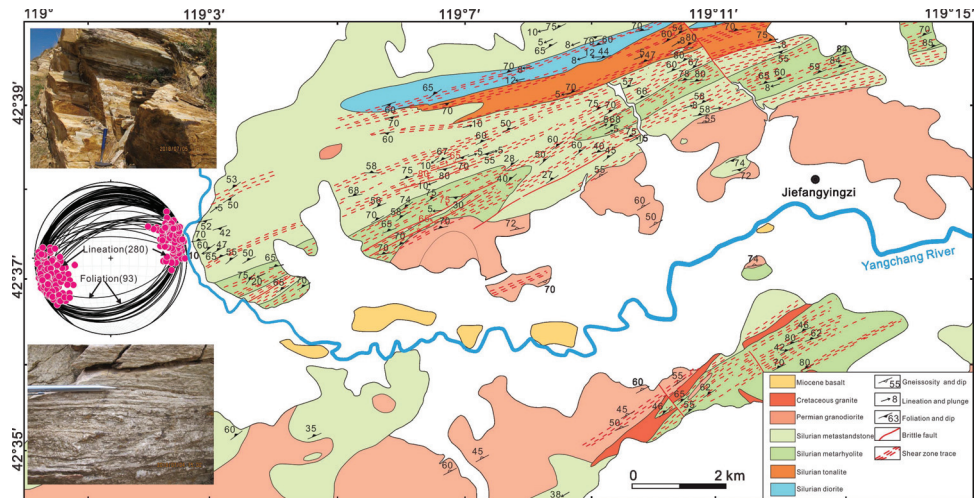


Fig. 14. Geological map of Jiefangyingzi region. A. Geological map. B. Felsic mylonite and quartz stretching lineation. C. Stereographic projection of mylonitic foliations and stretching lineation. D. Asymmetrical folds indicating dextral shearing.

distributed in an ENE direction. The margin of the granite pluton was deformed by ductile shearing with NEE-trending quartz-stretching lineation. Many dark mafic xenoliths of various sizes in the granite are obviously elongated in an ENE–WSW direction. The strike of the granite body and the stretching xenoliths are consistent with the ductile deformation zone. Recently, the emplacement age of syntectonic granite ( $229.7 \pm 0.8$  Ma) and the  $^{40}\text{Ar}/^{39}\text{Ar}$  plateau age of muscovite in the ductile shear zone ( $219.9 \pm 1.3$  Ma) indicate that ductile deformation occurred in the Late Triassic (Wang and Li, 2020).

*Other regions.*—In addition to the EW-trending ductile dextral shear zone in Linxi and Chifeng, dextral ductile shear zones were also found in Carboniferous carbonate rocks in the Changchun area (Liang and others, 2019), Jiapigou gold deposits (*ca.* 230 Ma, Deng and others, 2014) and Yingchengzi gold deposits (*ca.* 248 Ma, Chai and others, 2016) at the eastern end of the Xar Moron Shear Zone. The Carboniferous strata in the Chuangchun area are characterized by vertical foliations with east–west sub-horizontal stretching lineations with dextral kinematic indicators (Liang and others, 2019), which is similar to the deformation in other EW-trending dextral zones. We suggest that this deformation was caused by the same tectonic event, as argued by Liang and others (2019). The involvement of the Carboniferous strata in Chuangchun also indicates that deformation occurred after the Carboniferous.

The dextral ductile shear deformation in the Early Triassic was also reported from Chicheng, Huade and other areas in the northern margin of NCC (Wang and Wan, 2014). Pre-Cambrian metamorphic rocks and Late Paleozoic–Mesozoic granitic rocks were involved in the ductile deformation. The mylonitic foliations trend nearly E–W and dip to north/south at moderate to steep angles. The kinematic indicators such as feldspar porphyroclasts and S–C fabrics indicate dextral transpressional shearing (Wang 1996). The timing of the shear zone was constrained between 255 Ma and 241 Ma (Wang and Wan, 2014).

In addition to the EW-trending Xar Moron Shear Zone, the Xing’an–Mongolian orogenic belt changes to a NE–SW orientation to the east (fig. 1). The Keluo complex is located in the Hegenshan–Nenjiang–Heihe tectonic belt (HNHTB) (inset in fig. 15) and belongs to the junction of the Xing’an and Songnen blocks (inset in fig. 15; Liu

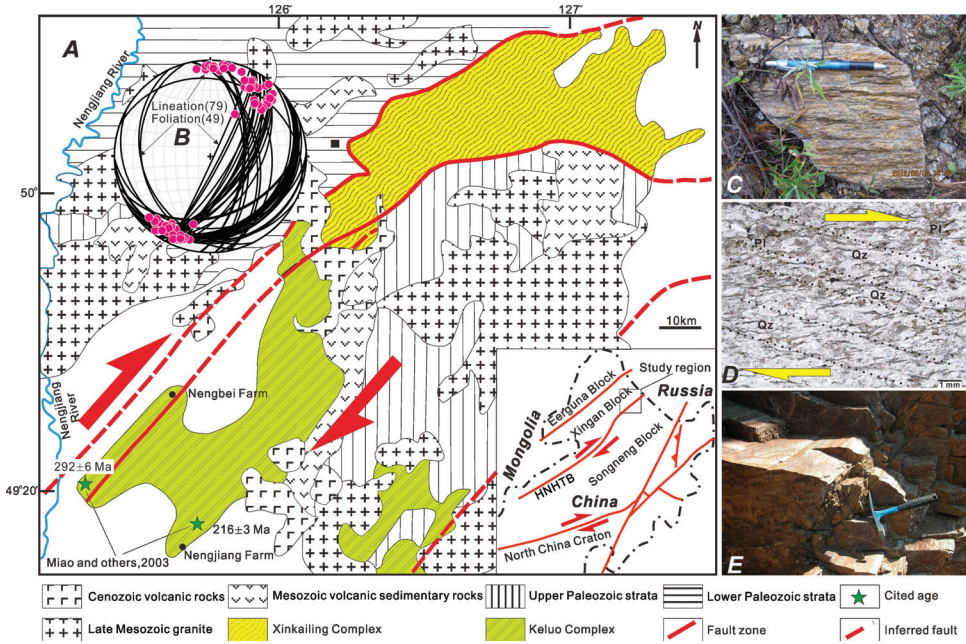


Fig. 15. Geological map of Keluo area. A. Geological map. B. Mylonitic foliations and quartz stretching lineation. C. Granitic mylonite and lineation. D. C' shear band in mylonite, indicating dextral shearing. E. Felsic mylonite. HNHTB-Hegenshan-Nenjiang-Heihe tectonic belt.

and others, 2017). A mylonite belt with a length of more than 100 km and a width of dozens of km developed (Miao and others, 2015; Zhao and others, 2017). Mylonite exposed in the Keluo area is mainly felsic. The foliation is NE-trending and dips to southeast (fig. 15). Quartz-stretching lineation is developed, nearly horizontally (fig. 15). The foliation may have been subjected to later folding (Zhao and others, 2017), and the later Devonian granite was involved in the ductile shear zone (Li and others, 2010).

The Keluo complex is composed of typical high-grade metamorphic rocks with migmatites, including garnet-bearing biotite plagioclase gneiss, garnet-bearing biotite hornblende plagioclase gneiss, garnet-bearing biotite hornblende plagioclase granulite and plagioclase hornblende gneiss. The complex was intruded by later Early-Middle Jurassic or Early Cretaceous granites (Miao and others, 2004; Zhao and others, 2017). On the outcrop and microscopic scales, dextral-shearing structures were found (fig. 15D), indicating the dextral movement of the Xing'an Block relative to the Songnen Block (fig. 15). Because of intensely subsequent deformation, the exact ages of ductile shearing in Keluo region and its kinematics are still needed to be determined.

DISCUSSION

*Late Ductile Shear Zones along the Southern CAOB*

In addition to the nearly EW-trending ductile shear zones from the Beishan to the Xing'an-Mongolian orogenic belt mentioned above, late Paleozoic dextral shear zones are also common in the Tianshan (fig. 1), including the Qiugemingtashi-Huangshan ductile shear zone (Chen and others, 2005; Wang and others, 2010; He and others, 2021), the ductile shear zone on the northern margin of the Central Tianshan (that is, the Main Tianshan Shear Zone, Allen and others, 1993; Shu and

others, 1999; Laurent-Charvet and others, 2003; de Jong and others, 2009; Cai and others, 2012), the southern margin of the Central Tianshan, the Xinger ductile shear zone in the northern Kuruktag, and the Kuruktag-Xingdi ductile shear zone (Cai and others, 2012). Kinematic indicators from field outcrops and microfabrics show concordant dextral shearing, and they are basically parallel in map view; there are also connected secondary shear zones among them (Shu and others, 1999; Laurent-Charvet and others, 2002, 2003; Chen and others, 2005; de Jong and others, 2009; Wang and others, 2010; Cai and others, 2012).

The shear system along the southern CAOBS may extend into the Kazakhstan orocline to the west (fig. 1). The Kazakhstan orocline is one of the most striking structures in the CAOBS and is composed of the folded Devonian Volcanic Belt and the Late Devonian to Carboniferous Balkhash-Yili arc (Li and others, 2018). The Kazakhstan orocline is thought to be the convergence of the large cratons of Baltica, Siberia and Tarim (Şengör and others, 1993; Van der Voo and others, 2006; Li and others, 2018). The formation period of this giant orocline is disputed; for example, in the late Carboniferous–Early Permian (Van der Voo, 2004), Devonian and Early Carboniferous and completed by the Late Carboniferous (Levashova and others, 2012), Late Devonian to Permian (Choulet and others, 2012; Li and others, 2018), or even Late Permian to the Early Triassic (Van der Voo and others, 2006; Xiao and others, 2015). As some dextral shear zones, such as the Central Kazakhstan Fault (CKF) and Chingiz-Alakol-North Tianshan Fault (CANTF, *ca.* 263 Ma, de Jong and others, 2009), have cut into the orocline (fig. 1), the orocline should have formed before these shear zones, that is, before the Middle Permian.

Regionally, the vast area between the Baltic, Siberian and Tarim cratons underwent intense deformation in the late Paleozoic during the convergence of the three cratons. Shear deformation also developed in the Ural orogenic belt. Although the orogenic belt formed in the Devonian-Carboniferous (Puchkov, 1997; Brown and others, 2006a), ductile deformation still occurred along the nearly NS-trending Main Uralian Fault in the central part of the orogenic belt from the end of Late Permian to the Early Triassic (250–240 Ma); however, the kinematics of the shearing are in dispute because of limited evidence (Ayarza and others, 2000; Hetzel and Glodny, 2002; Brown and others, 2006b). Whether the deformation along the Main Uralian Fault at 250–240 Ma was shortening or strike slipping, the deformation at the end of the late Paleozoic in the Ural and the dextral shear along the southern CAOBS were not only formed at the same time, but also resulted from the further convergence of the three cratons (Van der Voo and others, 2006). Therefore, we suggest that the late Paleozoic dextral shear zone in the southern CAOBS may be connected with the Main Uralian Fault in the west.

The shear zone along the southern CAOBS branches eastward into Greater Xing'an. There are different views on the late Paleozoic-Mesozoic tectonic framework in Northeast China (Wu and others, 2007; Zhou and others, 2009, Zhou and Wilde, 2013; Liu and others, 2017; Li and others, 2015). Most studies have suggested that the final closure of the CAOBS in NE China occurred during the Triassic (Liu and others, 2017 and references therein). The tectonic evolution is complicated because of the subduction of the Paleo-Pacific Ocean to the east and the closure of the Mongolia-Okhotsk Ocean to the northwest (Wu and others, 2007; Zhou and others, 2014; Liu and others, 2017).

After the closure of the Paleo-Asian Ocean, NE China experienced oceanic plate subduction in the Mesozoic, and several subduction-related complexes such as the "Heilongjiang Group" to the west and the Yuejinshan Complex and Raohe Complex to the east, developed (Zhou and Wilde, 2013; Zhou and others, 2014). At present, there are different standpoints on the evolution and formation of Heilongjiang

complex in NE China, but many studies have agreed that it is a subduction accretionary complex, which is also called the Jihei high-pressure metamorphic belt due to the discovery of high-pressure metamorphic rocks such as glaucophane schist (Zhou and Wilde, 2013). With the accumulation of zircon U–Pb ages and magmatic rock data, some scholars believe that the metamorphic rocks of the Heilongjiang Group were the products of the closure of a Permian to Jurassic ocean basin (Heilongjiang/Mudanjiang Ocean) (Zhou and Wilde, 2013). Some scholars believe that the Heilongjiang/Mudanjiang ocean basin was formed in the Early Permian and is a part of the Paleo-Pacific Ocean, which was subducted from the Late Triassic to the Late Jurassic (Ge and others, 2016, 2018), while others believe that it opened in the late Early Triassic (Long and others, 2020). In addition, when the Heilongjiang/Mudanjiang Ocean began to subduct is also unknown. Some studies have indicated that it began to subduct westward under the Songnen Block as early as the Permian (Dong and others, 2017; Ge and others, 2018; Li and others, 2022). Permian metamorphism has also been reported for the complex (Li and others, 2010), but others argue that it was mainly subducted and closed in the early and middle Mesozoic (Wu and others, 2007; Zhou and others, 2009; Zhou and Wilde, 2013). At present, because Mesozoic structural data are sparse in NE China, the eastward extension of the EW-trending ductile shear zone is unknown, and we still do not know how EW-trending ductile shearing transformed to the east or the relationship between EW-trending shear zones and NE-trending structures in NE China. We prefer that the EW-trending ductile shearing may have transformed to the convergence of the ocean regime in NE China such as the Heilongjiang/Mudanjiang Ocean (Li and others, 2022) or even the Paleo-Pacific Ocean.

In addition, Miao and others (2004) considered that the Keluo complex in the Hegenshan-Heihe tectonic belt was the product of collision and amalgamation between two terranes, and its metamorphic age is  $216 \pm 3$  Ma, suggesting that the belt represents an Indosinian collision zone. Li and others (2009, 2010) also believed that the Songnen Block collided with the Jiamusi Block in the Middle and Late Triassic. Moreover, the tectonic reconstruction map of Metelkin and others (2010) based on paleomagnetism also shows the Middle and Late Triassic amalgamation of blocks. We have to admit that there are few structural studies in the NE China focusing on the ductile deformation, many key data such as ages and kinematics are rare, and further work is also needed to determine the transform relationship in NE China with the EW-trending segment of shear system along the southern CAOB.

In conclusion, we suggest that the dextral ductile shear system along the southern CAOB extends eastward from the Ural orogenic belt, connects with Tianshan in China through the Kazakhstan orocline, goes through the northern margin of the NCC through the Beishan and the Alxa Block eastward, and finally connects with the nearly north–south-trending Jihei high-pressure belt and Hegenshan-Heihe tectonic belt in the east, forming a large “U”-type structure extending more than 5000 km (fig. 16). In addition, coeval gold deposits in the region appear to be spatially associated with the shear system, and mineralization might be related to this shearing event across the Eurasian continent (fig. 1).

Large shear zones on the continent often show a shear system composed of a series of secondary shear zones (Merzer and Freund, 1976). Since the end of the Permian was the final formation period of the Pangea Supercontinent (Zhao and others, 2018; Şengör and others, 2019a), the formation of the CAOB was a part of supercontinent development. At the end of the Permian, a large intracontinental transform structure composed of a group of dextral ductile shear zones also developed along the Variscan orogenic belt in Europe (Arthaud and Matte, 1977; Gates and others, 1986; Matte, 1991, 2001; Shelley and Bossière, 2000; Franke and Żelaźniewicz, 2002; Martínez Catalán, 2011; Şengör, 2013; Pfiffner, 2017; Şengör and others, 2019a) (fig. 17B).

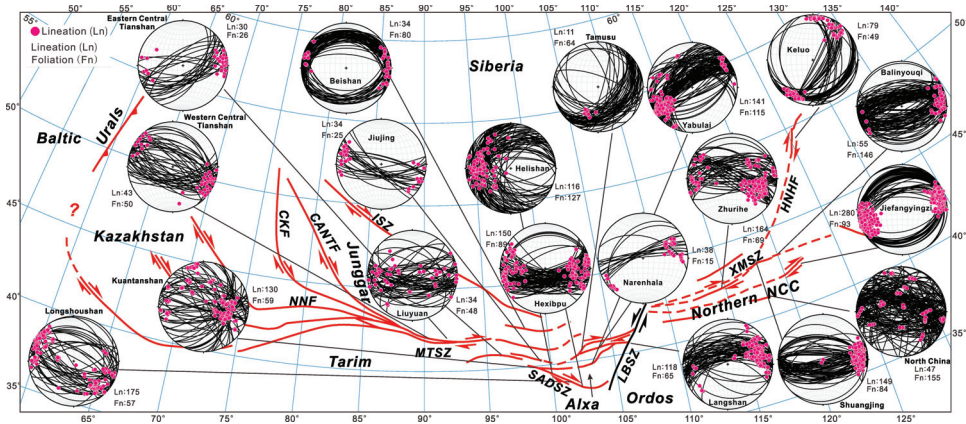


Fig.16. Distribution of dextral ductile shear zones along the southern CAOB during the late Paleozoic and early Mesozoic (see fig. 1 for the names of shear zones).

Previous studies have shown that with the formation of the Variscan orogenic belt, the African Plate continued to move westward relative to southern North America and Europe. A large deformation regime connects the Ural orogenic belt and the Variscan orogenic belt with the southern Appalachian orogenic belt in North

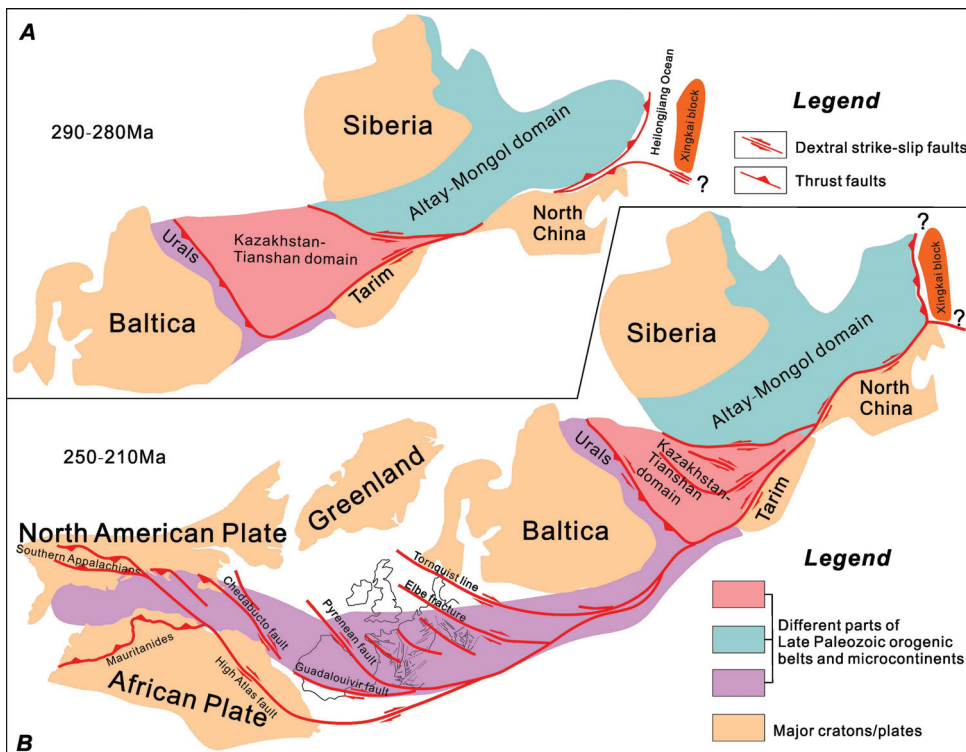


Fig.17. Formation of Intra-Pangean Megashear (IPM) (the paleogeographic positions of major blocks are according to Van der Voo and others, 2006, the locations of Europe-Africa-North America is according to Arthaud and Matte, 1977). A. 290–280 Ma. B. 250–210Ma.

America and the Mauritanides in West Africa (Arthaud and Matte, 1977). The age of this deformation event was the Late Permian (Şengör, 2013) or 250 Ma (Arthaud and Matte, 1977). A series of large dextral ductile shear zones, such as the Central Bohemian shear zone, Tornquist line, Elbe fracture, North Pyrenean fault and Kelvin fault, developed in this deformation regime. Some scholars have argued that the late Paleozoic deformation of the South Appalachian orogenic belt in North America and the contemporaneous deformation in the Ural orogenic belt were connected by a giant intracontinental shear zone along the southern Variscan orogenic belt in southern Europe, forming a giant intracontinental transform structure in Europe (Arthaud and Matte, 1977; Martínez Catalán, 2011).

In Asia, the late Paleozoic deformation of the Ural orogenic belt may also correlated with the dextral ductile shear deformation along the southern CAOB in the east (see above). This study and many previous studies show that these late Paleozoic dextral shear zones in the southern CAOB either appeared as strike-slip duplex structures (Alxa-Beishan) or strike-slip stacking structures (Scythian-Turan domain; Natal'in and Şengör, 2005) or a series of nearly parallel shear zones (Tianshan and the northern margin of the NCC), forming a relatively wide megashear zone in the eastern Eurasian Plate (fig. 16). At the same time, the late Paleozoic dextral shear systems in the Ural orogenic belt, Central Asia and the eastern Variscan orogenic belt were active and are considered to constitute a transcontinental shear zone (Natal'in and Şengör, 2005). Due to the similar kinematics and ages, we suggest that the late Paleozoic-early Mesozoic intracontinental transform structure along the southern CAOB can be connected with the transform structure of the European part, forming a giant intracontinental transform structure system across Eurasia, southern North America and northwestern Africa (fig. 17). Since the shear zone was developed in the central Pangea supercontinent, we call it the Intra-Pangean Megashear (IPM) after Irving (2004) because he first named it in the western part of this system.

Previous studies have shown that many large-scale intracontinental shear zones (such as the San Andreas and the North Anatolian shear zones) in the world were formed along previous suture zones or orogenic belts; the main reason for this that the materials in the sutures or orogenic belts are less competent than the surrounding tectonic units (Şengör and others, 2019a and references therein). The IPM in the central Pangea supercontinent is no exception; it mainly developed along the southern Variscan orogenic belt in Europe and the southern CAOB in Asia. These orogenic belts surrounded the relatively stable cratons (Siberia, Baltic, Tarim and North China cratons). Therefore, the later intracontinental deformation was mainly distributed or concentrated in the weak areas surrounding the cratons (Şengör and others, 2019b; Zhang and others, 2021f).

#### *Ages*

The age of dextral ductile shear in the eastern IPM has been restricted to some extent. Previous studies have focused on the Tianshan and Kazakhstan regions in the west and the Xar Moron Shear Zone and the northern margin of the NCC in the east. Our recent work focused on the Beishan and Alxa regions (this study, Zhang and others, 2021a, 2021b; Zhao and others, 2022). In this study, we systematically collected the ages of dextral ductile shear along the southern CAOB from the late Paleozoic to the early Mesozoic, which mainly includes the  $^{40}\text{Ar}/^{39}\text{Ar}$  ages of metamorphic minerals and the emplacement ages of syntectonic intrusive rocks. The deformation age gradually becomes younger to the east (fig. 18).

In the Tianshan, Chen and others (2005) reported the  $^{40}\text{Ar}/^{39}\text{Ar}$  ages of the Qiugemingtashi-Huangshan ductile shear zone and concluded that the main active period of dextral shearing was at 262–242 Ma, and the active age gradually becomes

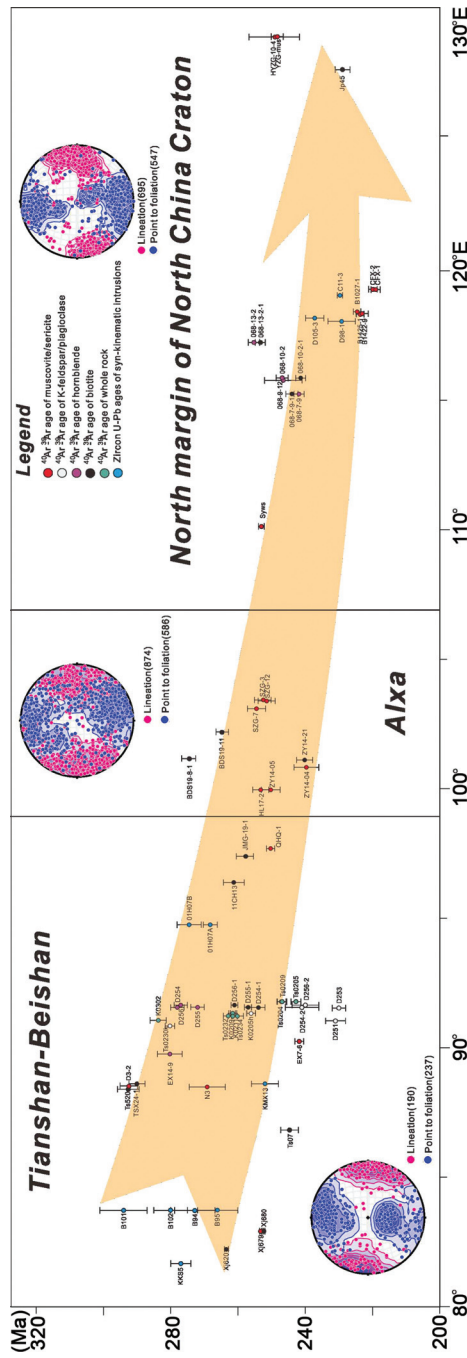


Fig. 18. Age distribution of Late Paleozoic-early Mesozoic dextral shear zones along the southern CAOB (X-axis: longitude of samples, Y-axis: ages; the stereographic projections show mylonite foliations and mineral stretching lineation of the dextral shear zones in main segments) (data from Laurent-Charvet and others, 2003; Chen and others, 2005; Ma, 2009; de Jong and others, 2009; Cai and others, 2012; Wang and others, 2007, 2008; Wang and Wan, 2014; Li and others, 2007; Zhang and others, 2021b; Wang and Li, 2020; Ding, 2021; Zhao and others, 2022; this study).

younger to the east. Wang and others (2010) dated syntectonic granite in the shear zone, thus constraining dextral shearing to 270–254 Ma. Cai and others (2012) dated the mylonite in the ductile shear zone of the northern margin of the Central Tianshan with  $^{40}\text{Ar}/^{39}\text{Ar}$  dating and obtained  $367 \pm 3$  Ma (dolomite),  $290 \pm 2$  Ma (biotite) and  $241 \pm 1$  Ma (biotite). It is believed that the youngest age indicates dextral shear deformation. The  $^{40}\text{Ar}/^{39}\text{Ar}$  dating of muscovite from mylonitic granite in the shear zone yielded an age of  $269 \pm 5$  Ma, and the K-Ar dating of biotite yielded an age of 281 Ma (Shu and others, 1999). Laurent-Charvet and others (2003) also reported biotite  $^{40}\text{Ar}/^{39}\text{Ar}$  ages (240–250 Ma) from the western segment of the northern margin of Central Tianshan. According to the  $^{40}\text{Ar}/^{39}\text{Ar}$  dating of amphibole, biotite and muscovite in mylonite developed on the southern margin of the Central Tianshan-Xingxingxia ductile shear zone and the Kuruktag-Xinger ductile shear zone, Cai and others (2012) argued that the active age of the former is between 298 and 280 Ma, while the latter is between 290 and 277 Ma. Laurent-Charvet and others (2003) also used the  $^{40}\text{Ar}/^{39}\text{Ar}$  age of biotite in the middle section of the Xingxingxia ductile shear zone on the southern margin of the Central Tianshan Mountains to constrain its active age to 290–300 Ma. The whole-rock  $^{40}\text{Ar}/^{39}\text{Ar}$  ages of the two samples in the central and eastern parts of the North Tianshan shear zone are 285–255 Ma and 275–263 Ma, respectively (Allen and others, 1993; de Jong and others, 2009).

In addition, the well-known Erqis shear zone extends from the Altay region of China to Kazakhstan from southeast to northwest and is one of the large strike-slip shear zones in the southern CAOB (Şengör and others, 1993; Buslov and others, 2004a, 2004b; Briggs and others, 2007; Li and others, 2015, 2021). Muscovite of the syntectonic granites in the Erqis shear zone yielded a  $^{40}\text{Ar}/^{39}\text{Ar}$  age of 290 Ma (Mitrokhin and others, 1997; Melnikov and others, 1998). Zhang and others (2012) obtained a zircon U–Pb age of  $252.4 \pm 2.6$  Ma for the undeformed granodiorite intruding the shear zone, and muscovite, biotite and amphibole  $^{40}\text{Ar}/^{39}\text{Ar}$  dating of mylonitized gneisses in the shear zone also indicates that the peak period of the dextral ductile shear zone in the Erqis was 275 Ma. Vladimirov and others (1997) and Travin and others (2001) performed  $^{40}\text{Ar}/^{39}\text{Ar}$  dating of muscovite, amphibole and K-feldspar in the shear zone, which constrained its age to 283–263 Ma. Based on the  $^{40}\text{Ar}/^{39}\text{Ar}$  dating of biotite and amphibole from the mylonites in the Erqis shear zone in China, Laurent-Charvet and others (2003) suggested that the shear zone was active from 290 to 245 Ma. Li and others (2015) also defined the upper limit of the age of the shear zone as 252 Ma according to the zircon U–Pb age of the granitic dike swarms intruded into the Erqis shear zone near Fuyun County. The timing of the Erqis shear zone is coeval with those of dextral shear zones along the Tianshan. However, studies have shown that the Erqis shear zone was a sinistral shear zone (Laurent-Charvet and others, 2002, 2003; Li and others, 2015, 2021), which will be discussed later.

Figure 18 shows that the main active time of the Central Tianshan shear zone and the southern margin of the “Silk Road Arc” in the western section was *ca.* 280–240 Ma (Laurent-Charvet and others, 2002, 2003; Natal’in and Şengör, 2005; Wang and others, 2007; Charvet and others, 2011). One biotite  $^{40}\text{Ar}/^{39}\text{Ar}$  age of the Jinmiaogou dextral ductile shear zone in the southern Beishan was obtained recently, and their plateau ages are  $258.1 \pm 2.7$  Ma (JMG-19-1; fig. S1, see Supplementary Data for details).

In the Alxa Block, the age of dextral ductile shear zone is rarely published. At present, the Langshan shear zone has been constrained to have formed at approximately 250 Ma according to the age of intrusive but undeformed dikes (Tian and others, 2020). We obtained the muscovite and biotite  $^{40}\text{Ar}/^{39}\text{Ar}$  ages of the Longshoushan ductile shear zone to the south, which are concentrated from 260–250

Ma (Zhang and others, 2021b), and the muscovite  $^{40}\text{Ar}/^{39}\text{Ar}$  ages of the Yabrai dextral shear zone are approximately 254–251 Ma (Zhao and others, 2022). Therefore, the development of the Yabrai shear zone can also be constrained between the Late Permian and Early Triassic.

In the eastern segment, many studies have been performed to date the shear zones on the northern margin of the NCC. Gao (ms, 2004) obtained  $^{40}\text{Ar}/^{39}\text{Ar}$  ages of K-feldspar (159 Ma), biotite (197 Ma) and muscovite (183 Ma, 192 Ma and 227 Ma) from the Shuangjing schist. Ma (2009) obtained a muscovite  $^{40}\text{Ar}/^{39}\text{Ar}$  age from Shuangjing mylonitized rocks, which was 224–225 Ma. Zhao and others (2015) obtained a muscovite  $^{40}\text{Ar}/^{39}\text{Ar}$  age of mylonitized granite, which was 209 Ma. Some Shuangjingzi intrusions were typical syntectonic intrusions (Zhao and others, 2015; fig. 13); therefore, their emplacement age represents the age of shear zone activity, and the age of Shuangjingzi intrusions ranges from 260 to 230 Ma (Li and others, 2007, 2014; Zhao and others, 2015). It can be determined that the formation age of the shear zone in the Shuangjing area may be 260–230 Ma. Most mica  $^{40}\text{Ar}/^{39}\text{Ar}$  ages obtained at present may be cooling ages, and the  $^{40}\text{Ar}/^{39}\text{Ar}$  dating results may also be affected by the superposition of multiple magmatic activities and tectonic events (Li and others, 2014) in the Xar Moron Shear Zone in a later stage. In addition, a series of nearly EW-trending dextral ductile shear zones were found in the Yanshan area on the northern margin of the NCC, and the shearing age is approximately 245 Ma (Wang and Wan, 2014).

It can be summarized from the data obtained thus far that the age of ductile dextral shearing activity of the Asian part of the IPM was mainly between 280 Ma and 230 Ma (fig. 18), and the ages of the western segment are older and gradually younger to the east (fig. 18). This phenomenon may indicate the gradual development of the shear zone from west to east. In the European part of the IPM, the age of shear deformation in the Ural area is 250–240 Ma (Hetzl and Glodny, 2002). Arthaud and Matte (1977) believed that the dextral shear age on the southern margin of the Variscan orogenic belt was approximately 250 Ma, although no accurate test methods and ages were given at that time. Although the exact ages are still relatively few, most scholars have constrained the age of this deformation in Europe to the Late Carboniferous–Late Permian (Matte, 2001; Muttoni and others, 2003, 2009; Martínez Catalán, 2011; Şengör, 2013). Compared with the Asian part, the age of IPM in Europe is older, and the IPM gradually becomes younger eastward, which may represent the gradual evolution and development process of the shear zone from west to east and may imply a continuous adjustment process within the Pangea Supercontinent.

### *Displacement*

It is difficult to determine the displacement of the IPM. On the one hand, the tectonic belt is a shear system, and the displacement obtained by a single shear zone cannot represent the displacement of the whole system. On the other hand, the shear system may gradually evolve from west to east, and the displacements of different segments will be very different. In addition, because both ends of the system are compressional, the length of the system will become shorter with deformation (Şengör and others, 2019a), and the system has a series of secondary structures in different segments; they will further absorb part of the strain of the main shear zone; therefore, the displacement of different segments of the whole system will be greatly different.

As far as the current studies are concerned, the displacement of the IPM in Europe was approximately 2500–3000 km (Pangea B to Pangea A, Irving, 1977, 2004; Muttoni and others, 2003, 2009; Şengör, 2013). These studies were mainly based on paleomagnetic work, which may determine the displacement of the whole transform system. The dextral displacement of the eastern end of the Variscan orogenic belt

could reach approximately 300–350 km (Natal'in and Şengör, 2005), while the dextral shear displacement of the Kazakhstan-Tianshan region in the same period was  $1165 \pm 630$  km (Zhu and others, 2018) or  $1160 \pm 380$  km (Wang and others, 2007). In the East Tianshan and Beishan, there is no relevant research. Farther east in the Alxa region, we have only provided constraints on the displacements of some shear zones, such as the Longshoushan (40–50 km), Yabrai (25–30 km) and Langshan (45–85 km) shear zones in the central and southern regions. However, several coeval shear zones, such as shear zones in the Engeer Us, Zhushileng and Yagan regions have been poorly studied in the northern Alxa region (fig. 10). These shear zones display comparable scales (fig. 10) and likely share similar displacements ( $\sim 40$ – $50$  km), but we have little information about these shear zones. Assuming that overall displacement was partitioned into these shear zones, the bulk displacement of  $\sim 130$ – $315$  km across the megashear system in the Alxa region can be generally estimated. Moreover, we think that there are still some small-scale shear zones occurring in the Alxa region that have not been reported, and a larger offset would be expected. Therefore, the  $\sim 130$ – $315$  km is the minimum limit. In the east, along the northern margin of the NCC and the Xar Moron shear zone, there have been few studies on dextral shear displacement. Our preliminary analysis on the northern margin of the NCC and Ondor Sum area shows that the dextral displacements were 270 km (fig. 2) and 102–124 km (fig. 11F), respectively.

The estimated displacement of the IPM by geological methods was obviously less than that inferred from paleomagnetic data. There are still many shear zones without displacement constraints in the eastern CAOB. We calculate their displacements by a shear strain of 5 as the minimum limits (Ramsay and Graham, 1970; Simpson, 1983; Fossen and Cavalcante, 2017) and show them in table 1; however, further field work is needed in the future, especially in segments in eastern Asia. The following several factors may be considered when the displacement is measured.

First, the bulk displacement of the IPM along the southern CAOB was highly underestimated because we only constrained the shear zones that we know, and there are still some shear zones lacking important constraints and study in the eastern CAOB.

Second, numerous studies have suggested that various factors can result in a displacement decrease from the center to the end of the shear zone. For example, the most common one is that the lateral motion is absorbed by thrust faults and related folds, as in the case of the Altyn Tagh fault (Zhang and others, 2020, 2021c). The diachronous east–west-trending shear system along the southern CAOB displays a decreasing trend in the displacement from  $>2000$  km in the western portion, 1000–1600 km in Central Asia,  $\sim 130$ – $315$  km in Alxa,  $\sim 270$  km along the northern margin of the NCC and approximately 100 km in the farthest eastern portion. It is worth noting that these displacements are the minimum limits of the eastern CAOB because there are still some large-scale shear zones (especially in the eastern Xing'an-Mongolian orogenic belt) without any information due to a lack of study. In addition, the reason for the eastward reduction in lateral offset can be explained by NE-trending thrusts in NE China or even by the subduction of Paleo-Pacific Ocean (Li and others, 2022).

Third, the displacement inferred from paleomagnetism is based on the overall wrench between Laurentia and Gondwana. However, field-based geological studies have focused on specific geological bodies or markers, such as tectonic belts, plutons, strata boundaries. These units are generally located on one side of shear systems, or only in them, which cannot decipher the bulk offset across a broad shear system. Unrecognized shear zones, degrees of research in different regions and some other

factors result in a large difference in the offset from inferred paleomagnetism and geological records.

Although there are few actual measured data, the overall characteristics can be estimated; that is, the western part of the IPM has the largest displacement and the displacement decreases eastward. This feature is also consistent with the feature that the shear system gradually becomes younger to the east (fig. 18).

#### *Pangea A and B*

In the early reconstruction of the supercontinent, intercontinental shearing was suggested in the Pangea supercontinent, such as the “Tethys twist” (Van Hilten, 1964), but now it has been confirmed that the deformation age given by the author is not correct. In later work using paleomagnetism to reconstruct the Pangea Supercontinent, different scholars have noticed that the Pangea Supercontinent may have different shapes (Pangea A1, A2, B, or C) in different stages; that is, there was strong internal deformation (Van der Voo and French, 1974; Irving, 1977, 2004; Muttoni and others, 2003, 2009; Le Pichon and others, 2019; Pastor-Galána, 2022) rather than the early thought that there was basically no significant internal deformation (Pangea A1) (Bullard, 1965).

Ever since Pangea B was first proposed (Irving, 1977), it has been in dispute even to the present (Weil and others, 2001; Muttoni and others, 2003, 2009; Irving, 2004; Domeier and others, 2012, 2021; Torsvik and others, 2012; Le Pichon and others, 2019; Muttoni and Kent, 2019; Kent and Muttoni, 2020; Wu and others, 2021). In our opinion, in the reconstruction of the Pangea Supercontinent, the role of Adria in northern Italy and dextral displacement are the focus of the discussion.

Whether Adria is part of Africa or Gondwana is the key question. On the one hand, authors arguing for Pangea B suggest that Adria is a promontory of Africa, and its paleomagnetic poles represent the poles of Gondwana (Muttoni and others, 2003; Muttoni and Kent, 2019; Kent and Muttoni, 2020); however, Domeier and others (2012, 2021) argued that Adria has rotated relative to stable Africa, and the paleopoles of Adria should be excluded in the reconstruction of the Pangea Supercontinent. On the other hand, studies such as Torsvik and others (2012) and Domeier and others (2012, 2021) suggested that Adria cannot represent Gondwana and are based on data dominated by sedimentary poles that are likely to be biased by inclination error because the application of an expedient blanket correction for inclination error to the sedimentary unit results may result in larger effects on the mean poles (Kent and Muttoni, 2020). To resolve this problem, Kent and Muttoni (2020) only chose data from intrusive and extrusive igneous rocks from Adria, which could exclude the possibility of sedimentary inclination error. They found that the mean of the Adria poles for the Early Permian was similar to that of Gondwana at the same time, and they argued for the tectonic coherence of Adria with NW Africa in the Permian. Two recent studies also provided paleomagnetic data or new interpretations of the assembly of the Pangea Supercontinent, which all support a Pangea A in the Early Permian or even before (Domeier and others, 2021; Wu and others, 2021). However, Wu and others (2021) argued for an oblique convergence between Gondwana and Laurussia, which may explain the relative dextral movement between the two continents. Domeier and others (2021) also indicated that possible dextral movement between units in northwestern Africa is an important problem to be unraveled. Therefore, relative dextral movement may occur during the convergence or even later, and the question among different studies is its timing.

Regarding the dextral displacement, although the amount of dextral strike slip at the end of the late Paleozoic constrained by geological methods is significantly different from that constrained by the paleomagnetic method, constraints from the eastern

CAOB are also lacking. There are many reasons for this, which has been mentioned above. It should be emphasized that although there are obvious differences, ductile shear deformation from the end of the late Paleozoic to the early Mesozoic generally existed from the core of the Pangea Supercontinent to its eastern margin, which is the consensus of geological researchers from various regions. For example, a large number of contemporaneous dextral shear zones have been found in the southern margin of the Variscan orogenic belt in Europe (Arthaud and Matte, 1977; Gates and others, 1986; Shelley and Bossière, 2000; Matte, 2001; Franke and Żelaźniewicz, 2002; Martínez Catalán, 2011; Şengör, 2013; Le Pichon and others, 2019) and the southern CAOBS (Laurent-Charvet and others, 2002, 2003; Wang and others, 2007, 2010; Charvet and others, 2011; Zhang and others, 2021b; Zhao and others, 2022).

Although their formation mechanisms are not clear, their displacements are also disputed (Arthaud and Matte, 1977; Şengör, 2013; Şengör and others, 2019a; Le Pichon and others, 2019, 2021). The development of this intracontinental-scale deformation zone cannot be answered only by coincidence, and the displacement of this deformation zone across the Pangea Supercontinent should also be objective. At the same time, in addition to the geological evidence, the constraints from paleontology (Cisneros and others, 2012) and paleoclimatology (Kent and Muttoni, 2020) also indirectly reflect the existence of Pangea B. In the discussion of Pangea B and A, most paleomagnetic studies may be inappropriate in denying their significance because of the small amount of displacement determined by geology. Even if there was no long displacement of 2500–3000 km, those paleomagnetic studies against Pangea B need to consider or explain the reason for the intensely ductile shear deformation developed in the core of the supercontinent, rather than simply denying its significance. Given the above reasons, we prefer the interpretations made by paleomagnetic studies supporting Pangea B and the conjecture of the Intra-Pangean Megashear (Irving, 2004).

#### *Tectonic Setting*

The IPM across the central Pangea supercontinent is a giant structure. At the end of the late Paleozoic (*ca.* 275–240 Ma), the Variscan orogenic belt and the CAOBS were all in the intracontinental stage. Previous studies were mostly limited to the regional scope in discussing the formation mechanisms or backgrounds. Shu and others (1999) and Chen and others (2005) considered that the dextral ductile shear zone in the North Tianshan was the reactivation of the early Paleozoic Tianshan orogenic belt caused by the collision between the Siberian Craton and the Tarim Craton, reflecting the characteristics of intracontinental deformation after the collision. The relative rotation among the Siberian Craton, Junggar block and Tarim Craton in the late Paleozoic also resulted in the dextral ductile shear zone on the northern margin of the East Tianshan (Allen and others, 1995; Laurent-Charvet and others, 2002, 2003; Cai and others, 2012). Wang and others (2010) suggested that the formation of the dextral shear zone on the northern margin of the Tianshan was related to intracontinental deformation during the post collisional period, mainly because the extension of the West Siberian region led to the eastward migration of the whole CAOBS in the late Paleozoic. Natal'in and Şengör (2005) suggested that it was related to the oblique subduction of the Paleo-Tethys Ocean.

When discussing the role of the Erqis shear zone, Li and others (2015) suggested that the shear along the Erqis shear zone absorbed the sinistral movement of the Peri-Siberian orogenic system relative to the Kazakhstan orogenic system. The sinistral shear movement, together with the dextral shear movement in the Tianshan, was formed in the eastward migration of the Kazakhstan orogenic system. It is further believed that the eastward migration of the orogenic belt may have been related to

the continuous convergence of the Siberian, Tarim and Baltic cratons in the late Paleozoic. The eastward migration of orogenic materials in this period is also supported by paleomagnetic data in the Yili Block (Wang and others, 2007). It was found that there was no obvious relative movement between the Yili and Junggar blocks since the Carboniferous. However, in the Late Carboniferous and Late Permian, the Yili-Junggar Block migrated eastward relative to the Tarim and Siberian cratons, resulting in the formation of a dextral ductile shear zone in North Tianshan and an Erqis sinistral ductile shear zone in the late Paleozoic. A recent study on the EW seismic profile across the Junggar Block showed that a strong tectonic event occurred in the eastern and western parts of the block in the late Paleozoic, resulting in the shortening of the Junggar Basin by nearly 35% (He and others, 2018). The formation of this shortening structure was probably caused by the eastward wedging of the Yili-Junggar Block between the Tarim Craton and the Siberian Craton in the late Paleozoic.

In the eastern part of the IPM, previous scholars believed that dextral shearing along the northern margin of the NCC in the late Paleozoic-Triassic was caused by the collision of the Yangtze Craton and NCC in the south and the subduction of the Mongol-Okhotsk Ocean in the north (Zhao and others, 2015). Wang and Wan (2014) emphasized continuous oblique compression during the closure of the Paleo-Asian Ocean. However, after recent geological mapping in different regions in different segments of the eastern CAOB (figs. 6, 11, 12), we found that dextral shearing occurred after the closure of the Paleo-Asian Ocean. For example, in the northeastern Alxa Block, the EW-trending ductile dextral strike-slip shear zone cuts the Mid-Late Permian contraction deformation related to the closure of the Paleo-Asian Ocean in the Langshan region (fig. 6; Zhang and others, 2021a, 2022) and postcollisional granite (Hui and others, 2021). In the eastern CAOB, the Permian accretionary wedge was thrust to the south over the early Paleozoic accretionary wedge and was then transformed by dextral shearing into a giant Z-type fold in the Ondor Sum region (fig. 11A). In the Linxi region, the Xar Moon Shear Zone cuts the Permian ophiolite and accretionary wedge, and folds related to the closure of the Paleo-Asian Ocean (fig. 12; Zhao and others, 2015; Zhang and others, 2021e). A similar process may have also occurred in the Beishan region (Zhang and Cunningham, 2012). We therefore suggest that the latest Permian-Triassic dextral shearing along the CAOB, especially along the eastern CAOB occurred after the closure of the Paleo-Asian Ocean, and not by the oblique subduction of the Paleo-Asian Ocean.

Although different scholars have proposed many models in different regions, most studies have suggested that the dextral shear in the eastern segment of the IPM at the end of the late Paleozoic may have been related to the interaction among the Siberian, North China and Tarim cratons. However, this cannot explain the formation of the segment of the IPM in Europe and its 2500–3000 km displacement. This may have been related to the evolution of the Pangea Supercontinent and Tethys regime.

Almost all results of Pangea supercontinent reconstruction show that the supercontinent in the Southern Hemisphere encircled oceanic basins, and the Paleo-Tethys Ocean occupied the main region of the basins during most of the Permian (Irving, 1977, 1979; Muttoni and others, 2003, 2009; Şengör and others, 2019a). During the transitional period from the Late Permian to the Early Triassic, the Neo-Tethys Ocean in the south began to expand (fig. 19; Muttoni and others, 2009).

As the IPM formed during the assembly of the Pangea, it should have been related to the formation of this supercontinent, which was controlled by mantle convections of different scales (Zhong and others, 2007; Mitchell and others, 2021). During the formation of Pangea Supercontinent, two types of orogens developed along the periphery and in the core of Pangea (that is, the external and internal

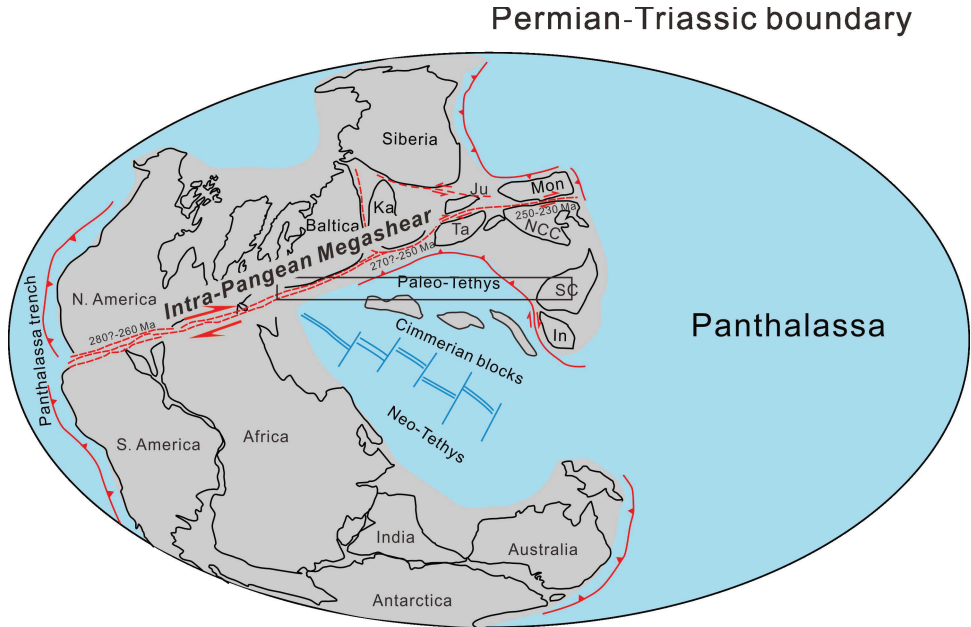


Fig. 19. Pangea A, distribution of IPM and tectonic setting during the Late Permian-early Mesozoic (SC-South China, Ka-Kazakhstan, In-Indochina, NCC-North China Craton, Ta-Tarim, Ju-Junggar).

orogenic systems, respectively) (Collins and others, 2011; Murphy and others, 2011). The external orogenic system formed at the stable boundary between the two global-scale mantle convection cells (that is, Panthalassan cell and Pangean cell); however, the internal system formed within the internal part of the Pangean convection cell (Collins, 2003; Collins and others, 2011). The boundary between these two cells was a curtain of subduction slabs down to at least a 400 km depth around most parts of the periphery of Pangea (Murphy and others, 2011; Collins and others, 2011; Stampfli and others, 2013), which led to thermal isolation, heating, and accumulation of hot plume materials beneath Pangea that prevented mixing between the two cells (Lenardic and others, 2011; Le Pichon and others, 2019, 2021). In the Pangea Supercontinent, the aspect ratio of the continental masses occupied by Laurasia in the north and Gondwana in the south was approximately 2 because the Tethys Oceans occupied the other half of the region in the south, which decreased the resulting heating of the underlying upper mantle in the south (Le Pichon and others, 2019). Therefore, the Tethyan Oceans in the south acted as an escape window for the asthenosphere below Pangea, and the lithosphere of northern Pangea was hotter than that of southern Pangea (Le Pichon and others, 2019), as indicated by many extensional basins in Europe and the Siberian Traps (Şengör and others, 2019a; Le Pichon and others, 2019; Kent and Muttoni, 2020). The warm mantle therefore spread laterally and dragged continental fragments toward peripheral subduction zones (Le Pichon and others, 2021), such as the Khangai-Khantey accretionary zone or Mongolia-Okhotsk subduction zone to the east of the supercontinent (Şengör and Natal'in, 1996; Zorin, 1999). Therefore, northern Pangea may have moved to the east relative to Gondwana to the south. In addition, the difference between horizontal principal stresses imposed on the lithosphere from mantle flow by subducted slabs or upwelling flow from the large low shear-wave velocity provinces was nearly zero in the

Paleo-Tethys region but remained relatively large across all northern Pangea and gradually decreased from west to east (Mitchell and others, 2021).

According to the deformation of different areas on the northern side of the Pangea Supercontinent, we suggest that the interaction of different cratons on the Laurasia continent to the north resulted in continuous EW shortening in the west (South Appalachian orogenic belt of North America), the middle (Ural orogenic belt) and the east (Xing'an-Mongolian orogenic belt), while the heated lithosphere of northern Pangea by plumes and its lateral (eastward) spreading may have been the main reason. Under the control of these factors, the IPM formed.

#### *Comparison with Other Continental Transform Faults or Large Shear Systems*

There are many large continental transform systems or shear systems in the world, most of which were active during the Cenozoic (for example, Norris and Toy, 2014; Şengör and others, 2019a). Compared to the Intra-Pangea Megashear or shear system described in this study, some continental transform faults, such as the San Andreas Fault of California, the Alpine Fault of New Zealand, and the Anatolian Fault Zone of northern Turkey are narrower. We suggest that three main reasons can account for the differential structures in the large-scale continental transform faults.

First, the structures and rheological features of strike-slip shear zones vary with depth. The width of the shear zone hinges on the exposed depth of the shear zones because the shear zone widens into a broad zone with increasing depth (for example, Storti and others, 2003; Lusk and Platt, 2020). The shear system we observed in the southern CAOB is highly exhumed and displays the middle crustal structures. Most modern continental transform faults as mentioned above present a relatively narrow zone, which is a fundamental characteristic of large-scale strike-slip faults in the brittle upper crust.

Second, the thermal structure of the crust, which determines rock rheology, is another important factor affecting the width of shear zones. In the late Paleozoic, profound magmatism occurred in the CAOB and highly influenced the thermal status of the crust. In this circumstance, the development of broad shear networks was facilitated. This was the same case in the NE Pan-African Orogen, where intense magmatism influenced the structures of the shear zones. Both shear activities occurred in a ~20 Ma interval after the emplacement of voluminous plutons. The widest part of the shear networks along the southern CAOB is in the Beishan-Alxa region where massive plutons developed, and many were also involved in the ductile deformation.

Third, the high heterogeneity of the accretional orogenic belt influences the scale of transcurrent systems. The CAOB is a composite collage, including microcontinents, islands, seamounts, ophiolites, arc-related basins, *etc.* The highly heterogeneous crust could influence the geometric and kinematic boundary conditions on ductile shearing, and anastomosing shear zones could be induced. A modern example is the broad intra-continental deformation in the region between the Tibetan Plateau and Mongolia Plateau, where a network of disconnected transpressive fault zones is controlled by pre-existing crustal structures, which favor the localization of strain (for example, Cunningham, 2013). A much older system is the Borborema Strike-Slip Shear Zone System (NE Brazil), which is more than 5,000 km long with a width of more than ~700 km and was formed on the basement of the older accretionary Pan-African Orogenic Belt (Neves and others, 2021; Fossen and others, 2022). Continental transform systems or shear systems are therefore controlled by the structures and temperatures of the crust. The types of previous orogenic belts on which continental transform systems form are also important, and accretionary orogenic belts are preferred.

## CONCLUSION

An intracontinental transform structure is an important form of continental deformation. Strike-slip faults played an important role in the formation and transformation of the CAOB. With the closing of the Paleo-Asian Ocean in the late Paleozoic, the Pangea Supercontinent was formed, and then a group of nearly EW-trending ductile dextral shear zones developed on the southern margin of the Variscan orogenic belt and the southern CAOB. The shear zone along the southern CAOB started from the Urals to the west, cut through the Kazakhstan orocline and passed through the Tianshan in China in the east and connected with the Beishan. It is connected with the strike-slip system of the Alxa area in the middle and continues eastward along the northern margin of the NCC, extending to the east of Greater Xing'an. We named this EW-trending shear zone in central Pangea the "Intra-Pangean Megashear" (IPM). The tectonic belt affected almost all rocks and structures before the Triassic. The regional strike-slip duplex system developed and strongly deformed the early orogenic belt. Its age ranges from 280 Ma to 230 Ma and is younger eastward. This tectonic belt connects the shortening in the Ural orogenic belt with the convergence in the east and forms the intracontinental transform structure in the central Pangea Supercontinent. The east west distance is more than 9000 km in the whole Eurasian Plate, and the dextral strike-slip displacement decreases eastward from approximately 2500 km in the west, *ca.* 1000 km in the middle part and ~130–315 km in the eastern segment, which is similar to the notable Altyn Tagh fault in the Cenozoic and transformed some strike slipping to oblique thrusting/shortening in the easternmost region due to a change in the strike of the system. The fact that the Baltic and Siberian cratons rotated close to each other from the end of late Paleozoic to the early Mesozoic and that the northern Pangean lithosphere was heated by plumes with lateral (eastward) spreading may have caused the development of the IPM and intracontinental deformation from Pangea B to Pangea A.

## ACKNOWLEDGMENTS

We thank Prof. Zongjin Ma from Institute of Geology, China Earthquake Administration for nearly 10 years' discussion on the global tectonics with the first author, although he is not able to work and suffering from Alzheimer's disease now. The authors are grateful for constructive reviews from Dr. Paul Eizenhöfer and the other two anonymous reviews. Meanwhile, Associate editor Prof. Guochun Zhao is gratefully acknowledged for his detailed and in-depth comments and encouragement. This research was funded by the National Natural Science Foundation of China (Nos. 41972224, 42102272, 42002228), China Postdoctoral Science Foundation (2021M703020), the National Key Research and Development Program of China from the Ministry of Science and Technology of China (No. 2017YFC0601301), and the China Geological Survey (DD20190004, 20221649). This is a contribution to IGCP-662 Project.

## SUPPLEMENTARY DATA

<https://earth.eps.yale.edu/~ajs/SupplementaryData/2022/Zhang/>

Fig. S1.  $^{40}\text{Ar}/^{39}\text{Ar}$  released spectra of samples from the Beidashan and Jinmiaogou ductile shear zones (see fig. 1)

Fig. S2. Zircon U-Pb ages of basic-Intermediate Dyke Swarms in Alxa Block, concordia diagrams, CL images of representative zircons. A and B. Diabase dikes in Hongshagang; C and D. Diorite dikes in Tukemu

Table S1 Results of  $^{40}\text{Ar}/^{39}\text{Ar}$  measurements of samples from the Beidashan

Table S2 U-Pb geochronologic analyses of zircons by LA-ICP-MS spectrometry

## REFERENCES

- Allen, M. B., Windley, B. F., Zhang, C., and Guo, J. H., 1993, Evolution of the Turfan basin, Chinese central Asia: *Tectonics*, v. 12, n. 4, p. 889–896, <https://doi.org/10.1029/93TC00598>
- Allen, M. B., Şengör, A. M. C., and Natal'in, B. A., 1995, Junggar, Turfan and Alakol basins as Late Permian to? Early Triassic extensional structures in a sinistral shear zone in the Altaid orogenic collage, *Central Asia: Journal of the Geological Society, London*, v. 152, p. 327–338, <https://doi.org/10.1144/gsjgs.152.2.0327>
- Arthaud, F., and Matte, P., 1977, Late Paleozoic strike-slip faulting in southern Europe and northern Africa: result of a right-lateral shear zone between the Appalachians and the Urals: *Geological Society of America Bulletin*, v. 88, n. 9, p. 1305–1320, [https://doi.org/10.1130/0016-7606\(1977\)88<1305:LPSFIS>2.0.CO;2](https://doi.org/10.1130/0016-7606(1977)88<1305:LPSFIS>2.0.CO;2)
- Ayarza, P., Brown, D., Alvarez-Marrón, J., and Juhlin, C., 2000, Contrasting tectonic history of the arc–continent suture in the Southern and Middle Urals: implications for the evolution of the orogen: *Journal of the Geological Society*, v. 157, n. 5, p. 1065–1076, <https://doi.org/10.1144/jgs.157.5.1065>
- BGMRIMAR (Bureau of Geology and Mineral Resources of Inner Mongolia Autonomous Region), 1991, *Regional Geology of Nei Mongol (Inner Mongolia) Autonomous Region*: Beijing, China, Geological Publishing House, 725 p.
- Briggs, S. M., Yin, A., Manning, C. E., Chen, Z. L., Wang, X. F., and Grove, M., 2007, Late Paleozoic tectonic history of the Ertix Fault in the Chinese Altai and its implications for the development of the Central Asian Orogenic System: *Geological Society of America Bulletin*, v. 119, n. 7–8, p. 944–960, <https://doi.org/10.1130/B26044.1>
- Brown, D., Puchkov, V., Alvarez-Marron, J., Bea, F., and Perez-Estaún, A., 2006b, Tectonic processes in the Southern and Middle Urals: an overview: *Geological Society, London, Memoirs*, v. 32, no. 1, p. 407–419, <https://doi.org/10.1144/GSL.MEM.2006.032.01.24>
- Brown, D., Spadea, P., Puchkov, V., Alvarez-Marron, J., Herrington, R., Willner, A. P., Hetzel, R., Gorozhanina, Y., and Juhlin, C., 2006a, Arc–continent collision in the Southern Urals: *Earth-Science Reviews*, v. 79, n. 3–4, p. 261–287, <https://doi.org/10.1016/j.earscirev.2006.08.003>
- Bullard, E., Everett, J. E., and Smith, A. G., 1965, The fit of the continents around the Atlantic: *Philosophical Transactions of the Royal Society of London, Series A, Mathematical and Physical Sciences*, v. 258, n. 1088, p. 41–51, <https://doi.org/10.1098/rsta.1965.0020>
- Buslov, M. M., 2011, Tectonics and geodynamics of the Central Asian Foldbelt: the role of Late Paleozoic large-amplitude strike-slip faults: *Russian Geology and Geophysics*, v. 52, n. 1, p. 52–71, <https://doi.org/10.1016/j.rgg.2010.12.005>
- Buslov, M. M., Fujiwara, Y., Iwata, K., and Semakov, N. N., 2004a, Late Paleozoic–Early Mesozoic Geodynamics of Central Asia: *Gondwana Research*, v. 7, n. 3, p. 791–808, [https://doi.org/10.1016/S1342-937X\(05\)71064-9](https://doi.org/10.1016/S1342-937X(05)71064-9)
- Buslov, M. M., Watanabe, T., Fujiwara, Y., Iwata, K., Smirnova, L. V., Safonova, I. Y., Semakov, N. N., and Kiryanova, A. P., 2004b, Late Paleozoic faults of the Altai region, Central Asia: tectonic pattern and model of formation: *Journal of Asian Earth Sciences*, v. 23, n. 5, p. 655–671, [https://doi.org/10.1016/S1367-9120\(03\)00131-7](https://doi.org/10.1016/S1367-9120(03)00131-7)
- Cai, Z. H., Xu, Z. Q., He, B. Z., and Wang, R. R., 2012, Age and tectonic evolution of ductile shear zones in the eastern Tianshan-Beishan orogenic belt: *Acta Petrologica Sinica*, v. 28, n. 6, p. 1875–1895.
- Chai, P., Sun, J. G., Xing, S. W., Li, B., and Lu, C., 2016, Ore geology, fluid inclusion and  $^{40}\text{Ar}/^{39}\text{Ar}$  geochronology constraints on the genesis of the Yingchengzi gold deposit, southern Heilongjiang Province, NE China: *Ore Geology Reviews*, v. 72, Part 1, p. 1022–1036, <https://doi.org/10.1016/j.oregeorev.2015.09.026>
- Charvet, J., Shu, L. S., Laurent-Charvet, S., Wang, B., Faure, M., Cluzel, D., Chen, Y., and de Jong, K., 2011, Palaeozoic tectonic evolution of the Tianshan belt, NW China: *Science China Earth Sciences*, v. 54, n. 2, p. 166–184, <https://doi.org/10.1007/s11430-010-4138-1>
- Chen, B. L., Wu, G. G., Yang, N., Ye, D. J., Shu, B., and Liu, X. C., 2007, Baidunzi-Xiaoxigong ductile shear zone and its ore-controlling effect in the southern Beishan Area, Gansu: *Journal of Geomechanics*, v. 13, n. 2, p. 99–109.
- Chen, W., Sun, S., Zhang, Y., Xiao, W. J., Wang, Y. T., Wang, Q. L., Jiang, L. Z., and Yang, J. T., 2005,  $^{40}\text{Ar}/^{39}\text{Ar}$  geochronology of the Qiugemingtashi-Huangshan ductile shear zone in east Tianshan, Xinjiang, NW China: *Acta Geologica Sinica*, v. 79, n. 6, p. 790–804.
- Choulet, F., Faure, M., Cluzel, D., Chen, Y., Lin, W., and Wang, B., 2012, From oblique accretion to transpression in the evolution of the Altaid collage: new insights from West Junggar, northwestern China: *Gondwana Research*, v. 21, n. 2–3, p. 530–547, <https://doi.org/10.1016/j.gr.2011.07.015>
- Cisneros, J. C., Abdala, F., Atayman-Güven, S., Rubidge, B. S., Şengör, A. M. C., and Schultz, C. L., 2012, Carnivorous dinocephalian from the Middle Permian of Brazil and tetrapod dispersal in Pangaea: *Proceedings of the National Academy of Sciences of the United States of America*, v. 109, n. 5, p. 1584–1588, <https://doi.org/10.1073/pnas.1115975109>
- Collins, W. J., 2003, Slab pull, mantle convection, and Pangaeian assembly and dispersal: *Earth and Planetary Science Letters*, v. 205, n. 3–4, p. 225–237, [https://doi.org/10.1016/S0012-821X\(02\)01043-9](https://doi.org/10.1016/S0012-821X(02)01043-9)
- Collins, W. J., Belousova, E. A., Kemp, A. I. S., and Murphy, J. B., 2011, Two contrasting Phanerozoic orogenic systems revealed by hafnium isotope data: *Nature Geoscience*, v. 4, n. 5, p. 333–337, <https://doi.org/10.1038/ngeo1127>
- Corsini, M., Vauchez, A., and Caby, R., 1996, Ductile duplexing at a bend of a continental-scale strike-slip shear zone: example from NE Brazil: *Journal of Structural Geology*, v. 18, n. 4, p. 385–394, [https://doi.org/10.1016/0191-8141\(95\)00102-J](https://doi.org/10.1016/0191-8141(95)00102-J)

- Cui, X., Wang, G. H., Wang, Z. Y., Liu, D. W., Lei, C. C., and Tang, Y., 2019, Discovery of structural schist belt in Huobuher area of Ejinaqi, Inner Mongolia: Implication for its tectonic significance: *Journal of Mineralogy and Petrology*, v. 39, n. 2, p. 81–89.
- Cunningham, D., 2013, Mountain building processes in intracontinental oblique deformation belts: Lessons from the Gobi Corridor, Central Asia: *Journal of Structural Geology*, v. 46, p. 255–282, <https://doi.org/10.1016/j.jsg.2012.08.010>
- de Jong, K., Xiao, W. J., Windley, B. F., Masago, H., and Lo, C. H., 2006, Ordovician  $^{40}\text{Ar}/^{39}\text{Ar}$  phengite ages from the blueschist-facies Ondor Sum subduction-accretion complex (Inner Mongolia) and implications for the Early Paleozoic history of continental blocks in China and adjacent areas: *American Journal of Science*, v. 306, n. 10, p. 799–845, <https://doi.org/10.2475/10.2006.02>
- de Jong, K., Wang, B., Faure, M., Shu, L. S., Cluzel, D., Charvet, J., Ruffet, G., and Chen, Y., 2009, New  $^{40}\text{Ar}/^{39}\text{Ar}$  age constraints on the late Palaeozoic tectonic evolution of the western Tianshan (Xinjiang, northwestern China), with emphasis on Permian fluid ingress: *International Journal of Earth Sciences*, v. 98, n. 6, p. 1239–1258, <https://doi.org/10.1007/s00531-008-0338-8>
- Deng, J., Yuan, W. M., Carranza, E. J. M., Yang, L. Q., Wang, C. M., Yang, L. Y., and Hao, N. N., 2014, Geochronology and thermochronometry of the Jiapigou gold belt, northeastern China: New evidence for multiple episodes of mineralization: *Journal of Asian Earth Sciences*, v. 89, p. 10–27, <https://doi.org/10.1016/j.jseas.2014.03.013>
- Dewey, J. F., 2002, Transtension in arcs and orogens: *International Geology Review*, v. 44, n. 5, p. 402–439, <https://doi.org/10.2747/0020-6814.44.5.402>
- Ding, S. H., 2021,  $^{40}\text{Ar}-^{39}\text{Ar}$  age of sericite and its geological significance in Qianhongquan gold deposit, Beishan Area, Gansu Province: *Gold Science and Technology*, v. 29, n. 2, p. 173–183.
- Domeier, M., Van der Voo, R., and Torsvik, T. H., 2012, Paleomagnetism and Pangea: the road to reconciliation: *Tectonophysics*, v. 514–517, p. 14–43, <https://doi.org/10.1016/j.tecto.2011.10.021>
- Domeier, M., Font, E., Youbi, N., Davies, J., Nemkin, S., Van der Voo, R., Perrot, M., Benabbou, M., Boumehdi, M. A., and Torsvik, T. H., 2021, On the Early Permian shape of Pangea from paleomagnetism at its core: *Gondwana Research*, v. 90, p. 171–198, <https://doi.org/10.1016/j.gr.2020.11.005>
- Dong, Y., Ge, W. C., Yang, H., Bi, J. H., Wang, Z. H., and Xu, W. L., 2017, Permian tectonic evolution of the Mudanjiang Ocean: Evidence from zircon U-Pb-Hf isotopes and geochemistry of a N-S trending granitoid belt in the Jiamusi Massif, NE China: *Gondwana Research*, v. 49, p. 147–163, <https://doi.org/10.1016/j.gr.2017.05.017>
- Eizenhöfer, P. R., Zhao, G. C., Zhang, J., and Sun, M., 2014, Final closure of the Paleo-Asian Ocean along the Solonker Suture Zone: constraints from geochronological and geochemical data of Permian volcanic and sedimentary rocks: *Tectonics*, v. 33, n. 4, p. 441–463, <https://doi.org/10.1002/2013TC003357>
- Feng, L. M., Lin, S. F., Li, L. M., Davis, D. W., Song, C. Z., Li, J. H., Ren, S. L., Han, X., Ge, Y. P., and Lu, K. J., 2020, Constraints on the tectonic evolution of the southern central Asian orogenic belt from early Permian–middle Triassic granitoids from the central Dunhuang orogenic belt, NW China: *Journal of Asian Earth Sciences*, v. 194, 104283, <https://doi.org/10.1016/j.jseas.2020.104283>
- Fossen, H., and Cavalcante, G. C. G., 2017, Shear zones – A review: *Earth-Science Reviews*, v. 171, p. 434–455, <https://doi.org/10.1016/j.earscirev.2017.05.002>
- Fossen, H., Harris, L. B., Cavalcante, C., Archanjo, C. J., and Ávila, C. F., 2022, The Patos-Pernambuco shear system of NE Brazil: Partitioned intracontinental transcurrent deformation revealed by enhanced aeromagnetic data: *Journal of Structural Geology*, v. 158, 104573, <https://doi.org/10.1016/j.jsg.2022.104573>
- Franke, W., and Żelaźniewicz, A., 2002, Structure and evolution of the Bohemian Arc: *Geological Society, London, Special Publication*, v. 201, p. 279–293, <https://doi.org/10.1144/GSL.SP.2002.201.01.13>
- Gao, J., Jiang, T., Wang, X. S., Li, J. L., Zhai, Q. G., Hu, P. Y., and Qian, Q., 2022, The Junggar, Tianshan and Beishan ophiolites: Constraint on the evolution of oceanic and continental framework along the southwestern margin of the Central-Asian Orogenic Belt: *Chinese Journal of Geology*, v. 57, n. 1, p. 1–42, <https://doi.org/10.12017/dzxx.2022.001>
- Gao, L. M., ms, 2004, Basic characteristics and dynamic significance of Xarmoron River fault zone: Master Thesis, Beijing, China, Chinese Academy of Geological Sciences (Beijing), 40 p.
- Gao, Y., Ding, H. L., Guo, R. J., Liu, Y. Y., and Wang, J. B., 2016, Structural deformation of Gonglujing—Sangejing ductile shear zone in the Beishan orogenic belt, and its geological significance: *Geological Survey of China*, v. 3, n. 1, p. 26–34, <https://doi.org/10.19388/j.zgdzdc.2016.01.005>
- Gates, A. E., Simpson, C., and Glover, L. III, 1986, Appalachian Carboniferous dextral strike-slip faults: an example from Brookneal, Virginia: *Tectonics*, v. 5, n. 1, p. 119–133, <https://doi.org/10.1029/TC005i001p00119>
- Ge, M. H., Zhang, J. J., Liu, K., Ling, Y. Y., Wang, M., and Wang, J. M., 2016, Geochemistry and geochronology of the blueschist in the Heilongjiang Complex and its implications in the late Paleozoic tectonics of eastern NE China: *Lithos*, v. 261, p. 232–249, <https://doi.org/10.1016/j.lithos.2015.11.019>
- Ge, M. H., Zhang, J. J., Li, L., and Liu, K., 2018, A Triassic–Jurassic westward scissor-like subduction history of the Mudanjiang Ocean and amalgamation of the Jiamusi Block in NE China: Constraints from whole-rock geochemistry and zircon U-Pb and Lu-Hf isotopes of the Lesser Xing’an-Zhangguangcai Range granitoids: *Lithos*, v. 302–303, p. 263–277, <https://doi.org/10.1016/j.lithos.2018.01.004>
- Goldfarb, R., Qiu, K. F., Deng, J., Chen, Y. J., and Yang, L. Q., 2019, Orogenic Gold Deposits of China, in Chang, Z., and Goldfarb, R. J., editors, *Mineral Deposits of China: Society of Economic Geologists Special Publications*, v. 22, p. 263–324.
- Gong, J. H., Zhang, J. X., Wang, Z. Q., Yu, S. Y., and Wang, D. S., 2018, Late Ordovician–Carboniferous tectonic evolutionary history of the Alxa Block: Constrained by the multistage magmatic–metamorphic–deformation events in Beidashan area: *Acta Petrologica et Mineralogica*, v. 37, n. 5, p. 771–798.

- Graham, S. A., Hendrix, M. S., Johnson, C. L., Badamgarav, D., Badarch, G., Amory, J., Porter, M., Barsbold, R., Webb, L. E., and Hacker, B. R., 2001, Sedimentary record and tectonic implications of Mesozoic rifting in southeast Mongolia: *Geological Society of America Bulletin*, v. 113, n. 12, p. 1560–1579, [https://doi.org/10.1130/0016-7606\(2001\)113<1560:SRATIO>2.0.CO;2](https://doi.org/10.1130/0016-7606(2001)113<1560:SRATIO>2.0.CO;2)
- Guan, J., ms, 2010, Study of the Aergashun ductile shear zone in Tamusu region of Alxa Youqi, Inner Mongolia: Master Thesis, Beijing, China, China University of Geosciences (Beijing), 49 p.
- Han, Y. G., Zhao, G. C., Sun, M., Eizenhöfer, P. R., Hou, W. Z., Zhang, X. R., Liu, Q., Wang, B., Liu, D. X., and Xu, B., 2016, Late Paleozoic subduction and collision processes during the amalgamation of the Central Asian Orogenic Belt along the South Tianshan suture zone: *Lithos*, v. 246–247, p. 1–12, <https://doi.org/10.1016/j.lithos.2015.12.016>
- Hart, C. J. R., Goldfarb, R. J., Qiu, Y. M., Snee, L., Miller, L. D., and Miller, M. L., 2002, Gold deposits of the northern margin of the North China Craton: multiple late Paleozoic–Mesozoic mineralizing events: *Mineralium Deposita*, v. 37, p. 326–351, <https://doi.org/10.1007/s00126-001-0239-2>
- He, D. F., Zhang, L., Wu, S. T., Li, D., and Zhen, Y., 2018, Tectonic evolution stages and features of the Junggar Basin: *Oil and Gas Geology*, v. 39, n. 5, p. 845–861.
- He, Z., Wang, B., Ni, X., De Grave, J., Scaillet, S., Chen, Y., Liu, J., and Zhu, X., 2021, Structural and kinematic evolution of strike-slip shear zones around and in the Central Tianshan: insights for eastward tectonic wedging in the southwest Central Asian Orogenic Belt: *Journal of Structural Geology*, v. 144, p. 104279, <https://doi.org/10.1016/j.jsg.2021.104279>
- Hetzl, R., and Glodny, J., 2002, A crustal-scale, orogen-parallel strike-slip fault in the Middle Urals: age, magnitude of displacement, and geodynamic significance: *International Journal of Earth Sciences*, v. 91, n. 2, p. 231–245, <https://doi.org/10.1007/s005310100208>
- Heumann, M. J., Johnson, C. L., Webb, L. E., Taylor, J. P., Jalbaa, U., and Minjin, C., 2014, Total and incremental left-lateral displacement across the East Gobi Fault Zone, southern Mongolia: Implications for timing and modes of polyphase intracontinental deformation: *Earth and Planetary Science Letters*, v. 392, p. 1–15, <https://doi.org/10.1016/j.epsl.2014.01.016>
- Hoskin, P. W. O., and Schaltegger, U., 2003, The composition of zircon and igneous and metamorphic petrogenesis: *Reviews in Mineralogy and Geochemistry*, v. 53, n. 1, p. 27–62, <https://doi.org/10.2113/0530027>
- Huang, T. K., 1945, On the major tectonic forms of China: National Geological Survey of China, *Geological Memoirs, Ser. A*, v. 20, p. 1–165.
- Hui, J., Zhang, K. J., Zhang, J., Qu, J. F., Zhang, B. H., Zhao, H., and Niu, P. F., 2021, Middle–late Permian high-K adakitic granitoids in the NE Alxa block, northern China: Orogenic record following the final closure of Paleo-Asian oceanic branch?: *Lithos*, v. 400–401, p. 106379, <https://doi.org/10.1016/j.lithos.2021.106379>
- Irving, E., 1977, Drift of the major continental blocks since the Devonian: *Nature*, v. 270, n. 5635, p. 304–309, <https://doi.org/10.1038/270304a0>
- Irving, E., 1979, Pole positions and continental drift since the Devonian, *in* McElhinny, M. W., editor, *The Earth its origins, structure and evolution*: Waltham, Massachusetts, Academic Press, p. 567–593.
- Irving, E., 2004, The case for Pangea B, and the Intra-Pangaean Megashear: *Geophysical Monograph Series*, v. 145, p. 13–27 <https://doi.org/10.1029/145GM02>
- Jahn, B. M., Wu, F. Y., and Chen, B., 2000, Granitoids of the Central Asian Orogenic Belt and continental growth in the Phanerozoic: *Earth and Environmental Science Transactions of the Royal Society of Edinburgh*, v. 91, n. 1–2, p. 181–193, <https://doi.org/10.1017/S0263593300007367>
- Jiang, H. B., Yang, H. Q., Dong, F. C., Tan, W. J., Zhao, G. B., and Ren, H. N., 2012, Division of metallogenic unit in the East Tianshan-Beishan area: *Northwestern Geology*, v. 45, n. 3, p. 1–12.
- Jiang, Y. D., Schulmann, K., Sun, M., Weinberg, R. F., Štípská, P., Li, P. F., Zhang, J., Chopin, F., Wang, S., Xia, X. P., and Xiao, W. J., 2019, Structural and geochronological constraints on Devonian suprasubduction tectonic switching and Permian collisional dynamics in the Chinese Altai, Central Asia: *Tectonics*, v. 38, n. 1, p. 253–280, <https://doi.org/10.1029/2018TC005231>
- Jourdon, A., Peti, C., Rolland, Y., Loury, C., Bellahsen, N., Guillot, S., Le Pourhiet, L., and Ganino, C., 2017, New structural data on Late Paleozoic tectonics in the Kyrgyz Tien Shan (Central Asian Orogenic Belt): *Gondwana Research*, v. 46, p. 57–78, <https://doi.org/10.1016/j.gr.2017.03.004>
- Kent, D. V., and Muttoni, G., 2020, Pangea B and the Late Paleozoic Ice Age: *Palaeogeography, Palaeoclimatology, Palaeoecology*, v. 553, p. 109753, <https://doi.org/10.1016/j.palaeo.2020.109753>
- Khain, E. V., Bibikova, E. V., Kröner, A., Zhuravlev, D. Z., Sklyarov, E. V., Fedotova, A. A., and Kravchenko-Berezhnoy, I. R., 2002, The most ancient ophiolite of the Central Asian fold belt: U–Pb and Pb–Pb zircon ages for the Duzhugur Complex, Eastern Sayan, Siberia, and geodynamic implications: *Earth and Planetary Science Letters*, v. 199, n. 3–4, p. 311–325, [https://doi.org/10.1016/S0012-821X\(02\)00587-3](https://doi.org/10.1016/S0012-821X(02)00587-3)
- Laurent-Charvet, S., Charvet, J., Shu, L. S., Ma, R. S., and Lu, H. F., 2002, Palaeozoic late collisional strike-slip deformations in Tianshan and Altay, Eastern Xinjiang, NW China: *Terra Nova*, v. 14, n. 4, p. 249–256, <https://doi.org/10.1046/j.1365-3121.2002.00417.x>
- Laurent-Charvet, S., Charvet, J., Monie, P., and Shu, L. S., 2003, Late Paleozoic strike-slip shear zones in eastern central Asia (NW China): New structural and geochronological data: *Tectonics*, v. 22, n. 2, 1009, <https://doi.org/10.1029/2001TC901047>
- Le Pichon, X., Şengör, A. M. C., and Imren, C., 2019, Pangea and the lower mantle: *Tectonics*, v. 38, n. 10, p. 3479–3504, <https://doi.org/10.1029/2018TC005445>
- Le Pichon, X., Jellinek, M., Lenardic, A., Şengör, A. M. C., and Imren, C., 2021, Pangea migration: *Tectonics*, v. 40, n. 6, p. e2020TC006585, <https://doi.org/10.1029/2020TC006585>
- Lenardic, A., Moresi, L., Jellinek, A. M., O’Neill, C. J., Cooper, C. M., and Lee, C. T., 2011, Continents, supercontinents, and mantle thermal mixing, and mantle thermal isolation: Theory, numerical simulations,

- and laboratory experiments: *Geochemistry, Geophysics, Geosystems*, v. 12, n. 10, p. Q10016, <https://doi.org/10.1029/2011GC003663>
- Levashova, N. M., Degtyarev, K. E., and Bazhenov, M. L., 2012, Oroclinal bending of the Middle and Late Paleozoic volcanic belts in Kazakhstan: Paleomagnetic evidence and geological implications: *Geotectonics*, v. 46, n. 4, p. 285–302, <https://doi.org/10.1134/S0016852112030041>
- Li, C. L., Li, S. R., Yuan, M. W., Du, B. Y., Li, W. L., Masroor, A., Liu, D. Y., and Liu, H., 2020, Genesis of the Keluo Au deposit in the Nenjiang-Heihe tectonic mélange belt, Heilongjiang Province: evidence from chemical composition and pyrite He-Ar, S, Pb isotopes: *Earth Science Frontiers*, v. 27, n. 5, p. 99–115, <https://doi.org/10.13745/j.esf.sf.2020.5.37>
- Li, G. Y., Zhou, J. B., Li, L., Chen, Z., and Wang, H. Y., 2022, Late Paleozoic to Mesozoic tectonic transition in northeastern Eurasia: Constraints from two island arc magmatic belts in eastern NE China: *Geological Society of America Bulletin*, <https://doi.org/10.1130/B36314.1>
- Li, J. Y., Gao, L. M., Sun, G. H., Li, Y. P., and Wang, Y. B., 2007, Shuangjingzi middle Triassic syn-collisional crust-derived granite in the east Inner Mongolian and its constraint on the timing of collision between Siberian and Sino-Korean paleo-plates: *Acta Petrologica Sinica*, v. 23, n. 3, p. 565–582.
- Li, P. F., Sun, M., Rosenbaum, G., Cai, K. D., and Yu, Y., 2015, Structural evolution of the Irtysh Shear Zone (northwestern China) and implications for the amalgamation of arc systems in the Central Asian Orogenic Belt: *Journal of Structural Geology*, v. 80, p. 142–156, <https://doi.org/10.1016/j.jsg.2015.08.008>
- Li, P. F., Sun, M., Rosenbaum, G., Yuan, C., Safonova, I., Cai, K., Jiang, Y., and Zhang, Y., 2018, Geometry, kinematics and tectonic models of the Kazakhstan Orocline, Central Asian Orogenic Belt: *Journal of Asian Earth Sciences*, v. 153, p. 42–56, <https://doi.org/10.1016/j.jseas.2017.07.029>
- Li, P. F., Sun, M., Yuan, C., Jourdan, F., Hu, W. W., and Jiang, Y. D., 2021, Late Paleozoic tectonic transition from subduction to collision in the Chinese Altai and Tianshan (Central Asia): New geochronological constraints: *American Journal of Science*, v. 321, n. 1–2, p. 178–205, <https://doi.org/10.2475/01.2021.05>
- Li, X. P., Jiao, L. X., Zheng, Q. D., Dong, X., Kong, F. M., and Song, Z. J., 2009, U-Pb zircon dating of the Heilongjiang complex at Huanan, Heilongjiang Province: *Acta Petrologica Sinica*, v. 25, n. 8, p. 1909–1916.
- Li, X. P., Kong, F. M., Zheng, Q. D., Dong, X., and Yang, Z. Y., 2010, Geochronological study on the Heilongjiang complex at Luobei area, Heilongjiang Province: *Acta Petrologica Sinica*, v. 26, n. 7, p. 2015–2024.
- Li, Y. L., Zhou, H. W., Brouwer, F. M., Xiao, W. J., Wijbrans, J. R., and Zhong, Z. Q., 2014, Early Paleozoic to Middle Triassic bivertent accretion in the Central Asian orogenic belt: Insights from zircon U-Pb dating of ductile shear zones in central Inner Mongolia, China: *Lithos*, v. 205, p. 84–111, <https://doi.org/10.1016/j.lithos.2014.06.017>
- Liang, C. Y., Liu, Y. J., Zheng, C. Q., Li, W. M., Neubauer, F., and Zhang, Q., 2019, Macro-and Micro-structural, Textural Fabrics and Deformation Mechanism of Calcite Mylonites from Xar Moron-Changchun Dextral Shear Zone, Northeast China: *Acta Geologica Sinica (English Edition)*, v. 93, n. 5, p. 1477–1499, <https://doi.org/10.1111/1755-6724.14357>
- Liu, B., Chen, Z. L., Yuan, F., Wu, B., Zhang, X. H., Han, F. B., Zhang, W. G., Huo, H. L., Li, J. L., Qu, M. M., Zhao, T. Y., Han, Q., Li, P., and Xia, D., 2022, Late Paleozoic deformation and tectonic significance of the South Central Tianshan Shear Zone, Kawabulake area, East Tianshan, NW China: Constraints from quartz fabrics and geochronologic data: *Journal of Asian Earth Sciences*, v. 227, p. 105074, <https://doi.org/10.1016/j.jseas.2021.105074>
- Liu, J. F., Li, J. Y., Chi, X. G., Zhao, Z. Z., Hu, Z. C., and Feng, Q. W., 2012, Petrogenesis of middle Triassic post-collisional granite from Jiefangyingzi area, southeast Inner Mongolia: Constraint on the Triassic tectonic evolution of the north margin of the Sino-Korean paleoplate: *Journal of Asian Earth Sciences*, v. 60, p. 147–159, <https://doi.org/10.1016/j.jseas.2012.08.012>
- Liu, Q., Zhao, G., Han, Y., Zhu, Y., Wang, B., Eizenhöfer, P. R., Zhang, X., and Tsui, R. W., 2019, Timing of the final closure of the middle segment of the Paleo-Asian Ocean: Insights from geochronology and geochemistry of Carboniferous–Triassic volcanosedimentary successions in western Inner Mongolia, China: *Geological Society of America Bulletin*, v. 131, n. 5–6, p. 941–965, <https://doi.org/10.1130/B32023.1>
- Liu, Y. J., Li, W. M., Feng, Z. Q., Wen, Q. B., Neubauer, F., and Liang, C. Y., 2017, A review of the Paleozoic tectonics in the eastern part of Central Asian Orogenic Belt: *Gondwana Research*, v. 43, p. 123–148, <https://doi.org/10.1016/j.gr.2016.03.013>
- Long, X. Y., Xu, W. L., Guo, P., Sun, C. Y., and Luan, J. P., 2020, Opening and closure history of the Mudanjiang Ocean in the eastern Central Asian Orogenic Belt: Geochronological and geochemical constraints from early Mesozoic intrusive rocks: *Gondwana Research*, v. 84, p. 111–130, <https://doi.org/10.1016/j.gr.2020.03.003>
- Lu, C. G., Bai, S. M., and Yang, G., 2012, Geological characteristics and prospecting indicators of Narenhala gold mine in Inner Mongolia: *Ningxia Engineering Technology*, v. 11, n. 444, p. 297–300.
- Lu, J., ms, 2016, Inner Mongolia Alxa Bayan Nuru NW dike swarm study in public area: Master Thesis, Beijing, China, China University of Geosciences (Beijing), 41 p.
- Lusk, A. D. J., and Platt, J. P., 2020, The deep structure and rheology of a plate boundary-scale shear zone: constraints from an exhumed Caledonian shear zone, NW Scotland: *Lithosphere*, v. 2020, n. 1, p. 8824736, <https://doi.org/10.2113/2020/8824736>
- Ma, A. Y., 2009, <sup>40</sup>Ar-<sup>39</sup>Ar dating of muscovite in mylonite of Shangganggangkundui fault-New evidence for the main stage of Xar Moron river fault zone: *Xinjiang Geology*, v. 27, n. 2, p. 170–175.
- Mao, Q. G., Xiao, W. J., Windley, B. F., Han, C. M., Qu, J. F., Ao, S. J., Zhang, J. E., and Guo, Q. Q., 2012, The Liuyuan complex in the Beishan, NW China: a Carboniferous-Permian ophiolitic fore-arc sliver in

- the southern Altai: *Geological Magazine*, v. 149, n. 3, p. 483–506, <https://doi.org/10.1017/S0016756811000811>
- Martínez Catalán, J. R., 2011, Are the oroclines of the Variscan belt related to late Variscan strike-slip tectonics?: *Terra Nova*, v. 23, n. 4, p. 241–247, <https://doi.org/10.1111/j.1365-3121.2011.01005.x>
- Matte, P., 1991, Accretionary history and crustal evolution of the Variscan belt in Western Europe: *Tectonophysics*, v. 196, n. 3–4, p. 309–337, [https://doi.org/10.1016/0040-1951\(91\)90328-P](https://doi.org/10.1016/0040-1951(91)90328-P)
- Matte, P., 2001, The Variscan collage and orogeny (480–290 Ma) and the tectonic definition of the Armorica microplate: a review: *Terra Nova*, v. 13, n. 2, p. 112–128, <https://doi.org/10.1046/j.1365-3121.2001.00327.x>
- McDougall, I., and Harrison, T. M., 1999, *Geochronology and Thermochronology by the  $^{40}\text{Ar}/^{39}\text{Ar}$  method*: New York, USA, Oxford University Press, 269 p.
- Melnikov, A., Travin, A., Plotnikov, A., Smirnova, L., and Theunissen, K., 1998, Kinematics and  $^{40}\text{Ar}/^{39}\text{Ar}$  geochronology of the Irtysh Shear zone in the NE Kazakhstan: IGCP 420, Ottawa, Canada, International Union of Geological Sciences, 60 p.
- Merzer, A. M., and Freund, R., 1976, Equal spacing of strike-slip faults: *Geophysical Journal International*, v. 45, n. 1, p. 177–188, <https://doi.org/10.1111/j.1365-246X.1976.tb00319.x>
- Metelkin, D. V., Vernikovskiy, V. A., Kazansky, A. Y., and Wingate, M. T. D., 2010, Late Mesozoic tectonics of Central Asia based on paleomagnetic evidence: *Gondwana Research*, v. 18, n. 2–3, p. 400–419, <https://doi.org/10.1016/j.jgr.2009.12.008>
- Miao, L. C., Fan, W. M., Zhang, F. Q., Liu, D. Y., Jian, P., Shi, G. H., Tao, H., and Shi, Y. R., 2004, Zircon SHRIMP geochronology of the Xinkailing–Kele complex in the northwestern Lesser Xing’an Range, and its geological implications: *Chinese Science Bulletin*, v. 49, n. 2, p. 201–209, <https://doi.org/10.1360/03wd0316>
- Miao, L. C., Qiu, Y. M., Fan, W. M., Zhang, F. Q., and Zhai, M. G., 2005, Geology, geochronology, and tectonic setting of the Jiapijiao gold deposits, southern Jilin Province, China: *Ore Geology Reviews*, v. 26, n. 1–2, p. 137–165, <https://doi.org/10.1016/j.oregeorev.2004.10.004>
- Miao, L., Zhang, F., Zhu, M., and Liu, D., 2015, Zircon SHRIMP U–Pb dating of metamorphic complexes in the conjunction of the Greater and Lesser Xing’an ranges, NE China: Timing of formation and metamorphism and tectonic implications: *Journal of Asian Earth Sciences*, v. 114, p. 634–648, <https://doi.org/10.1016/j.jseaes.2014.09.035>
- Mitchell, R. N., Zhang, N., Salminen, J., Liu, Y. B., Spencer, C. J., Steinberger, B., Murphy, J. B., and Li, Z. X., 2021, The supercontinent cycle: *Nature Reviews Earth & Environment*, v. 2, n. 5, p. 358–374, <https://doi.org/10.1038/s43017-021-00160-0>
- Mitrokhin, D., Zazansky, A., Theunissen, K., and Berzin, N., 1997, Paleomagnetic and kinematic characteristics of the Irtysh shear zone near Predgornoye (East Kazakhstan), Preliminary Results: Tervuren, Belgium, Royal Museum of Central Africa, Annual Report, v. 1995–1996, p. 187–201.
- Murphy, J. B., van Staal, C. R., and Collins, W. J., 2011, A comparison of the evolution of arc complexes in Paleozoic interior and peripheral orogens: Speculations on geodynamic correlations: *Gondwana Research*, v. 19, n. 3, p. 812–827, <https://doi.org/10.1016/j.jgr.2010.11.019>
- Muttoni, G., and Kent, D. V., 2019, Adria as promontory of Africa and its conceptual role in the Tethys Twist and Pangea B to Pangea A transformation in the Permian: *Rivista Italiana di Paleontologia e Stratigrafia*, v. 125, n. 1, p. 249–269, <https://doi.org/10.13130/2039-4942/11437>
- Muttoni, G., Kent, D. V., Garzanti, E., Brack, P., Abrahamsen, N., and Gaetani, M., 2003, Early Permian Pangea ‘B’ to Late Permian Pangea ‘A’: *Earth and Planetary Science Letters*, v. 215, n. 3–4, p. 379–394, [https://doi.org/10.1016/S0012-821X\(03\)00452-7](https://doi.org/10.1016/S0012-821X(03)00452-7)
- Muttoni, G., Gaetani, M., Kent, D. V., Sciuinbach, D., Angiolini, L., Berra, F., Garzanti, E., Mattei, M., and Zanchi, A., 2009, Opening of the Neo-Tethys Ocean and the Pangea B to Pangea A transformation during the Permian: *GeoArabia*, v. 14, n. 4, p. 17–48, <https://doi.org/10.2113/geoarabia140417>
- Natal’in, B. A., and Şengör, A. M. C., 2005, Late Palaeozoic to Triassic evolution of the Turan and Scythian platforms: The pre-history of the Palaeo-Tethyan closure: *Tectonophysics*, v. 404, n. 3–4, p. 175–202, <https://doi.org/10.1016/j.tecto.2005.04.011>
- Neves, S. P., Tommasi, A., Vauchez, A., and Carrino, T. A., 2021, The Borborema Strike-Slip Shear Zone System (NE Brazil): Large-Scale Intracontinental Strain Localization in a Heterogeneous Plate: *Lithosphere*, v. 2021, Special 6, p. 6407232, <https://doi.org/10.2113/2021/6407232>
- Norris, R. J., and Toy, V. G., 2014, Continental transforms: A view from the Alpine Fault: *Journal of Structural Geology*, v. 64, p. 3–31, <https://doi.org/10.1016/j.jsg.2014.03.003>
- Passchier, C. W., and Trouw, R. A. J., 2005, *Microtectonics*, 2nd edition: Berlin Heidelberg, Germany, Springer-Verlag, 366 p.
- Pastor-Galana, D., 2022, From supercontinent to superplate: Late Paleozoic Pangea’s inner deformation suggests it was a short-lived superplate: *Earth-Science Reviews*, v. 226, p. 103918, <https://doi.org/10.1016/j.earscirev.2022.103918>
- Peng, R., Zhang, G. S., Qiu, H. X., Liu, T. T., Fan, X. X., and Zhao, J. C., 2020, Petrogenesis and tectonic significance of the late Paleozoic mafic dykes in the Beishan area in Gansu Province: *Bulletin of Mineralogy, Petrology and Geochemistry*, v. 39, n. 2, <https://doi.org/10.19658/j.issn.1007-2802.2019.38.121>
- Pfiffner, O. A., 2017, Thick-Skinned and Thin-Skinned Tectonics: A Global Perspective: *Geosciences*, v. 7, n. 3, 71, <https://doi.org/10.3390/geosciences7030071>
- Puchkov, V. N., 1997, Structure and geodynamics of the Uralian orogen: Geological Society, London, Special Publications, v. 121, n. 1, p. 201–236, <https://doi.org/10.1144/GSL.SP.1997.121.01.09>
- Qi, Q., Wang, Y. H., Feng, M. X., Yang, J. G., Yu, J. Y., Wang, L., and Wang, X. H., 2016, Geochronology, geochemistry and tectonic significance of dike swarms in Beishan, Gansu: *Acta Geologica Sinica (English Edition)*, v. 90, n. s1, p. 114–115, <https://doi.org/10.1111/1755-6724.12919>

- Ramsay, J. G., and Graham, R. H., 1970, Strain variation in shear belts: *Canadian Journal of Earth Sciences*, v. 7, n. 3, p. 786–813, <https://doi.org/10.1139/e70-078>
- Sengör, A. M. C., 2013, The Pyrenean Hercynian Keirogen and the Cantabrian Orocline as genetically coupled structures: *Journal of Geodynamics*, v. 65, p. 3–21, <https://doi.org/10.1016/j.jog.2012.10.003>
- Sengör, A. M. C., and Natal'in, B. A., 1996, Paleotectonics of Asia: Fragments of a synthesis, *in* Yin, A., and Harrison, T. M., editors, *The tectonic evolution of Asia*: Cambridge, Britain: Cambridge University Press, p. 486–640.
- Sengör, A. M. C., Natal'in, B. A., and Burtman, V. S., 1993, Evolution of the Altaid tectonic collage and Palaeozoic crustal growth in Eurasia: *Nature*, v. 364, n. 6435, p. 299–307, <https://doi.org/10.1038/364299a0>
- Sengör, A. M. C., Natal'in, B. A., Sunal, G., and van der Voo, R., 2018, The tectonics of the Altai: Crustal growth during the construction of the continental lithosphere of Central Asia between ~750 and ~130 Ma ago: *Annual Review of Earth and Planetary Science*, v. 46, p. 439–494, <https://doi.org/10.1146/annurev-earth-060313-054826>
- Sengör, A. M. C., Zabi, C., and Natal'in, B. A., 2019a, Continental transform faults: Congruence and incongruence with normal plate kinematics, *in* Duarte, J. C., editor, *Transform plate boundaries and fracture zones*: Amsterdam, The Netherlands, Elsevier, chapter 9, p. 169–247, <https://doi.org/10.1016/B978-0-12-812064-4.00009-8>
- Sengör, A. M. C., Lom, N., and Sagdic, N. G., 2019b, Tectonic inheritance, structure reactivation and lithospheric strength: the relevance of geological history, *in* Wilson, R. W., Houseman, G. A., McCaffrey, K. J. W., Dore, A. G., and Buitter, S. J. H., editors, *Fifty Years of the Wilson Cycle Concept in Plate Tectonics*: Geological Society, London, Special Publications, v. 470, p. 105–135, <https://doi.org/10.1144/SP470.8>
- Shelley, D., and Bossière, G., 2000, A new model for the Hercynian Orogen of Gondwanan France and Iberia: *Journal of Structural Geology*, v. 22, n. 6, p. 757–776, [https://doi.org/10.1016/S0191-8141\(00\)00007-9](https://doi.org/10.1016/S0191-8141(00)00007-9)
- Shi, G. Z., Faure, M., Xu, B., Zhao, P., and Chen, Y., 2013, Structural and kinematic analysis of the Early Paleozoic Ondor Sum-Hongqi mélange belt, eastern part of the Altai (CAOB) in Inner Mongolia, China: *Journal of Asian Earth Sciences*, v. 66, p. 123–139, <https://doi.org/10.1016/j.jseas.2012.12.034>
- Shu, L. S., Chavert, J., Guo, L. Z., Lu, H. F., and Sébastien, L. C., 1999, A large-scale Palaeozoic dextral ductile strike-slip zone: the Aqikkudug-Weiya Zone along the Northern Margin of the Central Tianshan Belt, Xinjiang, NW China: *Acta Geologica Sinica*, v. 73, n. 2, p. 189.
- Simpson, C., 1983, Strain and shape-fabric variations associated with ductile shear zones: *Journal of Structural Geology*, v. 5, n. 1, p. 61–72, [https://doi.org/10.1016/0191-8141\(83\)90008-1](https://doi.org/10.1016/0191-8141(83)90008-1)
- Smith, A. G., Hurlley, A. M., and Briden, J. C., 1981, *Phanerozoic Paleogeographic World Maps*: Cambridge, United Kingdom, Cambridge University Press, 102 p.
- Stampfli, G. M., Hochard, C., Vèrard, C., Wilhelm, C., and VonRaumer, J., 2013, The formation of Pangea: *Tectonophysics*, v. 593, p. 1–19, <https://doi.org/10.1016/j.tecto.2013.02.037>
- Storti, F., Holdsworth, R. E., and Salvini, F., 2003, Intraplate Strike-Slip Deformation Belts: Geological Society, London, Special Publications, v. 210, p. 1–14, <https://doi.org/10.1144/GSL.SP.2003.210.01.01>
- Sun, D. Y., Liang, Y. H., and Zhang, Y. M., 1990, Ductile shear zone and gold deposits in Wuchuan-Guyang-Dashetai, Inner Mongolia: *Journal of Changchun University of Earth Science*, v. 20, n. 4, p. 399–406.
- Tang, K. D., 1990, Tectonic development of Paleozoic fold belts at the northern margin of the northern margin of the Sino-Korean craton: *Tectonics*, v. 9, n. 2, p. 249–260, <https://doi.org/10.1029/TC009i002p00249>
- Tang, K., and Yan, Z., 1993, Regional metamorphism and tectonic evolution of the Inner Mongolian suture zone: *Journal of Metamorphic Geology*, v. 11, n. 4, p. 511–522, <https://doi.org/10.1111/j.1525-1314.1993.tb00168.x>
- Tian, R. S., Xie, G. A., Zhu, W. B., Zhang, J., Zhang, B. H., Zhao, H., and Li, T., 2020, Late Paleozoic tectonic evolution of the Paleo-Asian ocean in the Northern Alxa Block (NW China): *Tectonics*, v. 39, e2020TC006359, <https://doi.org/10.1029/2020TC006359>
- Torsvik, T. H., Van der Voo, R., Preeden, U., Niocaill, C. M., Steinberger, B., Doubrovine, P. V., van Hinsbergen, D. J. J., Domeier, M., Gaina, C., Tohver, E., Meert, J. G., McCausland, P. J. A., and Cocks, L. R. M., 2012, Phanerozoic polar wander, palaeogeography and dynamics: *Earth-Science Reviews*, v. 114, n. 3–4, p. 325–368, <https://doi.org/10.1016/j.earscirev.2012.06.007>
- Travin, A. V., Vladimirov, V. G., and Boven, A., 2001, Implication of  $^{40}\text{Ar}/^{39}\text{Ar}$  data on the tectonothermal evolution of the Irtysh shear zone (Eastern Kazakhstan): Continental growth in the Phanerozoic: evidence from central Asia, ICGP 480 Conference Abstract Volume, p. 106–107.
- Van der Voo, R., 2004, Paleomagnetism, Oroclines, and Growth of the Continental Crust: *GSA Today*, v. 14, n. 12, p. 4–9, [https://doi.org/10.1130/1052-5173\(2004\)014<4:POAGOT>2.0.CO;2](https://doi.org/10.1130/1052-5173(2004)014<4:POAGOT>2.0.CO;2)
- Van der Voo, R., and Fench, R. B., 1974, Apparent polar wander for the Atlantic-bordering continents: late Carboniferous to Eocene: *Earth-Science Reviews*, v. 10, n. 2, p. 99–119, [https://doi.org/10.1016/0012-8252\(74\)90082-8](https://doi.org/10.1016/0012-8252(74)90082-8)
- Van der Voo, R., Levashov, N. M., Skrinnik, L. I., Kara, T. V., and Bazhenov, M. L., 2006, Late orogenic, large-scale rotations in the Tien Shan and adjacent mobile belts in Kyrgyzstan and Kazakhstan: *Tectonophysics*, v. 426, n. 3–4, p. 335–360, <https://doi.org/10.1016/j.tecto.2006.08.008>
- Van Hiltten, D., 1964, Evaluation of some geotectonic hypotheses by paleomagnetism: *Tectonophysics*, v. 1, n. 1, p. 3–71, [https://doi.org/10.1016/0040-1951\(64\)90028-9](https://doi.org/10.1016/0040-1951(64)90028-9)
- Vladimirov, A. G., Ponomareva, A. P., Shokalskii, S. P., Khalilov, V. A., Kostitsyn, Y. A., Ponomarchuk, V. A., Rudnev, S. N., Vystavnoi, S. A., Kruk, N. N., and Titov, A. V., 1997, Late Paleozoic early Mesozoic granitoid magmatism in Altai: *Russian Geology and Geophysics*, v. 38, n. 4, p. 715–729.

- Wang, B., Chen, Y., Zhan, S., Shu, L. S., Faure, M., Cluzel, D., Charvet, J., and Laurent-Charvet, S., 2007, Primary Carboniferous and Permian paleomagnetic results from the Yili Block (NW China) and their implications on the geodynamic evolution of Chinese Tianshan Belt: *Earth and Planetary Science Letters*, v. 263, n. 3–4, p. 288–308, <https://doi.org/10.1016/j.epsl.2007.08.037>
- Wang, T. Y., Zhang, M. J., Wang, J. R., and Gao, J. P., 1998, The characteristics and tectonic implications of the thrust belt in Eger Wusu, China: *Scientia Geologica Sinica*, v. 33, n. 4, p. 385–394.
- Wang, X. A., and Li, S. C., 2020, Late Triassic extensional deformation and magmatism in the eastern part of the Central Asian Orogenic Belt: Constraint from  $^{40}\text{Ar}/^{39}\text{Ar}$  and zircon U-Pb geochronology: *Acta Petrologica Sircica*, v. 36, n. 8, p. 2447–2462, <https://doi.org/10.18654/1000-0569/2020.08.11>
- Wang, Y., 1996, Tectonic processes of the Inner Mongolia–Yanshan Orogenic Belt in Eastern China during the Late of Late Paleozoic–Mesozoic: Beijing, China, Geological Publishing House, 142 p.
- Wang, Y., Li, J. Y., and Sun, G. H., 2008, Postcollisional Eastward Extrusion and Tectonic Exhumation along the Eastern Tianshan Orogen, Central Asia: Constraints from Dextral Strike-Slip Motion and  $^{40}\text{Ar}/^{39}\text{Ar}$  Geochronological Evidence: *The Journal of Geology*, v. 116, n. 6, p. 599–618, <https://doi.org/10.1086/591993>
- Wang, Y., Li, J. Y., and Sun, G. H., 2010, Postcollisional eastward extrusion and tectonic exhumation along the eastern Tianshan Orogen, Central Asia: Constraints from dextral strike-slip motion and  $^{40}\text{Ar}/^{39}\text{Ar}$  geochronological evidence: *The Journal of Geology*, v. 116, n. 6, p. 599–618, <https://doi.org/10.1086/591993>
- Wang, Z. H., and Wan, J. L., 2014, Collision-Induced Late Permian–Early Triassic transpressional deformation in the Yanshan Tectonic Belt, North China: *the Journal of Geology*, v. 122, n. 6, p. 705–716, <https://doi.org/10.1086/677843>
- Weil, A. B., Van der Voo, R., and van der Pluijm, B. A., 2001, Oroclinal bending and evidence against the Pangaea megashear: The Cantabria-Asturias Arc (northern Spain): *Geology*, v. 29, n. 11, p. 991–994, [https://doi.org/10.1130/0091-7613\(2001\)029<0991:OBAEAT>2.0.CO;2](https://doi.org/10.1130/0091-7613(2001)029<0991:OBAEAT>2.0.CO;2)
- Wilson, J. T., 1965, A new class of faults and their bearing on continental drift: *Nature*, v. 207, n. 4995, p. 343–347, <https://doi.org/10.1038/207343a0>
- Windley, B. F., Alexeev, D., Xiao, W. J., Kröner, A., and Badarch, G., 2007, Tectonic models for accretion of the Central Asian Orogenic Belt: *Journal of the Geological Society*, v. 164, n. 1, p. 31–47, <https://doi.org/10.1144/0016-76492006-022>
- Wu, F. Y., Yang, J. H., Lo, C. H., Wilde, S. A., Sun, D. Y., and Jahn, B. M., 2007, The Heilongjiang Group: A Jurassic accretionary complex in the Jiamusi Massif at the western Pacific margin of northeastern China: *Island Arc*, v. 16, n. 1, p. 156–172, <https://doi.org/10.1111/j.1440-1738.2007.00564.x>
- Wu, F. P., Zhang, W. J., and Wang, W., 2012, Discovery of the NNE ductile shear zone and its deformation age analysis of Tamusu area, inner Mongolia: *Xinjiang Geology*, v. 30, n. 2, p. 216–220.
- Wu, L., Murphy, J. B., Quesada, C., Li, Z. X., Waldron, J. W. F., Williams, S., Pisarevsky, S., and Collins, W. J., 2021, The amalgamation of Pangea: Paleomagnetic and geological observations revisited: *Geological Society of America Bulletin*, v. 133, n. 3–4, p. 625–646, <https://doi.org/10.1130/B35633.1>
- Xiao, W. J., Windley, B. F., Hao, J., and Zhai, M. G., 2003, Accretion leading to collision and the Permian Solonker suture, Inner Mongolia, China: Termination of the central Asian orogenic belt: *Tectonics*, v. 22, n. 6, p. 1069, <https://doi.org/10.1029/2002TC001484>
- Xiao, W. J., Mao, Q. G., Windley, B. F., Han, C. M., Qu, J. F., Zhang, J. E., Ao, S. J., Guo, Q. Q., Clevon, N. R., Lin, S. F., Shan, Y. H., and Li, J. L., 2010, Paleozoic multiple accretionary and collisional processes of the Beishan orogenic collage: *American Journal of Science*, v. 310, n. 10, p. 1553–1595, <https://doi.org/10.2475/10.2010.12>
- Xiao, W. J., Windley, B. F., Sun, S., Li, J. L., Huang, B. C., Han, C. M., Yuan, C., Sun, M., and Chen, H. L., 2015, A tale of amalgamation of three Permo-Triassic collage systems in Central Asia: Oroclines, sutures, and terminal accretion: *Annual Review of Earth and Planetary Sciences*, v. 43, p. 477–507, <https://doi.org/10.1146/annurev-earth-060614-105254>
- Xiao, W. J., Windley, B. F., Han, C. M., Liu, W., Wan, B., Zhang, J. E., Ao, S. J., Zhang, Z. Y., and Song, D. F., 2018, Late Paleozoic to early Triassic multiple roll-back and oroclinal bending of the Mongolia collage in Central Asia: *Earth-Science Reviews*, v. 186, p. 94–128, <https://doi.org/10.1016/j.earscirev.2017.09.020>
- Xin, H. T., Niu, W. C., Tian, J., Teng, X. J., and Duan, X. L., 2020, Spatio-temporal structure of Beishan orogenic belt and evolution of Paleo-Asian Ocean, Inner Mongolia: *Geological Bulletin of China*, v. 39, n. 9, 1297–1316.
- Xiong, S. Q., 2019, Atlas of aeromagnetic survey results of petroliferous basins in China: Beijing, China, Geological Publishing House, 151 p.
- Xu, H., Chen, T. H., Gong, Q. D., Liu, X. G., Liu, B., and Xie, Y. F., 2014, Relationship between ductile shear zone and gold deposit in Sunite Zuoqi, Inner Mongolia: *Journal of Mineral and Petrology*, v. 34, n. 2, p. 68–76, <https://doi.org/10.19719/j.cnki.1001-6872.2014.02.011>
- Yakubchuk, A., 2004, Architecture and mineral deposit settings of the Altaid orogenic collage: a revised model: *Journal of Asian Earth Sciences*, v. 23, n. 5, p. 761–779, <https://doi.org/10.1016/j.jseas.2004.01.006>
- Ye, K., Zhang, L., Wang, T., Shi, X. J., Zhang, J. J., and Liu, C., 2016, Geochronology, geochemistry and zircon Hf isotope of the Permian intermediate-acid igneous rocks from the Yabulai Mountain in western Alxa, Inner Mongolia, and their tectonic implications: *Acta Petrologica et Mineralogica*, v. 35, n. 6, p. 901–928.
- Yu, J. Y., Guo, L., Li, J. X., Li, Y. G., Smithies, R. H., Wingate, M.T.D., Meng, Y., and Chen, S. F., 2016, The petrogenesis of sodic granites in the Niujuanzi area and constraints on the Paleozoic tectonic evolution of the Beishan region, NW China: *Lithos*, v. 256–257, p. 250–268, <https://doi.org/10.1016/j.lithos.2016.04.003>

- Zhang, J., and Cunningham, D., 2012, Kilometer-scale refolded folds caused by strike-slip reversal and intra-plate shortening in the Beishan region, China: *Tectonics*, v. 31, n. 3, p. TC3009, <https://doi.org/10.1029/2011TC003050>
- Zhang, B. H., Zhang, J., Zhao, H., Qu, J. F., Zhang, Y. P., Niu, P. F., Hui, J., and Yun, L., 2021b, Kinematics and Geochronology of Late Paleozoic–Early Mesozoic Ductile Deformation in the Alxa Block, NW China: New Constraints on the Evolution of the Central Asian Orogenic Belt: *Lithosphere*, v. 2021, n. 1, p. 3365581, <https://doi.org/10.2113/2021/3365581>
- Zhang, C. L., Santosh, M., Zou, H. B., Xu, Y. G., Zhou, G., Dong, Y. G., Ding, R. F., and Wang, H. Y., 2012, Revisiting the “Irish tectonic belt”: Implications for the Paleozoic tectonic evolution of the Altai orogen: *Journal of Asian Earth Sciences*, v. 52, p. 117–133, <https://doi.org/10.1016/j.jseas.2012.02.016>
- Zhang, H. T., So, C. S., and Yun, S. T., 1999, Regional geologic setting and metallogenesis of central Inner Mongolia, China: guides for exploration of mesothermal gold deposits: *Ore Geological Reviews*, v. 14, n. 2, p. 129–146, [https://doi.org/10.1016/S0169-1368\(98\)00019-5](https://doi.org/10.1016/S0169-1368(98)00019-5)
- Zhang, J., Li, J. Y., Xiao, W. X., Wang, Y. N., and Qi, W. H., 2013, Kinematics and geochronology of multi-stage ductile deformation along the eastern Alxa block, NW China: New constraints on the relationship between the North China Plate and the Alxa block: *Journal of Structural Geology*, v. 57, p. 38–57, <https://doi.org/10.1016/j.jsg.2013.10.002>
- Zhang, J., Li, J. Y., Li, Y. F., Qi, W. H., and Zhang, Y. P., 2014, Mesozoic-Cenozoic intraplate deformations at the Langshan region and their tectonic implication: *Acta Geologica Sinica (English Edition)*, v. 88, n. 1, p. 78–102, <https://doi.org/10.1111/1755-6724.12184>
- Zhang, J., Zhang, Y. P., Xiao, W. X., Wang, Y. N., and Zhang, B. H., 2015a, Linking the Alxa Terrane to the eastern Gondwana during the Early Paleozoic: Constraints from detrital zircon U–Pb ages and Cambrian sedimentary records: *Gondwana Research*, v. 28, n. 3, p. 1168–1182, <https://doi.org/10.1016/j.gr.2014.09.012>
- Zhang, J. J., Wang, T., Zhang, L., Tong, Y., Zhang, Z. C., Shi, X. J., Guo, L., Huang, H., Yang, Q. D., Huang, W., Zhao, J. X., Ye, K., and Hou, J. Y., 2015b, Tracking deep crust by zircon xenocrysts within igneous rocks from the northern Alxa, China: Constraints on the southern boundary of the Central Asian Orogenic Belt: *Journal of Asian Earth Sciences*, v. 108, p. 150–169, <https://doi.org/10.1016/j.jseas.2015.04.019>
- Zhang, J., Li, J. Y., Zhang, B. H., and Zhao, H., 2016, Timing of amalgamation of the Alxa Block and the North China Block: Constraints based on detrital zircon U–Pb ages and sedimentologic and structural evidence: *Tectonophysics*, p. 668–669, p. 65–81, <https://doi.org/10.1016/j.tecto.2015.12.006>
- Zhang, J. R., Wei, C. J., and Chu, H., 2018, Multiple metamorphic events recorded in the metamorphic terranes in central Inner Mongolia, Northern China: Implication for the tectonic evolution of the Xing’an-Inner Mongolia Orogenic Belt: *Journal of Asian Earth Sciences*, v. 167, p. 52–67, <https://doi.org/10.1016/j.jseas.2018.04.007>
- Zhang, J., Yun, L., Zhang, B. H., Qu, J. F., Zhao, H., Hui, J., Wang, Y. N., and Zhang, Y. P., 2020, Deformation at the easternmost Altyn Tagh fault: constraints on the growth of the northern Qinghai-Tibetan Plateau: *Acta Geologica Sinica (English Edition)*, v. 94, n. 4, p. 988–1006, <https://doi.org/10.1111/1755-6724.14555>
- Zhang, J., Qu, J. F., Zhang, B. H., Zhao, H., Zheng, R. G., Zhang, Q. L., Zhao, S., Liu, J. F., Zhang, Y. P., Niu, P. F., Hui, J., Yun, L., Tian, R. S., Amirdin, A., Li, F. H., and Xie, G. A., 2021a, China Geological Survey: 1: 50,000 Geological Map of Bayan Hara (K48E021017) in Inner Mongolia: Beijing, China: Geoscientific Data & Discovery Publishing System, 95 p., <http://dcc.ngac.org.cn/cn/geologicalData/details/doi/10.35080/data.C.2021.P12>
- Zhang, J., Cunningham, D., Ynn, L., Qu, J. F., Zhao, H., Zhang, B. H., Niu, P. F., and Hui, J., 2021c, Kinematic variability of late Cenozoic fault systems and contrasting mountain building processes in the Alxa block, western China: *Journal of Asian Earth Sciences*, v. 205, p. 104597, <https://doi.org/10.1016/j.jseas.2020.104597>
- Zhang, J. J., Zhang, S. H., Zhao, Y., Hu, G. H., and Gao, H. L., 2021d, Identification of an early Neoproterozoic gabbro sill emplaced into the Zha’ertai Group in the Guyang area, Inner Mongolia and its geological significance: *Acta Geologica Sinica*, v. 95, n. 3, p. 667–685, <https://doi.org/10.19762/j.cnki.dizhixuebao.2021125>
- Zhang, J., Qu, J. F., Liu, J. F., Wang, Y. N., Zhao, H., Zhao, S., Zhang, B. H., Zheng, R. G., Yun, L., Yang, Y. Q., and Niu, P. F., 2021e, The nature and evolution of the Xar Moron tectonic belt in the eastern Central Asian Orogenic Belt: constraints from deformation and low-temperature thermochronology: *Sedimentary Geology and Tethyan Geology*, v. 41, n. 2, p. 190–217, <https://doi.org/10.19826/j.cnki.1009-3850.2021.02010>
- Zhang, J., Wang, Y. N., Qu, J. F., Zhang, B. H., Zhao, H., Yun, L., Li, T. Y., Niu, P. F., Nie, F. J., Hui, J., and Zhang, Y. P., 2021f, Mesozoic intracontinental deformation of the Alxa Block in the middle part of Central Asian Orogenic Belt: A review: *International Geological Review*, v. 63, n. 12, p. 1490–1520, <https://doi.org/10.1080/00206814.2020.1783583>
- Zhang, J., Cunningham, D., Qu, J. F., Zhang, B. H., Zhao, H., Zheng, R. G., Niu, P. F., Hui, J., Yun, L., Zhao, S., Zheng, R., and Zhang, Y. P., 2022, Poly-phase accretionary, collisional and intraplate tectonism in the Langshan region of the Alxa Block, China: Unravelling the complex structural evolution of the southern Central Asian Orogenic Belt: *Gondwana Research*, v. 105, p. 25–50, <https://doi.org/10.1016/j.gr.2021.12.007>
- Zhang, W., ms. 2013, Late Paleozoic granitoids in Beishan-northern Alxa area (NW China) and their tectonic implications: Ph.D Dissertation, Peking University, Beijing, China, 200 p.
- Zhang, Y. Y., Yuan, C., Sun, M., Long, X. P., Xia, X. P., Wang, X. Y., and Huang, Z. Y., 2015c, Permian doleritic dikes in the Beishan Orogenic Belt, NW China: Asthenosphere–lithosphere interaction in response to slab break-off: *Lithos*, v. 233, p. 174–192, <https://doi.org/10.1016/j.lithos.2015.04.001>

- Zhang, Y., Yuan, C., Sun, M., Long, X., Wang, Y., Jiang, Y., and Lin, Z., 2017, Arc magmatism associated with steep subduction: Insights from trace element and Sr–Nd–Hf–B isotope systematics: *Journal of Geophysical Research: Solid Earth*, v. 122, n. 3, p. 1816–1834, <https://doi.org/10.1002/2016JB013289>
- Zhao, G. C., Sun, M., Wilde, S. A., and Li, S. Z., 2005, Late Archean to Paleoproterozoic evolution of the North China Craton: key issues revisited: *Precambrian Research*, v. 136, n. 2, p. 177–202, <https://doi.org/10.1016/j.precamres.2004.10.002>
- Zhao, G. C., Wang, Y. J., Huang, B. C., Dong, Y. P., Li, S. Z., Zhang, G. W., and Yu, S., 2018, Geological reconstructions of the East Asian blocks: From the breakup of Rodinia to the assembly of Pangea: *Earth-Science Reviews*, v. 186, p. 262–286, <https://doi.org/10.1016/j.earscirev.2018.10.003>
- Zhao, H., Zhang, J., Wang, Y.N., and Zhang, B. H., 2017, The Deformation Features, Phases and Significance of Keluo Complex in Nenjiang Area, Heilongjiang Province: *Geotectonica et Metallogenia*, v. 41, n. 4, p. 617–637, <https://doi.org/10.16539/j.ddgzycxk.2017.04.001>
- Zhao, H., Zhang, J., Zhang, B. H., Qu, J. F., Zhang, Y. P., Niu, P. F., Hui, J., and Wang, Y., 2022, Structures and chronology of the Yabrai shear zone in the Alxa, NW China: constraints on the late Paleozoic shear system in central segment of the Central Asian orogenic belt: *Journal of Structural Geology*, v. 142, p. 104575, <https://doi.org/10.1016/j.jsg.2022.104575>
- Zhao, P., Faure, M., Chen, Y., Shi, G. Z., and Xu, B., 2015, A new Triassic shortening-extrusion tectonic model for Central-Eastern Asia: Structural, geochronological and paleomagnetic investigations in the Xilamulun Fault (North China): *Earth and Planetary Science Letters*, v. 426, p. 46–57, <https://doi.org/10.1016/j.epsl.2015.06.011>
- Zheng, R. G., Wu, T. R., Zhang, W., Xu, C., Meng, Q. R., and Zhang, Z. Y., 2014, Late Paleozoic subduction system in the northern margin of the Alxa block, Altaids: Geochronological and geochemical evidences from ophiolites: *Gondwana Research*, v. 25, n. 2, p. 842–858, <https://doi.org/10.1016/j.gr.2013.05.011>
- Zheng, R. G., Li, J. Y., Xiao, W. J., and Wang, L. J., 2018, A new ophiolitic mélange containing boninitic blocks in Alxa region: Implications for Permian subduction events in southern CAOB: *Geoscience Frontiers*, v. 9, n. 5, p. 1355–1367, <https://doi.org/10.1016/j.gsf.2018.02.014>
- Zheng, R. G., Li, J. Y., Zhang, J., Xiao, W. J., and Wang, Q. J., 2020, Permian oceanic slab subduction in the southmost of Central Asian Orogenic Belt: Evidence from adakite and high-Mg diorite in the southern Beishan: *Lithos*, v. 358–359, p. 105406, <https://doi.org/10.1016/j.lithos.2020.105406>
- Zheng, Y. D., Wang, S., and Wang, Y., 1991, An enormous thrust nappe and extensional metamorphic core complex newly discovered in Sino-Mongolian boundary area: *Science in China, Series B*, v. 34, n. 9, p. 1145–1152.
- Zhong, S. J., Zhang, N., Li, Z. X., and Roberts, J. H., 2007, Supercontinent cycles, true polar wander, and very long-wavelength mantle convection: *Earth and Planetary Science Letters*, v. 261, n. 3–4, p. 551–564, <https://doi.org/10.1016/j.epsl.2007.07.049>
- Zhou, J. B., and Wilde, S. A., 2013, The crustal accretion history and tectonic evolution of the NE China segment of the Central Asian Orogenic Belt: *Gondwana Research*, v. 23, n. 4, p. 1365–1377, <https://doi.org/10.1016/j.gr.2012.05.012>
- Zhou, J. B., Wilde, S. A., Zhang, X. Z., Zhao, G. C., Zheng, C. Q., Wang, Y. J., and Zhang, X. H., 2009, The onset of Pacific margin accretion in NE China: Evidence from the Heilongjiang high-pressure metamorphic belt: *Tectonophysics*, v. 478, n. 3–4, p. 230–246, <https://doi.org/10.1016/j.tecto.2009.08.009>
- Zhou, J. B., Cao, J. L., Wilde, S. A., Zhao, G. C., Zhang, J. J., and Wang, B., 2014, Paleo-Pacific subduction-accretion: Evidence from geochemical and U–Pb zircon dating of the Nadanhada accretionary complex, NE China: *Tectonics*, v. 33, n. 12, p. 2444–2466, <https://doi.org/10.1002/2014TC003637>
- Zhou, X. C., Zhang, H. F., Luo, B. J., Pan, F. B., Zhang, S. S., and Guo, L., 2016, Origin of high Sr/Y-type granitic magmatism in the southwestern of the Alxa Block, Northwest China: *Lithos*, v. 256–257, p. 211–227, <https://doi.org/10.1016/j.lithos.2016.04.021>
- Zhu, X., Wang, B., Chen, Y., Liu, H., Hornig, C. S., Choulet, F., Faure, M., Shu, L. S., and Xue, Z. H., 2018, First Early Permian paleomagnetic pole for the Yili Block and its implications for late Paleozoic post-orogenic kinematic evolution of the SW Central Asian Orogenic Belt: *Tectonics*, v. 37, n. 6, p. 1709–1732, <https://doi.org/10.1029/2017TC004642>
- Zorin, Y. A., 1999, Geodynamics of the western part of the Mongolia–Okhotsk collisional belt, Trans-Baikal region (Russia) and Mongolia: *Tectonophysics*, v. 306, n. 1, p. 33–56, [https://doi.org/10.1016/S0040-1951\(99\)00042-6](https://doi.org/10.1016/S0040-1951(99)00042-6)
- Zuo, G. C., and He, G. Q., 1990, Plate tectonics and metallogenic regularities in Beishan region: Beijing, China, Geological Publishing House, 224 p.
- Zuo, G. C., and Zheng, Y. D., 1991, Great breakthroughs in the field investigation of Beishan lithosphere in 1990, eight regional ductile shear zones and major thrust faults: *Gansu Geological Science and Technology Information*, n. 1, p. 1–4.
- Zuo, G. C., Zhang, S. L., He, G. Q., and Zhang, Y., 1990, Early Paleozoic plate tectonics in Beishan area: *Scientia Geologica Sinica*, v. 25, n. 4, p. 305–314.